NOVEL METHODS FOR PREPARATION OF MODIFIED 1-DIMENSIONAL NANOMATERIALS OF TITANIUM DIOXIDE FOR ENVIRONMENTAL ENGINEERING APPLICATIONS

A Dissertation

presented to

the Faculty of the Graduate School

at the University of Missouri

In Partial Fulfillment

of the Requirements for the Degree

Doctor of Philosophy

---

by

HUY QUANG NGUYEN

Dr. Baolin Deng, Dissertation Supervisor

DECEMBER 2012

The undersigned, appointed by the dean of the Graduate School, have examined the dissertation entitled

NOVEL METHODS FOR PREPARATION OF MODIFIED 1-DIMENSIONAL NANOMATERIALS OF TITANIUM DIOXIDE FOR ENVIRONMENTAL ENGINEERING APPLICATIONS

presented by Huy Quang Nguyen,

a candidate for the degree of doctor of philosophy of Civil Engineering,

and hereby certify that, in their opinion, it is worthy of acceptance.

Professor Baolin Deng

Professor Qingsong Yu

Professor Thomas E. Clevenger

Professor Zhiqiang Hu

DEDICATIONS

This dissertation is dedicated to my father Chuong Nguyen for his endless encouragement and to my mother Tho Le, my wife Khanh Nguyen, my son Minh Nguyen, and my sister Trang Nguyen for their love and support during my 5 years staying away from home.

ACKNOWLEDGEMENTS

I would like to express my sincerest appreciation to my advisor and mentor, Dr. Baolin Deng, for his insightful and careful advice, and especially for the great support throughout the research which not only is wholly new to me but also presents a great deal of challenges during the study course. Your time, understanding, and supporting are truly appreciated.

I am grateful to Dr. Qingsong Yu of the Department of Material and Aerospace Engineering for his generosity in allowing me using many facilities of his lab for carrying out my research. Most of my research would not be possible without your help and support.

I would like to thank Vietnam Education Foundation and the Department of Civil and Environmental Engineering of the University of Missouri to provide me with financial support and an opportunity to pursuit doctoral training in the United States. I also would like to thank the US Geological Survey for funding a part of my research project.

I also thank my other dissertation committee members: Dr. Thomas E. Clevenger and Dr. Hu Zhiqiang who have generously provided their time and valuable suggestions to my dissertation.

Finally, I would like to send my appreciations to many colleagues and friends who had help me a lot during my training in the US: Dr. Enoss Inniss, Dr. Lisa Wuff, Mr. Dan Crosby, Dr. Armelle Braud, Dr. Eunsik Kim, and Yun Jin of the Department of Civil and Environmental Engineering for their assistance in my lab works; John Jones and Dr. Andrew Ritts of the Department of Material and Aerospace Engineering for their assistance in operating the plasma equipment; Mr. Lou Ross and Ms. Cheryl Jensen of Electron Microscopy Core for their teaching and assistance in SEM and TEM characterization, Dr. Joseph Mathai of the Department of Electrical Engineering for helping with UV-VIS reflection test; Dr. Junhua Guo of the Department of Geology for helping with XRD scanning; Ms. Mary McCush, Ms. Jennifer Keyzer-Andre, and Ms. April Klug for their administrative works; and my friends Dr. C.J. Nelson, Dr. Joseph Hobbs, Dr. Sang Kim, Nazmul Hussain, Ryan Admunson, Scott Gaines, Thanh Vu, Chau Nguyen, Ha Nguyen, Thuy Vu, Thang La and Phuong Nguyen for their great support and care to make me feel living in the family although of being thousands miles away from home.

TABLE OF CONTENTS

LIST OF ILLUSTRATIONS

LIST OF TABLES

NOVEL METHODS FOR PREPARATION OF

MODIFIED 1-DIMENSIONAL NANOMATERIALS OF TITANIUM DIOXIDE FOR

ENVIRONMENTAL ENGINEERING APPLICATIONS

Huy Quang Nguyen

Dr. Baolin Deng, Dissertation Supervisor

ABSTRACT

Photocatalytic processes of titanium dioxide have been discovered in the early 1980 and till now titanium dioxide nanomaterials are the most popular photocatalysts for scientific researches and industrial applications. In the environmental engineering field, titanium dioxide nanoparticles have been applied in water treatment such as disinfection of drinking water. It is well known that the photocatalytic efficiency of titanium dioxide nanomaterials is correlated with the total surface area and the optical absorption of the materials themself.

Original titanium dioxide nanomaterials can only be photo-activated with radiations in the ultra violet (UV) spectrum. As UV radiations make up less than 10% of total solar radiation to the earth's surface, the efficiency of original titanium dioxide nanomaterials is therefore limited under direct sunlight. As a result, extensive studies have been carried out to modify original titanium dioxide nanomaterials to achieve

activation in the visible light, and the most popular and effective modification method is doping titanium dioxide with nitrogen.

Titanium dioxide can be in various forms and recent developments have allowed the preparation of novel nanostructures of titanium dioxide nanomaterial. Particularly, the 1-Dimension (1-D) structures including nanorod, nanofiber, and nanotube are of great interest. These structures have not only a large surface area but also geometries that may improve the overall efficiency of titanium dioxide nanomaterials as heterogeneous photocatalyst. Moreover, 1-D titanium dioxide nanomaterials under forms such as mats, foils, and films provide better handling and utilization in term of engineering. As a result, 1-D titanium dioxide nanomaterials are considered as very promising catalyst for industrial applications, including in the environmental engineering field.

To fully capitalize on the advent of titanium dioxide surface doping and new titanium dioxide structures, modification of 1-D titanium dioxide nanomaterials is being widely studied to enable visible light activation. However, current modification methods, particularly nitrogen doping, still have shortcomings. For instance, nitrogen doping of titanium dioxide nanotubes requires high temperature settings or comes with unwanted damage to the 1-D structure.

The primary objective of this doctoral study is to develop novel methods of preparation and modifications of 1-D titanium dioxide nanomaterials for achieving activation with visible light while addressing shortcomings of currently available method.

Two types of 1-D titanium dioxide nanomaterials including nanotube and nanofiber are selected as the research targets. The secondary objective is to explore the possibility of applying the as prepared modified 1-D titanium dioxide nanomaterials in the photocatalytic degradation of hydrocarbon contaminants in water with only visible light as the radiation source. Produced water with aromatic hydrocarbon components are chosen as the model with a view to assess the effectiveness and efficiency of modified 1-D titanium dioxide nanomaterials. Moreover, produced water and oily water represent a large portion of wastewater source in the oil and gas production sector. Therefore it is desirable to develop an effective and sustainable treatment technique for produced water reuse.

In line with the research objectives, the following research activities have been implemented and accomplished: i) preparation, modification and characterization of visible light activated titanium dioxide nanotubes; ii) preparation, modification and characterization of visible light activated titanium dioxide nanofibers; and iii) assessment of the photocatalytic removal of model aromatic hydrocarbons with the modified 1-D titanium dioxide nanomaterials as prepared in visible light.

Titanium dioxide nanotubes were prepared through the popular anodization method with hydroflouride acid and dimethyl sulfoxide (DMSO) as solvent. After the structure being confirmed by SEM, titanium dioxide nanotubes were subjected to treatment by plasma processing techniques with either nitrogen and nitrogen/carbon monoxide as feeding gases. The plasma treated titanium dioxide nanotubes were

characterized by SEM, TEM, XRD, and UV-VIS reflection test. These characterization experiments showed that the plasma treated titanium dioxide nanotubes mostly retain the tubular structure. Titanium dioxide tubes are polycrystalline and anatase was found to be the dominant crystalline form within these nanotubes. The mat of plasma treated titanium dioxide nanotubes showed an increased optical absorption in the visible light. In subsequent photocatalytic experiments with methylene blue, the plasma treated titanium dioxide nanotubes exhibited activation with visible light as desired.

In the second research task, modified titanium dioxide nanofibers were successfully prepared by a novel method based on electrospinning which enables the *in situ* nitrogen doping of nanofibers simultaneously. An electrospinning dope was prepared from titanium isopropoxide, DMSO, acetone and polyacrylonitrile (PAN). The application of PAN was hypothesized to improve the stability of annealed titanium dioxide nanofibers and at same time to provide nitrogen for doping of the nanofibers during the preparation process. After being annealed, titanium dioxide/PAN nanofibers were again characterized by SEM, XRD, and UV-VIS reflection test. These characterizations showed that the annealed titanium dioxide/PAN nanofibers still retain the fibrous shape, with titanium dioxide deposited as "nodules" along fibers. This characteristic greatly increased the total surface area of the material. Anatase was the dominant crystalline form and the increased optical absorption in the visible light suggested that nitrogen doping had taken place as hypothesized. Similarly, subsequent photocatalytic experiments with methylene blue confirmed that annealed titanium dioxide/PAN nanofibers exhibited activation with visible light.

Lastly, the as prepared modified 1-D titanium dioxide nanomaterials were utilized in degradation experiments of aromatic hydrocarbons including Benzene, Toluene, Ethyl benzene and Xylene (BTEX) in water under visible light. The working solution with BTEX component was designed to resemble the produced water from oil and gas production activities. The removal of BTEX was assessed based on the total organic carbon (TOC). Experimental results showed that the as prepared modified 1-D titanium dioxide were able to degrade BTEX components in water via the photocatalytic processes initiated by visible lights. Comparing to current Best Available Techniques (flotation) and Best Possible Techniques (adsorption), it is assessed that treatment techniques of produced water built upon modified 1-D titanium dioxide nanomaterials is promising with high effectiveness and sustainability.

The findings reported in this dissertation have demonstrated the novel methods to prepare visible light-activated 1-D titanium dioxide nanomaterials. Particularly, with the ease in the preparation of N-doped titanium dioxide nanofibers and their high photocatalytic efficiency in visible light as observed, the research results bring up promising opportunities to prepare new types of titanium dioxide nanomaterials which are better suitable for removing harmful contaminants in air and water in environmental engineering applications.

CHAPTER 1

INTRODUCTION

Since the discovery of their photoactivity via the photocatalytic dissociation of water under UV radiation in 1972 (Fujishima and Honda 1972), titanium dioxide (TiO_2) nanomaterials has been attracted a wide interest among research and industry communities as a simple, inexpensive and effective photocatalyst. Other than the application in production of hydrogen from water in the energy field, applications also include the use of the reduction/oxidation processes initiated by these photocatalysts to kill bacteria and pathogens as well as to degrade unwanted contaminants in environmental engineering field (Yu, Yu et al. 2007). During past decades, photocatalytic degradation of a wide range of hazardous substances by advanced oxidation processes based on TiO_2 nanomaterial have been carried out (Chen and Mao 2007), of which the research results had confirmed that TiO_2 nanomaterial is an effective photocatalyst for the decomposition of harmful contaminants commonly found in water and air media.

Attempts of manufacturing and applying TiO_2 nanomaterials at industrial scale have also achieved some successes, such as self-cleaning glass and disinfection of drinking water (Zaleska 2008). However, original TiO_2 nanomaterial can only be activated by ultra-violet (UV) radiation due to its high energy band gap. Since less than 10% of the total solar radiation to the earth's surface is in the UV range, photocatalytic processes mediated by TiO_2 nanomaterial require an anthropogenic UV source. As a result, many efforts have recently been devoted to modify TiO_2 nanomaterial to achieve

activation in the visible light region (Asahi, Morikawa et al. 2001). Notably TiO_2 nanomaterial modified with nitrogen as a dopant is found capable of absorbing and activating with visible light (Asahi and Morikawa 2007; Yu, Yu et al. 2007). Several other elements such as carbon, sulfur, vanadium, and lanthanum have been reported to show similar effect when being doped into TiO_2 nanomaterial (Chen and Mao 2007). Nevertheless, the nitrogen doping process was found to be an efficient process due to the availability, low-cost, and diversity of substances available for doping.

In another aspect, the scientific communities are focusing on the development of new structures of TiO_2 nanomaterials. The first and most popular type of TiO_2 nanomaterial is nanoscaled particles, which is being manufactured at an industry-wide scale today. Despite of being inexpensive and possessing a large surface area important for photocatalytic efficiency, however TiO_2 nanoparticles have some limitations in engineering applications. For example, separation step is usually required to remove the photocatalyst from the working media. Therefore it is desirable to have other structures of TiO_2 nanomaterial to improve the applicability of this photocatalyst. Recent developments in this field have resulted in many types of TiO_2 nanomaterial such as nanotubes, nanowires, nanosheets and nanorods (Chen and Mao 2007).

While the two important aspects mentioned above are being studied actively, the applications of modified TiO_2 nanomaterials with novel structures have not been fully explored for water treatment. The goal of this study is to synthesize and characterize the visible light activated TiO_2 nanomaterials by using nitrogen as dopants, particularly those

nanofibers and nanotube having 1-dimension structures. The visible light absorption and high photocatalytic efficiency of modified TiO_2 nanomaterials will be evaluated based on their ability for the degradation of aromatic hydrocarbons benzene, toluene, ethyl benzene and xylene (BTEX) commonly found in petroleum products.

Petroleum hydrocarbons were selected in this study because they are generally considered important pollutants to the environment. With the continuous production and utilization of fuels and petrochemicals in the human society, petroleum hydrocarbons are being discharged to air, water and soil. Being hazardous compounds to public health, many petroleum hydrocarbons, particularly aromatic fractions, are strictly regulated. The maximum concentration limits (MCLs) in drinking water, as regulated by the U.S. Environmental Protection Agency (EPA), are 0.005, 1.0, 0.7, and 10 ppm, respectively, for benzene, toluene, ethyl benzene and xylene (BTEX) (Office of Ground and Drinking Water 2006). Such regulations call for effective and efficient environmental engineering processes for their treatment.

In this research, BTEX act as model contaminants for testing the effectiveness and efficiency of modified 1-D TiO_2 nanomaterials prepared with novel methods. The research presented in this dissertation also serve as an integral part of our long-term goal to prepare solid thin-film and nano-structured photocatalysts with a superior quantum yield and explore their environmental applications such as degradation of petroleum hydrocarbons, disinfection of treated municipal wastewater prior to final discharge to rivers and lakes, and destruction of indoor air pollutants.

The organization of this dissertation includes 7 chapters with Chapter 1 being this Introduction. Chapter 2 is a literature review on titanium dioxide nanomaterial as a photocatalyst, including the fundamental operating principles, preparations, applications, and recent trends in modification of nanoscale titanium dioxide to achieve activation with visible light. A brief introduction on plasma treatment and electrospinning techniques is also provided. Chapter 3 provides descriptions of related research tasks and activities, including techniques, instrument, and materials that are used to accomplish the proposed research. Detailed research implementation and experimental results are provided in Chapters 4, 5 and 6. Finally, Chapter 7 provides the summary of the dissertation, and personal perspective and recommendation for future works in the area.

REFERENCES

Asahi, R. and T. Morikawa (2007). "Nitrogen complex species and its chemical nature in TiO_2 for visible-light sensitized photocatalysis." Chemical Physics **339**(1-3): 57-63.

Asahi, R., T. Morikawa, T. Ohwaki, K. Aoki and Y. Taga (2001). "Visible-light photocatalysis in nitrogen-doped titanium oxides." Science **293**(5528): 269-271.

Chen, X. and S. S. Mao (2007). "Titanium dioxide nanomaterials: Synthesis, properties, modifications and applications." Chemical Reviews **107**(7): 2891-2959.

Fujishima, A. and K. Honda (1972). Nature **37**: 238-245.

Office of Ground, W. and O. W. Drinking Water (2006). "Drinking Water Contaminants." from http://www.epa.gov/safewater/contaminants/index.html#listmcl.

Yu, H., J. Yu and B. Cheng (2007). "Photocatalytic activity of the calcined H-titanate nanowires for photocatalytic oxidation of acetone in air." Chemosphere **66**(11): 2050-2057.

Zaleska, A. (2008). "Doped-TiO2: A review." Recent Patents on Engineering **2**(3): 157-164.

CHAPTER 2

BACKGROUND INFORMATION

2.1. TITANIUM DIOXIDE AND PHOTOCATALYTIC PROCESSES

2.1.1. General information of titanium dioxide

Titanium dioxide (TiO_2) in the crystal forms is known as photoactivated semiconductor. The crystal form of TiO_2 is consisting of chains of TiO_6 octahedra in which each Ti^{4+} cation is surrounded by six O^{2-} anions. Two major crystalline structures of TiO_2 are rutile and anatase. In rutile, each octahedron of TiO_6 connects with ten neighbor octahedrons. In anatase, each octahedron of TiO_6 connects with eight neighbor octahedrons. Anatase is a more common form in fine grain samples including both natural and synthetic sources. When heating, anatase transforms to rutile, a more stable form at high temperature. The band gap of bulk TiO_2 is 3.0 eV for rutile and 3.2 eV for anatase (Linsebigler, Lu et al. 1995; Yu, Yu et al. 2007; Fujishima, Zhang et al. 2008). Brookite with an orthorhombic structure, is the third type of TiO_2 structure. However, it is rarer and more difficult to prepare (Fujishima, Zhang et al. 2008), so has limited use as a photocatalyst (Chen and Mao 2007). Illustrations of 3 crystal structures of TiO_2 are provided in Fig 2.1 (Pelaez, Nolan et al. 2012).

a

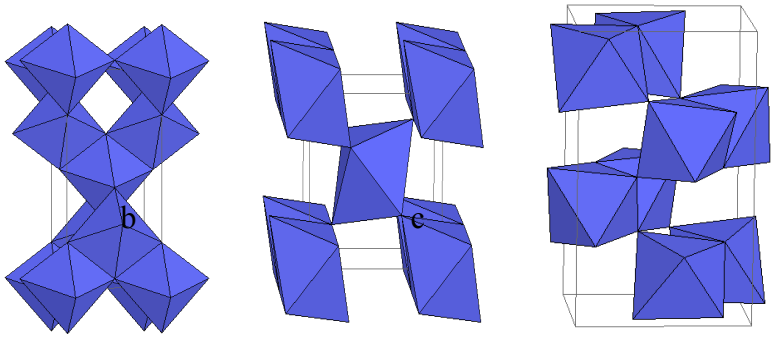

Figure 2.1. Crystal structures of titanium dioxide

a) Anatase; b) Rutile; c) Brookite

When TiO_2 crystallite particles absorb photons with energy higher than the band gap, electrons are excited from the valence band into the conduction band. This activation process leads to the creation of positive holes in the valence band. These charges can be recombined at trap sites or react with electron donor and acceptors absorbed at the particle surface. These fundamental processes can be expressed as follows (Linsebigler, Lu et al. 1995; Szczepankiewicz, Colussi et al. 2000; Emilio, Litter et al. 2006):

$$TiO_2 + hv \rightarrow e^- + h^+ \quad (1)$$

$$e^- + Ti(IV)O\text{-}H \rightarrow Ti(III)O\text{-}H^-(X) \quad (2)$$

$$h^+ + Ti(IV)O\text{-}H \rightarrow Ti(IV)O^-\text{-}H^+(Y) \quad (3)$$

$$h^+ + H_2O \rightarrow {}^{\cdot}OH + H^+ \quad (4)$$

$$h^+ + OH^- \rightarrow {}^{\cdot}OH \quad (5)$$

$$e\text{-} + O_{2,s} \rightarrow O_{2,s}^- \quad (6)$$

$$O_{2,s}^- + H^+ \rightarrow HO_{2,s} \quad (7)$$

$$h^+ + Ti(III)O\text{-}H^- \rightarrow Ti(IV)O\text{-}H \quad (8)$$

$$e^- + Ti(IV)O^{\cdot}\text{-}H^+ \rightarrow Ti(IV)O\text{-}H \quad (9)$$

$$O_{2,s} + Ti(IV)O^{\cdot}\text{-}H^+(Y) \rightarrow Ti(IV)O\text{-}H + O_{2,s} \quad (10)$$

The competition among those processes listed above determines the overall efficiency of photocatalytic applications of TiO_2. Reaction (1) is the starting point where a pair of electron-hole is generated. The generated electrons and holes then transport to the defect sites and are trapped by hydroxyl groups at the surface of TiO_2 particle through reactions (2) and (3). At the surface, these charges react with water and dissolve oxygen to form free hydroxyl radical $^{\cdot}OH$ and hydroperoxyl radical HO_2 as demonstrated in reactions (4) to (7). Reactions (8) to (10) illustrate recombination processes of electrons and holes at the surface of TiO_2 particle. The free hydroxyl radicals $^{\cdot}OH$ and hydroperoxyl radical HO_2 created from reactions (4-7) have high oxidation potential and are the principal agents oxidizing organic compounds via chain reactions for environmental engineering application (Yu, Yu et al. 2007). For example, ethanol is oxidized by $^{\cdot}OH$ as follows (Kwon, Fan et al. 2008):

$$CH_3CH_2OH + {}^{\cdot}OH \rightarrow CH_3C^{\cdot}HOH + H_2O \quad (11)$$

$$CH_3C^{\cdot}HOH + O_2 \rightarrow CH_3CH(OH)OO^{\cdot} \quad (12)$$

$$CH_3CH(OH)OO^{\cdot} + CH_3CH_2OH \rightarrow CH_3CH(OH)OOH + CH_3{}^{\cdot}HOH \quad (13)$$

$$CH_3CH(OH)OOH \rightarrow CH_3CHO + H_2O_2 \quad (14)$$

It should be noted that from reaction (14) H_2O_2 then can disintegrate and form two new free radicals of $^{\cdot}OH$, which enter the oxidative chain reaction subsequently. As a result, new $^{\cdot}OH$ radicals are supplied and the oxidation process is continuing until ethanol and organic intermediates are completely oxidized.

While the above oxidation reaction chain occurs inside the volume of one material phase, free holes that have positive charges on the surface of TiO_2 particle also act as oxidation sites. Because of the high surface area of TiO_2 particles, organic molecules in aqueous phase are attracted to TiO_2 solid surface. Consequently absorbed molecules donate electrons to positive holes and are oxidized at the interface of liquid-solid phases. Based on these processes, TiO_2 nanomaterials are applied as cleaning agents towards contaminants in air and water media when appropriate radiation conditions are provided. The overall decontamination process can be illustrated in Fig 2.2 below.

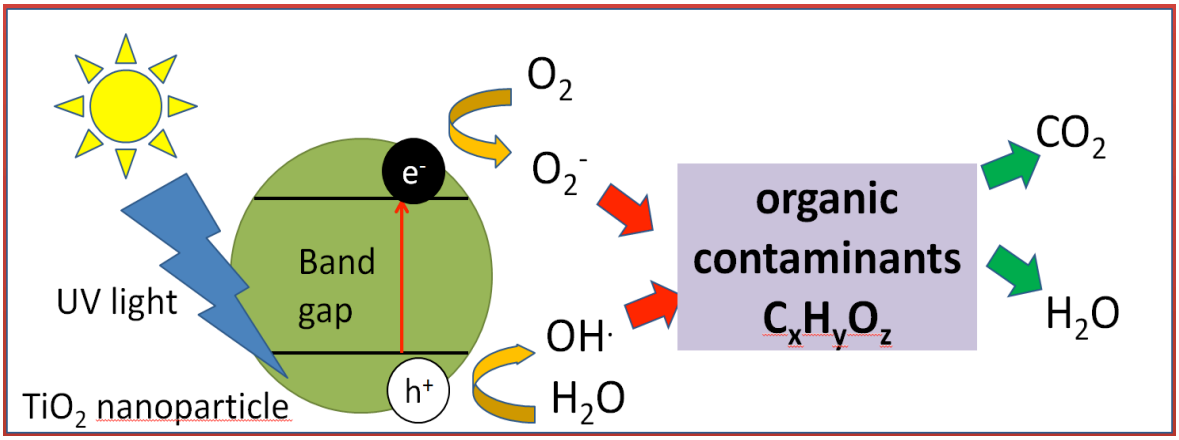

Figure 2.2. A simple illustration of photocatalytic processes of titanium dioxide nanomaterial for degradation of organic contaminants

2.1.2. Applications of titanium dioxide nanomaterials in environmental engineering

Among photocatalysts, TiO_2 has attracted by far the most attention of scientist and engineering communities. With the high oxidation potential of the positive hole and hydroxyl $^{\cdot}OH$ radicals as described above, the photocatalytic process induced by TiO_2 is capable of oxidizing a wide range of contaminants in water and air. Not only of showing a high photocatalytic activity, TiO_2 also has numerous advantages including chemical inertness, non-toxicity, mechanical stability and inexpensiveness.

To date, industrial applications of TiO_2 in the environmental engineering field include disinfection of microorganisms, control of odor, conversion of NOx, removal of mercury, conversion of SO_2, and particularly degradation volatile organic compounds (VOCs) (Kwon, Fan et al. 2008). Photocatalysts based on TiO_2 are still being developed to enhance the efficiency, as well as to reduce the energy consumption, to offer more sustainable and economical pollution control measures for air and water.

2.1.3. Significance of 1-dimensional titanium dioxide nanomaterials

The widely accepted definition of 1-Dimension (1-D) object is that an object has 1 dimension significantly larger than the other. Based on this definition, 1-D structures may include tube, column, long rod, and fiber. These structures not only provide high surface effective surface area but also well-defined geometrical patterns resulting from their unique geometrical characteristics. For a heterogeneous photocatalyst such as TiO_2

nanomaterial, the two features provided with 1-D structures listed above are considered as advantages that can greatly improve the efficiency of the photocatalytic processes (Pelaez, Nolan et al. 2012). More importantly these 1-D structures are usually built with fixed supporting substrates in the form of a solid thin film or a non-woven mat, which shall provide technical advantages in incorporating heterogeneous catalysts into the reactor. This is in contrast with particles used in powder forms, as suspensions. Application of solid catalysts in fine powder form usually requires extra separation steps in engineering applications, particularly in processes in aqueous phase. The application of 1-D structured materials with fixed and sizeable supporting substrates will not require such step and therefore provide a better engineering option.

As a result, many attempts have been made to prepare 1-D TiO_2 nanomaterials, such as nanotube, nanorod and nanofiber, and many of them have exhibited high photocatalytic efficiency (Macak, Tsuchiya et al. 2007). It is envisioned that modified 1-D TiO_2 nanomaterials with enhanced ability for visible light absorption may find wide environmental applications such as degradation of organic contaminants in produced waters associated with gas and oil production, cleanup of gasoline spills in surface water, disinfection of treated municipal wastewater prior to final discharge to rivers and lakes, and destruction of indoor air pollutants (e.g., aldehyde). In this study, we will focus on the synthesis and characterization of the materials, and demonstrate their potential environmental applications using produced water degradation as an example.

2.2. MODIFICATION OF TITANIUM DIOXIDE NANOMATERIALS TOWARDS VISIBLE LIGHT-ACTIVATED PHOTOCATALYST

2.2.1. Overview

Ultra-violet (UV) radiations in the solar radiation are strongly absorbed by the atmosphere before reaching the earth surface. As a result, UV radiations account for only ~10% of the total solar energy at the earth surface (Chen and Mao 2007). The fraction that has the highest energy throughput in solar radiation is the visible light section with wavelength 460-500nm (Asahi, Morikawa et al. 2001) as showed in Fig 2.3.

As original TiO_2 nanomaterials can only absorb UV radiation, the photocatalytic activity of TiO_2 is limited. In order to improve the efficiency, modifications of TiO_2 are highly sought after with the goal of reducing the high band gap and enabling TiO_2 to activate photoactivity with visible lights (Anpo 2000). The recent methods are (Yu, Yu et al. 2007; Zaleska 2008): i) doping TiO_2 crystals with atoms of other elements; ii) sensitizing TiO_2 nanomaterials with dyes or metal nanoparticles and iii) coupling collective oscillation of the electrons in conduction bands at particles surface between TiO_2 and another metal element. Among them, the doping process with various metallic and non-metallic elements plays the most important role in modifying TiO_2 for visible-light activation.

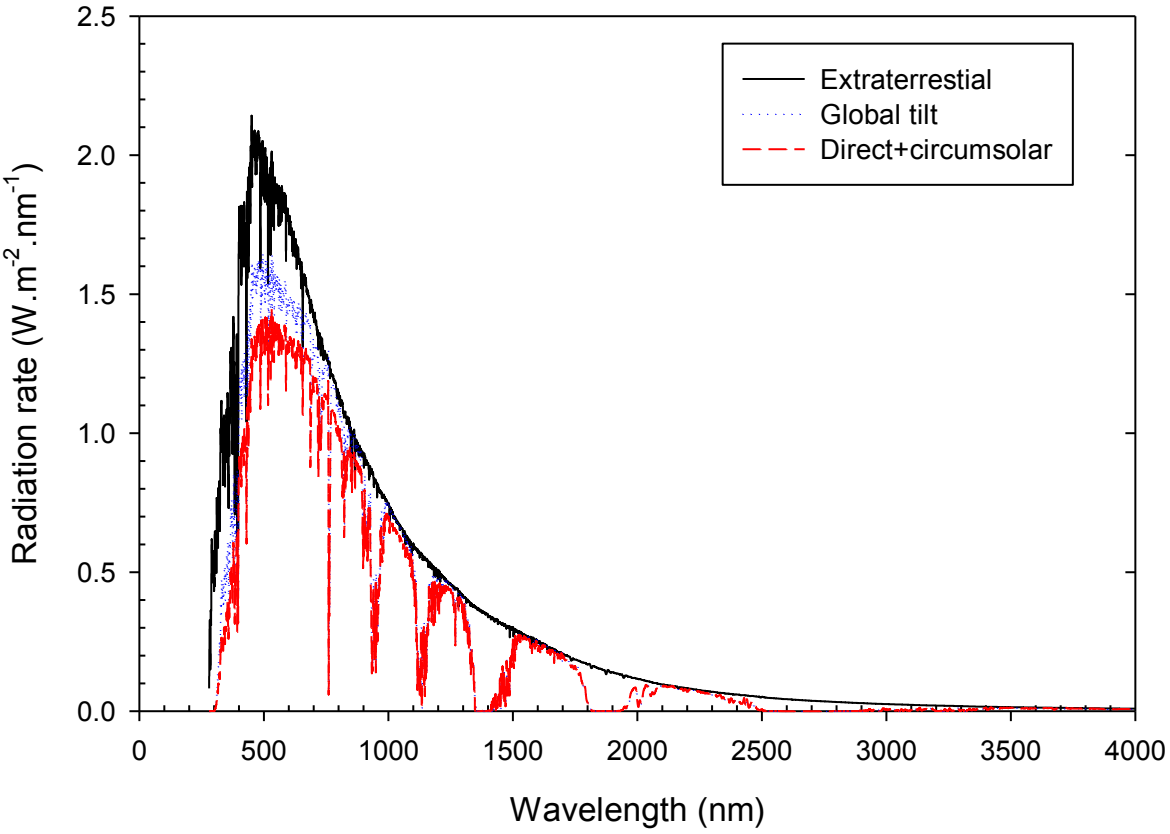

Figure 2.3. Standard solar spectrum according to ASTM G-173-03 (ASTM).

(Plot is reconstructed from tabular data)

2.2.2. Metal and non-metal doping of titanium dioxide

Doping method involves a partly substitution of other elements for Ti^{4+} or O^{2-} ions in TiO_2 crystal structure. Ti^{4+} is reported as easier to be replaced by transition metals and O^{2-} is more difficult to be substituted (Burda, Lou et al. 2003; Chen, Lou et al. 2003). After doping, the chemical composition of the material is altered, leading to changes in electronic properties, of which some can favor the desire of narrowing of the band gap.

Electronic structures in doped materials are analyzed by ab initio band calculations with the full-potential linearized augmented plane wave (FLAPW) method (Asahi, Morikawa et al. 2001; Umebayashi, Yamaki et al. 2002; Umebayashi, Yamaki et al. 2002). Based on theoretical calculations, band gap narrowing of TiO_2 have been reported as possible with both metallic and non-metallic dopants as illustrated in Fig 2.4 and Fig 2.5 respectively.

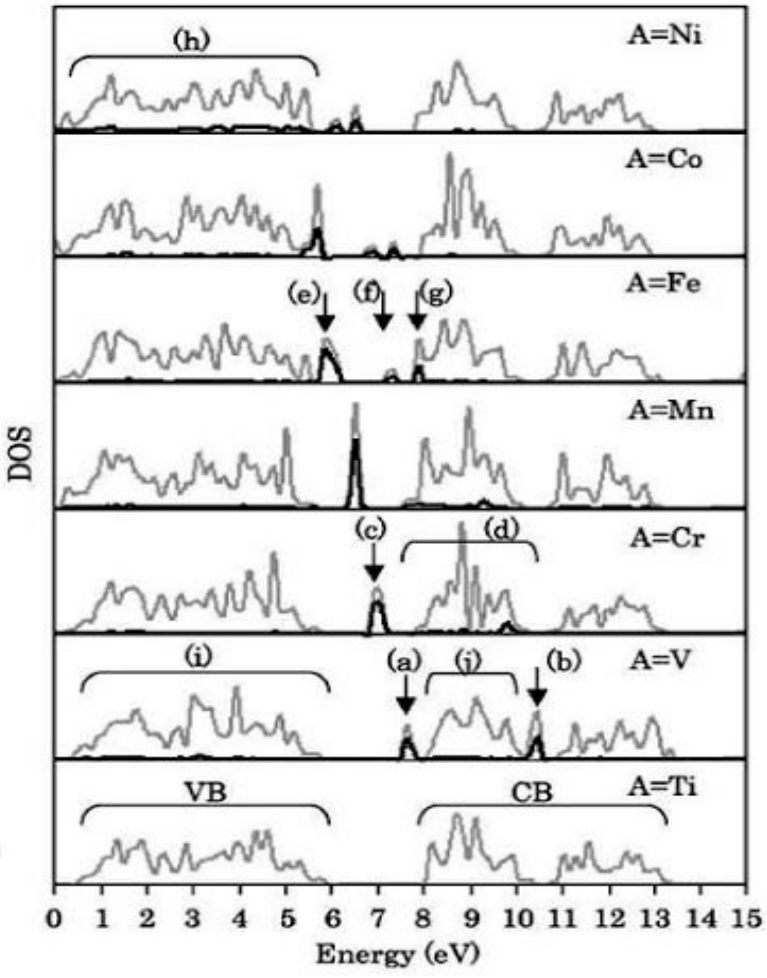

Figure 2.4. Density of States (DOS) of metal doped TiO_2 calculated by FLAPW. Gray solid line represents total DOS and black solid line represents DOS of dopants (Umebayashi, Yamaki et al. 2002).

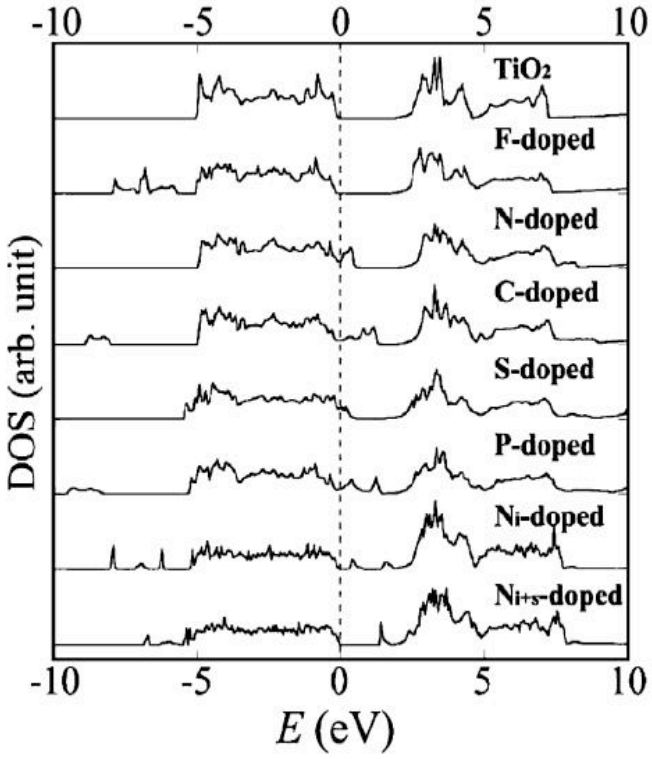

Figure 2.5. Density of States (DOS) of non-metal doped TiO_2 calculated by FLAPW

(Asahi, Morikawa et al. 2001)

Experimental results have confirmed these predictions, for example Li et al found Ni^{3+} can reduce TiO_2 band gap as much as 0.55 eV (Li, Wang et al. 2003) and Nakano et al found N-doping produce two deep levels at approximately 1.18 and 2.48 eV below the conduction band of TiO_2 (Nakano, Morikawa et al. 2006). With such changes in electronic structures, absorption of visible light was observed in metal-doped and non-metal-doped TiO_2 nanomaterials (Yu, Yu et al. 2007). Transitional metal ions including V, Cr, Mn, Fe and Ni were found to cause large shift in the absorption band towards visible light region (Anpo 2000; Anpo 2000; Anpo, Kishiguchi et al. 2001; Anpo and Takeuchi 2001; Anpo and Takeuchi 2003). Optical absorptions of N- and S-doped TiO_2

nanomaterials were in the range of 400-500 nm and 400-600 nm respectively (Ohno, Akiyoshi et al. 2004; Lin, Orlov et al. 2005). In most of cases, improvement of photocatalytic efficiency was also observed (Yu, Yu et al. 2007) but not all metal-doped TiO_2 nanomaterials exhibit higher photocatalytic activities than pure TiO_2, V-doped TiO_2 for example, showed reduced activity on the photooxidation of 4-chlorophenol (Martin, Morrison et al. 1994).

The subjects of this research are carbon and nitrogen doped 1-D TiO_2 materials, and the rationale to focus on these elements is detailed below.

2.2.3. Nitrogen and carbon doping of titanium dioxide

In 2001, Asahi et al applied FLAPW method to calculate potential band gap narrowing features in anatase when doped with various non-metals including carbon, sulfur, phosphorus and fluorine. The substitution of carbon and nitrogen for O^{2-} ions in the crystal structure was predicted as capable of band gap narrowing as showed in Fig, 2.5 above. In term of electron configuration, carbon and nitrogen has 2 and 3 electrons respectively in the outer 2p state, and the narrowing of TiO_2 band gap is found to be resulted from the mixing of 2p states of nitrogen and carbon atoms with 2p state of oxygen ions within the crystal structure. This mixing of 2p states, while is well screened and barely interacts with the band states of TiO_2, give rise to the bonding states below the oxygen 2p valence bands as well as antibonding states deep in the band gap, resulting in narrowing of the energy gap (Asahi, Morikawa et al. 2001; Umebayashi, Yamaki et al. 2002).

Moreover, from calculations showed in Figure 2.3 above, nitrogen doping is considered as one of the most effective dopant for TiO_2. Because not only the band gap of TiO_2 is narrowed, the p-states of nitrogen also well overlap with band states of TiO_2, which enables electrons to transit from the valence band to the conduction band, leaving holes inside the TiO_2 bulk and initiating the photocatalytic processes.

The nitrogen doped (N-doped) TiO_2 materials were then prepared by sputtering TiO_2 anatase powder in nitrogen/argon gas mixture and annealed at 550^{o}C in nitrogen atmosphere for 4 hours (Asahi, Morikawa et al. 2001). Optical absorption of the doped sample were significantly improved in visible lights having wavelength < 500 nm comparing to original TiO_2 as depicted in Fig 2.6. Improvement on photocatalytic efficency was also observed in the degradation of methylene blue and gaseous acetaldehyde.

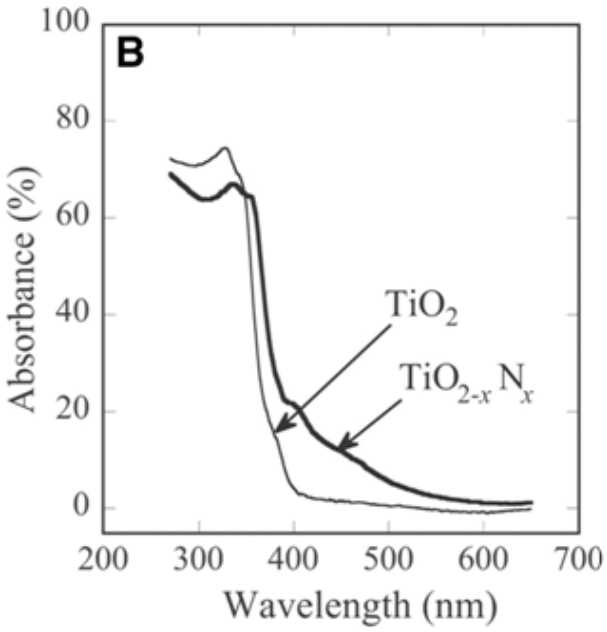

Figure 2.6. Red shift in optical property of N-doped TiO_2 nanomaterial
(Asahi, Morikawa et al. 2001)

Other studies found that the significant increase in photoactivity is due to the formation of O-Ti-N bondings inside crystal structure (Chen, Lou et al. 2004; Chen, Low et al. 2005). With the observed increase of electron trapping sites (Ti^{3+}) and oxygen vacancies, higher photocatalytic oxidation performance in degradation of a wide range of organic compounds in visible lights was found mainly through water intermediates (Nakamura, Tanaka et al. 2004) (see reactions (11) and (12) above).

Reproducible results on N-doped TiO_2 anatase nanoparticles and other nanomaterials were reported by other groups later (Asahi and Morikawa 2007). Other than the sputtering method that carried out by Asahi group, N-doped TiO_2 nanoparticles were prepared by various methods such as hydrolysis of TIIP in a water/amine mixture and post treatment of TiO_2 gel with amine (sol-gel method) (Burda, Lou et al. 2003; Chen, Low et al. 2005), ball milling of TiO_2 in NH_3 solution (Chen, Chen et al. 2005), heating TiO_2 nanoparticles under NH_3 flux at 500-600^oC (Diwald, Thompson et al. 2004; Nakamura, Tanaka et al. 2004), and by mildly oxidating TiN under control conditions.

Similarly, carbon doped (C-doped) TiO_2 nanomaterials have been prepared mostly via heating TiO_2 nanomaterials with a carbon substrate such as activated carbon and carbon nanotube (Chen and Mao 2007), or processing TiO_2 nanomaterials in an environment containing only methane CH_4. Co-doping of carbon and nitrogen to TiO_2 nanomaterial has been achieved by heating TiO_2 nanomaterials with urea (Rengifo-Herrera, Kiwi et al. 2009).

For 1-D TiO_2 nanomaterials, however, available carbon and nitrogen doping methods are limited, particularly for 1-D TiO_2 in forms of self-ordered nanotubes and nanofibers, the two research subjects of this dissertation. The most common doping method is to heat the nanomaterial in the presence of dopant. Beside of consuming a lot of energy, this method will destroy the polymer substrate in the case of TiO_2 nanofiber, resulting in nanofibers with low mechanic strength, which are easily broken in applications, so the desirable 1-dimensional characteristics are lost (Kim, Cho et al. 2010). In case of the TiO_2 self-ordered nanotubes, a common method of doping is ion implantation, which has been found to convert TiO_2 anatase crystals into amorphous TiO_2, which do not have photocatalytic effect, and damage the self-ordered nanotube structures. As a result, subsequent heat treatments were needed to reconvert amorphous TiO_2 into crystallite forms to reactivate photocatalytic effect. Nevertheless, the damage to the self-ordered nanotube structures was not reversible (Ghicov, Macak et al. 2006).

In this research, we propose to investigate the possible carbon and nitrogen doping at significantly lower temperature settings. For TiO_2 nanofiber, we propose to use a thermal resistant polymer containing carbon and nitrogen as fiber substrate for the electrospinning/annealing process; and use non-thermal plasma treatment technique for TiO_2 nanotubes. From our knowledge, these are the first attempts to modify the TiO_2 nanofiber and the self-ordered TiO_2 nanotubes respectively with these two modification techniques.

2.3. ELECTROSPINNING AND ELECTROSPINNING TECHNIQUES

2.3.1. Overview

The overall operating principle of electrospinning process is illustrated in Fig. 2.7. It is widely known that electrospinning is a process that produces fibers with diameters ranging from nanoscale to microscale by pushing a liquid jet through an opening such as a needle tip under the influence of an electrostatic field. Conventionally, when a liquid droplet at the tip of the needle is electrostatically charged by a high voltage, the combination of electrostatic repulsion and the surface tension will result in the formation of the well-known Taylor cone. When the whole system reaches the critical point, from the apex of the Taylor cone a single fluid jet is ejected. As the jet accelerates and dries during the flight in the electrostatic field, the jet becomes thinner and elongated until it is deposited on the collector (usually a conductive metal foil as target for electrospinning), resulted in a solid fiber. The diameter of the fiber can be in the range of nanometers, depending on the opening diameter of the needle tip, the electrostatic field, and the distance from the tip to the collector (target).

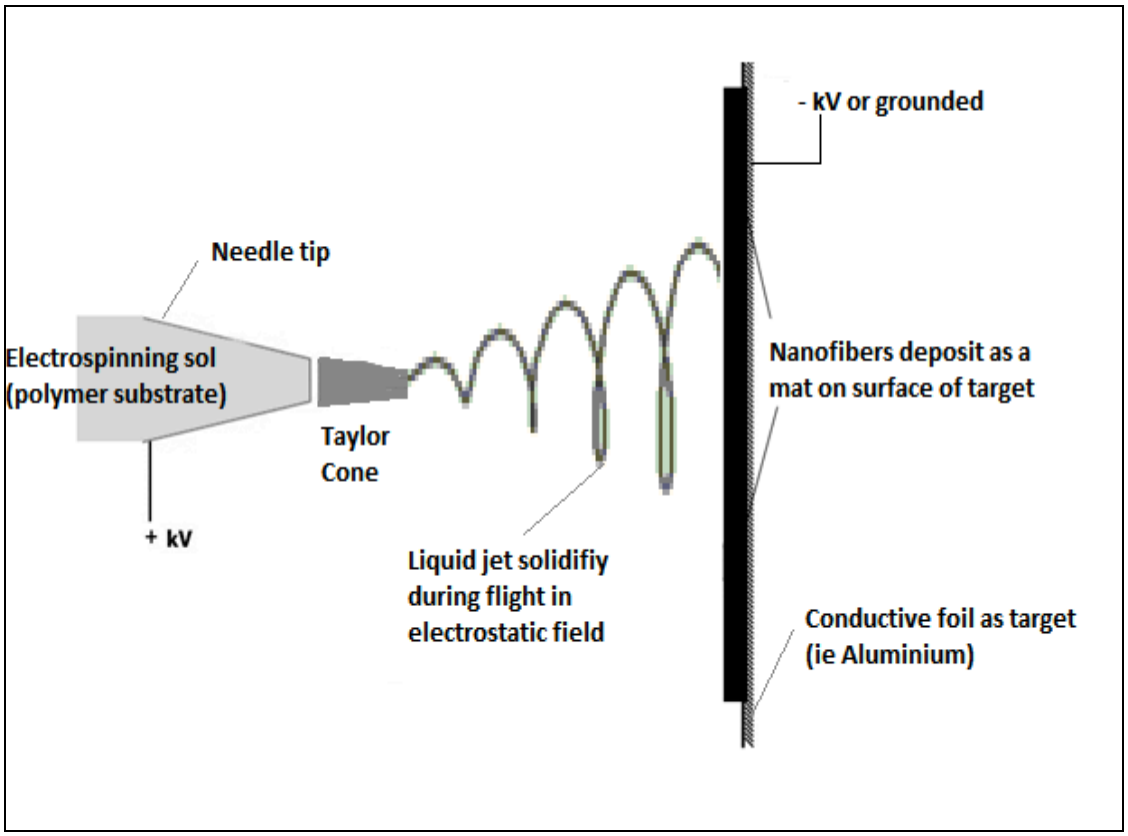

Figure 2.7. Principle of electrospinning process

With a diversity of polymers and solvents that can be used as feedstock, the electrospinning process has been widely applied to prepare non-woven plastic fabrics with different wettability and biocompatibility for various uses in engineering and biomedical applications. Moreover, recent developments in sol-gel chemistry have facilitated the electrospinning process to be capable of preparing solid ceramic / metal oxide nanofibers. In one conventional preparation, a sol containing a suitable polymer, solvent and metal oxide precursor is spun with electrospinning process to form nanofibers, which then subject to various chemical processes for the metal oxide to precipitate as solid nanomaterial while still retaining the fibrous shape inherited from the original substrate (Chandrasekar, Zhang et al. 2009).

In accordance to the conventional preparation of metal oxide nanofibers as mentioned above, TiO_2 nanofiber have been prepared by electrospinning processes with Ti precursors including titanium tetrachloride (Qiu and Yu 2008), titanium isopropoxide (Li and Xia 2003), titanium butoxide (Chandrasekar, Zhang et al. 2009), and even titanium dioxide nanoparticles (P25 Degussa) (Im, Kim et al. 2008). The most common polymer utilized among these preparations is polyvinylpyrrolidone (PVP) which has the chemical formula as follows.

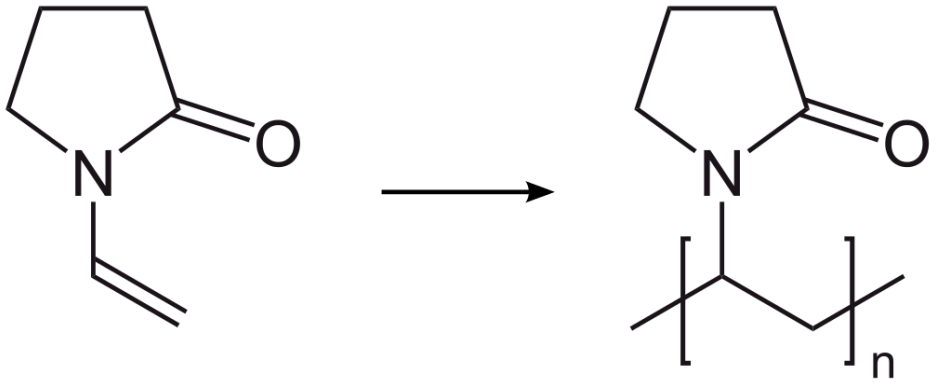

PVP monomer **PVP polymer**

PVP is soluble in water, ethanol and acetone, and have low toxicity with good spun-ability by electrospinning. These characteristics explain for the wide use of PVP in preparation of TiO_2 nanofibers by electrospinning processes. Other than PVP, other tested polymers include polyvinyl alcohol (PVA) (He and Gong 2003) and polyvinylidene flouride (PVDF) (Song, Kim et al. 2005). The preparation of TiO_2 nanofiber following this route has been found to be straightforward and effective. Moreover, it has been reported that by adding ions of other metallic elements as dopants

into the electrospinning sol, cobalt for example, a doped TiO_2 nanofiber can be acquired, which showed enhanced photocatalytic efficiency in the visible light region in accordance to the literature review as mentioned in section 2.2.2 above (Jia, Xie et al. 2007).

Other than using direct crystalized TiO_2 as precursor, the nanofibers prepared with the electrospinning processes always contain TiO_2 under amorphous form, which then need to be annealed at temperature > 500^oC to be converted into crystallized forms of anatase and rutile in order to exhibit photocatalytic effects. PVP with melting point of 150-180^oC, as well as other polymers currently used in preparing of TiO_2 nanofibers via electrospinning processes are not resistant to such high annealing temperature and therefore destroyed during the annealing process. Such treatment process results in mechanically unstable nanofibers, which are easily broken into smaller rods in utilization (Kim, Cho et al. 2010). In our research, we seek to enhance the mechanical properties of prepared TiO_2 nanofibers and at the same time modify them with carbon and nitrogen as dopants in order to achieve activation under visible lights and improve their photocatalytic efficiency.

2.3.2. Electrospinning techniques

The conventional and most common electrospinning technique is to utilize one syringe with steel needle connected to a high voltage DC power supply. The collector is a fixed metal foil which is also grounded. In some experiments, the fixed metal foil is

replaced by a constantly rotating metal drum for the purpose of achieving better distribution of nanofibers deposited on the collector surface (Chandrasekar, Zhang et al. 2009). Moreover, two or more electrospinning systems can target one collector for co-spinning different nanofibers into one mat (Kim, Cho et al. 2010).

The most recent development in the electrospinning techniques is the application of coaxial co-spinning system. The setup of this technique is illustrated in Fig.2.8 as below.

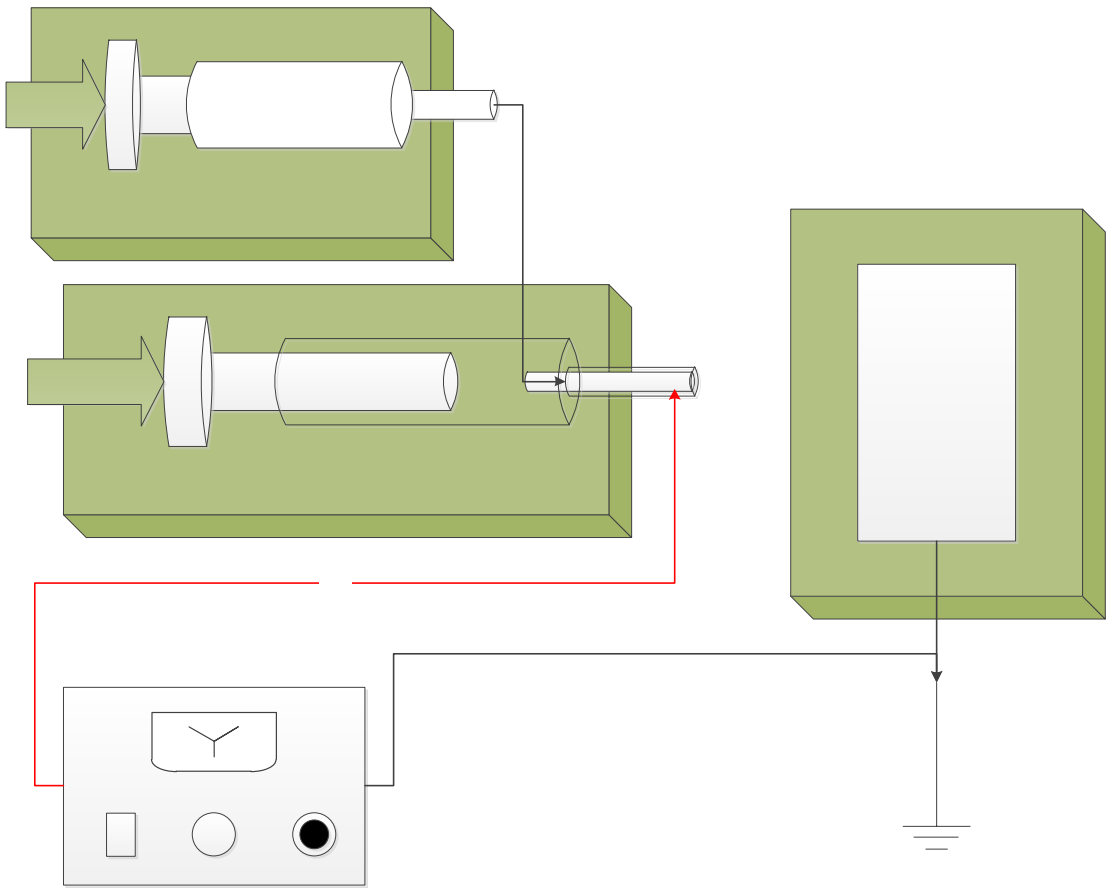

Figure 2.8. Coaxial co-spinning electrospinning technique setup

In a typical setup, the electric output is attached to the needle of primary syringe. Each syringe contains different materials which are immiscible to each other. With this setup, the secondary syringe provides a secondary liquid flow coaxially to the primary flow to the needle of primary syringe and both liquid are pull out together in one jet during the electrospinning process. As the resulted, the collected fiber will have the outer layer made of substrates of primary syringe, and the inner core made of substrates of secondary syringe. If this inner core is removed, the hollow nanofibers are acquired. This technique has been applied successfully by to prepare hollow TiO_2 nanofibers (Li and Xia 2004).

2.4. PLASMA CHEMISTRY AND PLASMA TREATMENT TECHNIQUES

2.4.1. Overview

Plasma is termed as the fourth state of matter, in which matters present under the form of ionized gases. In plasma, electrons and ions are balanced in number and the whole environment is neutral in term of charge, but these free particles make plasma electrically conductive, internally interactive, and strongly responsive to electromagnetic fields (Fridman 2008).

Man-made plasma in the laboratory and industry occur under a wide range of pressures, electron temperatures, and electron densities. Fig 2.9 below depicts the types of plasma depending on the electron densities and temperatures.

In engineering term, non-thermal plasmas are those generated at either low temperature or lower power levels. In many non-thermal plasma systems, electron temperature is about 1-3eV (1eV is approximate 11,600K), while the gas temperature is close to room temperature (Lieberman 2005; Fridman 2008). On the other hand, thermal plasmas are more powerful, having much -higher temperature and pressure. The glow discharge, which is the subject in our proposed research, is considered as the non-thermal plasma because it is created at the room temperature with low power input. Moreover, glow discharge can be created with either direct current (DC) driven electrodes or with radio frequency (RF) driven electrodes. With the RF plasma discharge system, the frequency of 13.56 MHz is common in industrial and laboratory practices.

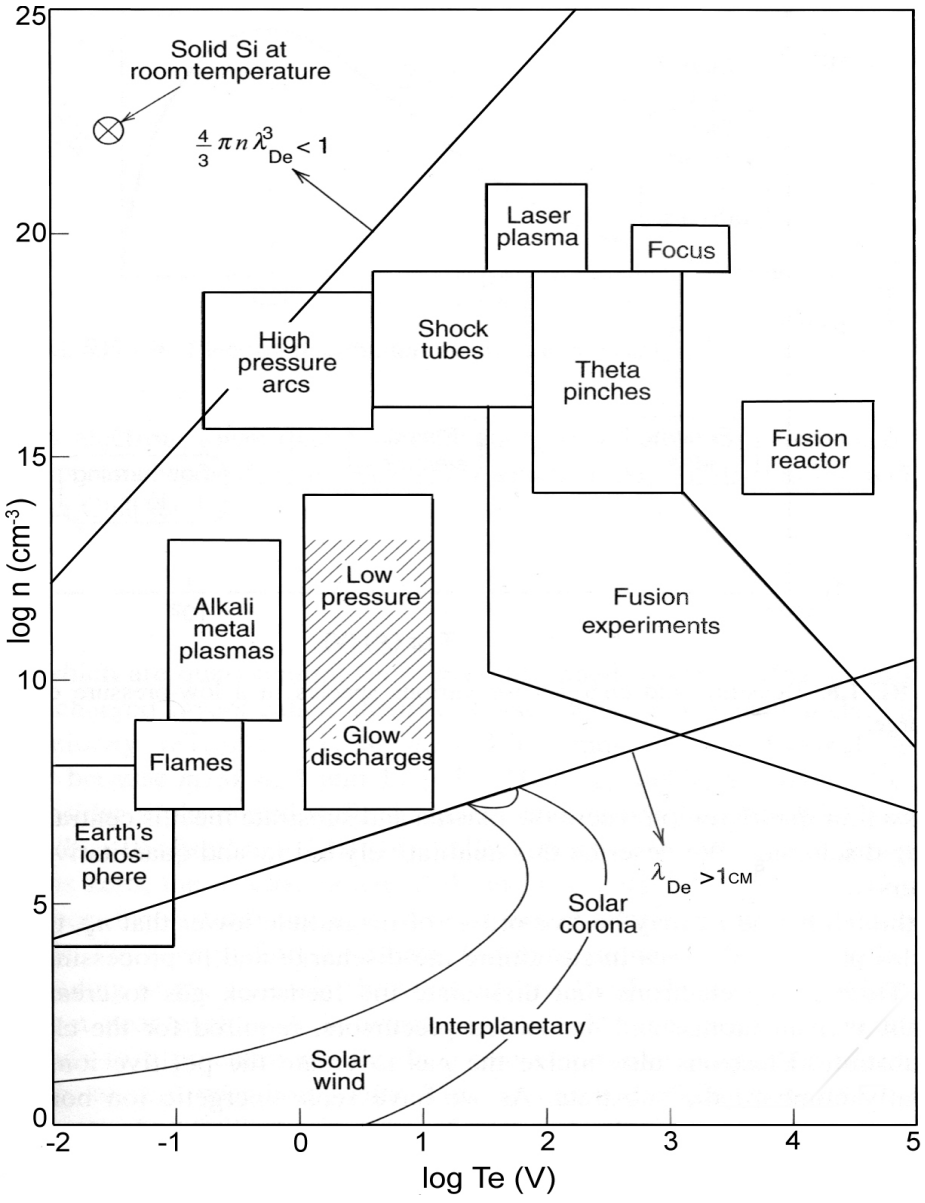

Figure 2.9. Space and laboratory plasmas based on concentrations and temperature of charged particles

(Lieberman 2005)

Chemically, plasma is a very reactive environment due to large concentrations of charged particles, excited atoms, free radicals, and photons. Moreover, such concentrations can often exceed those at the quasi-equilibrium systems by many orders of

magnitude at the same gas temperature (Fridman 2008). Furthermore, parameters of plasma can be controlled via pressure, temperature, and energy input, resulting in a good control of desired chemical reaction in term of direction and selectiveness.

2.4.2. Plasma treatment techniques

Plasma treatments are widely used in the industry to prepare and modify solid materials, particularly for thin solid films of micro- and nano-structured materials commonly used in electrical, electronic and mechanical devices. While there are many plasma processes available, ranging from sputtering deposition to polymerization, these processes can be categorized in three principal techniques. They are deposition, implantation and etching as briefly described below.

Plasma deposition technique

Plasma deposition techniques are used to deposit a thin film of solid material to the surface of a "substrate". The common methods are sputtering and plasma enhanced chemical vapor deposition (PECVD).

In the sputtering technique, an inert gas, argon for instance, is employed for making the plasma. When colliding with the target material inside the plasma environment, excited argon atoms with high kinetic energy sputter particles out of the

target, then these particles deposit to the substrate surface, creating a thin solid film. As a result, sputtering technique involves in mainly physical processes.

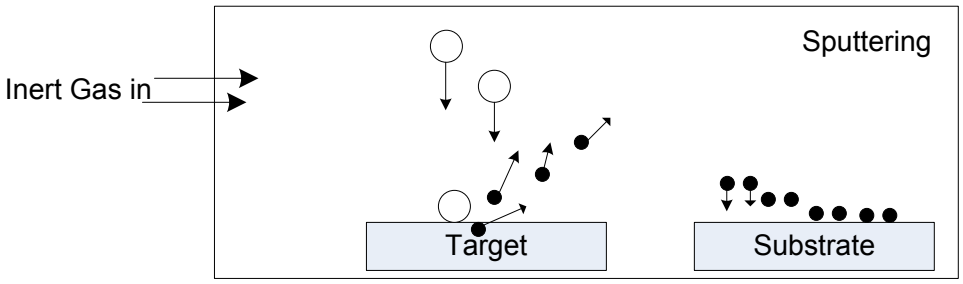

When the chosen gases utilized to create plasma are reactive with each other or with the substrate, chemical reactions will occurs with the final products in the form of solid particle depositing or attaching to the surface of the substrate. PECVD is the most prominent method following this principle, which is widely used to prepare micro- and nanoscale material in the industry. Other derivatives of this technique can be listed such as plasma polymerization, oxidation and reduction.

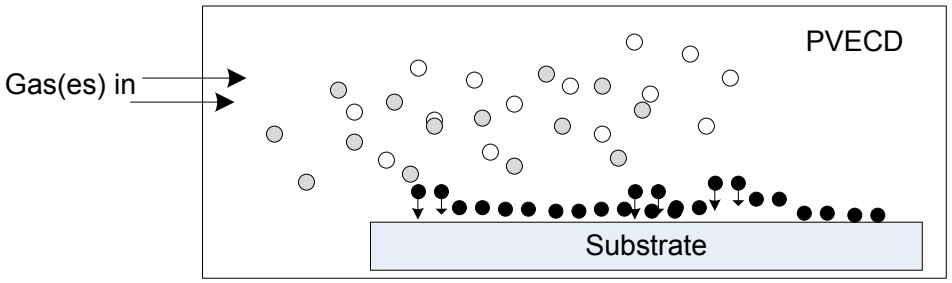

Sputtering and PECVD have been employed to prepare N-doped TiO_2 nanomaterials (Chen and Mao 2007). However, these methods have not been used to dope nitrogen into the self-ordered nanotubes of TiO_2 (Macak, Tsuchiya et al. 2007).

Plasma implantation technique

In the implantation technique, ionized particles are excited by the energy input to the level that the charged ions have enough kinetic energy to penetrate deeply into the crystal lattice of the colliding target. As a result, the crystal lattice of the target material is modified physically and chemically, leading to a change in the material properties.

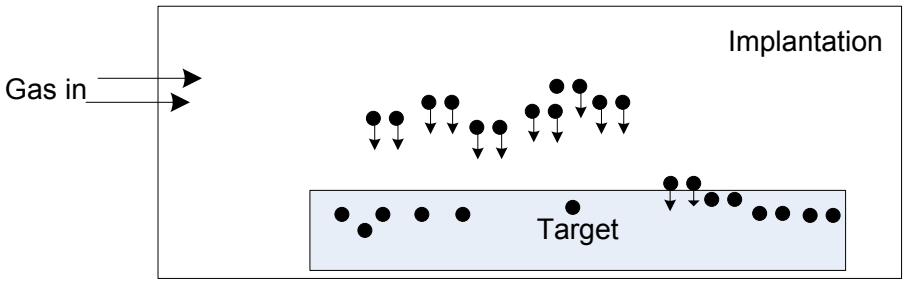

According to the literature review, the implantation technique is the only available plasma method to dope nitrogen into the self-ordered nanotubes of TiO_2 recently.

Plasma etching technique

Plasma etching involves in the use of a reactive gas, which can react with the substance at the surface of the treated object to form a volatile compound. For instance, carbon monoxide and hydrogen are popular reactive gases used to etch the surface of metal oxides because the end products of such chemical reactions are carbon dioxide and

water, respectively. By preparing the surface of the treated object, the etching process can be selectively controlled to create desired nano- and micro-structures at the solid surface.

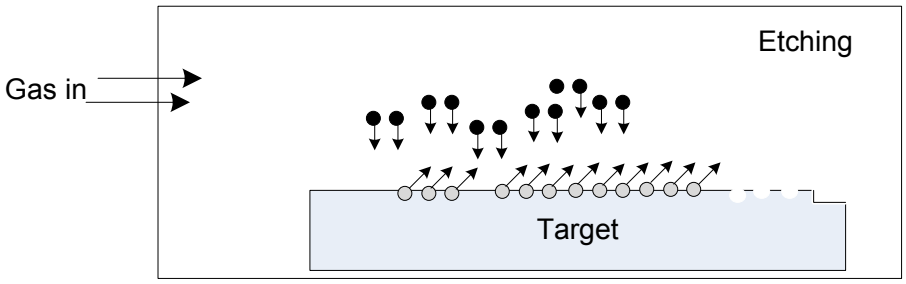

Our proposed plasma treatment method involves in using N_2 and CO gases. Therefore, this method can be viewed as the combination of both etching and deposition techniques.

2.5. PRODUCED WATER IN OIL AND GAS INDUSTRY

2.5.1. Introduction

In petroleum production activities, the water extracted from the oil/water separation process is termed as produced water. Sources of produce water can include formation water presenting together with the oil and injection water pumped down hole for lifting oil to surface. The term of produced water is also applied for the formation water extracted from the production of coal bed methane (Veil, Puder et al. 2004).

Produced water is by far the largest waste streams from the oil and gas extraction industries. In the United States, produced water comprises approximately 98% of the total volume of exploration and production waste generated by the oil and gas industry and is the largest volume waste stream generated by the oil and gas industry. Table 2.1. list the volumes (in thousand barrels, each barrel equals 117.34 liters) of produced water generated in the US onshore wells in 1985-2002 (Veil, Puder et al. 2004). Besides of these data, additional large volumes of produced water are still being generated at U.S. offshore wells and at thousands of wells in other countries.

Table 2.1. Quantities of produced water generated from US onshore oil and gas production

Unit: thousand barrels

State	1985	1995	2002	Source
Alabama	87,619	320,000	99,938	State
Alaska	97,740	1,090,000	813,367	State
Arizona	149	100	88	Estimate
Arkansas	184,536	110,000	90,331	Estimate
California	2,846,078	1,684,200	1,290,050	Estimate
Colorado	388,661	210,600	133,005	Estimate
Florida	NA	76,500	48,990	Estimate
Illinois	1,282,933	285,000	212,098	Estimate
Indiana	NA	48,900	34,531	Estimate
Kansas	999,143	683,700	1,174,641	State
Kentucky	90,754	3,000	2,411	Estimate

Louisiana	1,346,675	1,346,400	1,079,805	State
Michigan	76,440	52,900	33,207	Estimate
Mississippi	318,666	234,700	286,532	State
Missouri	NA	100	1,200	State
Montana	223,558	103,300	104,501	Estimate
Nebraska	164,688	61,200	51,191	State
Nevada	NA	6,700	2,765	Estimate
New Mexico	445,265	706,000	112,934	State
New York	NA	300	844	State
North Dakota	59,503	79,800	78,236	Estimate
Ohio	NA	7,900	6,416	State
Oklahoma	3,103,433	1,642,500	1,252,870	Estimate
Pennsylvania	NA	2,100	5,842	State
South Dakota	5,155	4,000	3,293	State
Tennessee	NA	400	275	Estimate
Texas	7,838,783	7,630,000	5,031,945	State
Utah	260,661	124,600	84,791	Estimate
Virginia	NA	300	550	Estimate
W. Virginia	2,844	6,000	4,284	Estimate
Wyoming	785,221	1,401,000	2,119,394	State
Total	**20,608,505**	**17,922,200**	**14,160,325**	

2.5.2. Treatment and the need to enhance reusability of produced water

Produced water always contains hydrocarbons and various chemical additives used in petroleum drilling and production activities. Among the constituents, hydrocarbons are of the most concern due to their abundance found in produced water; particularly, the aromatic fraction including BTEX which are more soluble and harmful to aquatic lives and human. Environmental risks of produced water are greatly amplified by the large discharged quantity. As a result, the treatment of produced water is mandatory and strictly regulated worldwide.

In the US, the discharge of produced water to navigable and coastal water is generally not permitted by EPA. For some regions of the US, onshore petroleum facilities can only discharge produced water to navigable water as long as the produced water is of good enough quality to be used for wildlife or livestock watering or other agricultural uses and produced water is actually put to such use during periods of discharge. Discharged produced water from offshore facilities to the sea is regulated with the effluent limitation guidelines of 42 mg/L and 29 mg/L of daily maximum and monthly average, respectively, concentrations of oil and grease (Veil, Puder et al. 2004).

Various technologies including absorption, gas flotation, and gravity separation are being applied to treat produced water, and the most focused treatment is removal of hydrocarbons. A sample of produced water treatment efficiencies between Best Available Technology (BAT) and Best Practicable Technology (BPT) is listed in the following

Table 2.2. In this review, the gas flotation method is determined as the BAT by EPA (EPA 1993).

Table 2.2. Produced water treatment efficiencies between BPTs and BAT

Constituent	**Concentration after BPT-Level Treatment (mg/L)**	**Concentration after BAT-Level Treatment (mg/L)**
Oil and grease	25	23.5
2-Butanone	1.03	0.41
2,4-Dimethylphenol	0.32	0.25
Anthracene	0.018	0.007
Benzene	2.98	1.22
Benzo(a)pyrene	0.012	0.005
Chlorobenzene	0.019	0.008
Di-n-butylphthalate	0.016	0.006
Ethylbenzene	0.32	0.062
n-Alkanes	1.64	0.66
Naphthalene	0.24	0.092
p-Chloro-m-cresol	0.25	0.010
Phenol	1.54	0.54
Steranes	0.077	0.033
Toluene	1.901	0.83
Triterpanes	0.078	0.031
Total xylenes	0.70	0.38
Aluminum	0.078	0.050

Arsenic	0.11	0.073
Barium	55.6	35.6
Boron	25.7	16.5
Cadmium	0.023	0.014
Copper	0.45	0.28
Iron	4.9	3.1
Lead	0.19	0.12
Manganese	0.12	0.074
Nickel	1.7	1.1
Titanium	0.007	0.004
Zinc	1.2	0.13
Radium 226 (in pCi/L)	0.00023	0.00020
Radium 228 (in pCi/L)	0.00028	0.00025

Source: EPA- 821-R-93-003

The results show the post-treatment concentrations of BTEX in produced water are 1.22-2.98 mg/L, 0.83-1.901 mg/L, 0.032-0.62 mg/L and 0.38-0.70 mg/L, respectively, for each component. Comparing with MCLs of BTEX in drinking water, which are 0.005, 1, 0.7, and 10 ppm, respectively; these treatment techniques do not meet the standards for drinking water supply.

Most recently, the Produced Water Utilization Act of 2009 has been passed by the US House of Representative. This Act aims to promote research, development, and demonstration of technologies for environmentally sustainable utilization of produced

water for agricultural, municipal, or industrial uses or other environmentally sustainable purposes. The act put up requirement for programs to be designed to maximize the utilization of produced water in the United States by increasing its quality and reducing its environmental impacts. Therefore, the need of enhancing reusability of produced water is real and necessary (Congress 2009).

Treatment of petroleum hydrocarbons in contaminated water by advanced oxidation processes with TiO_2/visible light has showed little success for BTEX and n-alkanes ranging from C_{10} to C_{20} (Cho, Kim et al. 2006) (Fig 2.10). Such limited successes were mainly due to the limited UV lights in solar radiation, and the TiO_2 nanoparticles used were not activated by visible light.

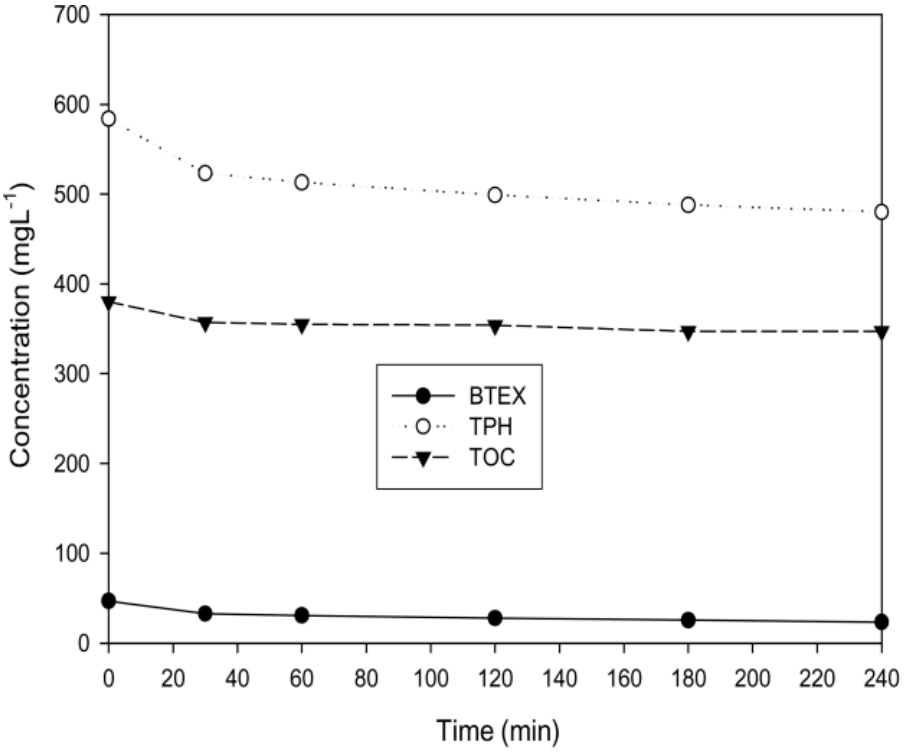

Figure 2.10. Removal of petroleum hydrocarbons by TiO_2/sunlight system

In this study, we aim to achieving the synthesis of modified 1-D TiO_2 nanomaterials by the non-thermal plasma treatment and electrospinning techniques, which are expected to significantly enhance their sorption of visible lights and result in faster and more effective degradation of contaminants (BTEX) in produced water comparing to the above reported results.

REFERENCES

Anpo, M. (2000). "Use of visible light. Second-generation titanium oxide photocatalysts prepared by the application of an advanced metal ion-implantation method." Pure and Applied Chemistry **72**(9): 1787-1792.

Anpo, M. (2000). "Utilization of TiO_2 photocatalysts in green chemistry." Pure and Applied Chemistry **72**(7): 1265-1270.

Anpo, M., S. Kishiguchi, Y. Ichihashi, M. Takeuchi, H. Yamashita, K. Ikeue, B. Morin, A. Davidson and M. Che (2001). "The design and development of second-generation titanium oxide photocatalysts able to operate under visible light irradiation by applying a metal ion-implantation method." Research on Chemical Intermediates **27**(4-5): 459-467.

Anpo, M. and M. Takeuchi (2001). Int. J. Photoenergy **3**: 89-94.

Anpo, M. and M. Takeuchi (2003). "The design and development of highly reactive titanium oxide photocatalysts operating under visible light irradiation." Journal of Catalysis **216**(1-2): 505-516.

Asahi, R. and T. Morikawa (2007). "Nitrogen complex species and its chemical nature in TiO_2 for visible-light sensitized photocatalysis." Chemical Physics **339**(1-3): 57-63.

Asahi, R., T. Morikawa, T. Ohwaki, K. Aoki and Y. Taga (2001). "Visible-light photocatalysis in nitrogen-doped titanium oxides." Science **293**(5528): 269-271.

ASTM ASTM G173 - 03e1 Standard Tables for Reference Solar Spectral Irradiances: Direct Normal and Hemispherical on 37° Tilted Surface. Philadelphia, American Society for Testing and Materials.

Burda, C., Y. Lou, X. Chen, A. C. S. Samia, J. Stout and J. L. Gole (2003). "Enhanced nitrogen doping in TiO_2 nanoparticles." Nano Letters **3**(8): 1049-1051.

Chandrasekar, R., L. Zhang, J. Y. Howe, N. E. Hedin, Y. Zhang and H. Fong (2009). "Fabrication and characterization of electrospun titania nanofibers." Journal of Materials Science **44**(5): 1198-1205.

Chen, S. F., L. Chen and S. Gao (2005). Chemical Physics Letters **413**: 404-409.

Chen, X., Y. Lou and C. Burda (2004). "Spectroscopic investigation of II-VI core-shell nanoparticles: CdSe/CdS." International Journal of Nanotechnology **1**(1-2): 105-118.

Chen, X., Y. Lou, A. C. Samia and C. Burda (2003). "Coherency strain effects on the optical response of core/shell heteronanostructures." Nano Letters **3**(6): 799-803.

Chen, X., Y. Low, A. C. S. Samia, C. Burda and J. L. Gole (2005). "Formation of oxynitride as the photocatalytic enhancing site in nitrogen-doped titania nanocatalysts: Comparison to a commercial nanopowder." Advanced Functional Materials **15**(1): 41-49.

Chen, X. and S. S. Mao (2007). "Titanium dioxide nanomaterials: Synthesis, properties, modifications and applications." Chemical Reviews **107**(7): 2891-2959.

Cho, I. H., Y. G. Kim, J. K. Yang, N. H. Lee and S. M. Lee (2006). "Solar-chemical treatment of groundwater contaminated with petroleum at gas station sites: Ex situ remediation using solar/TiO_2 photocatalysis and solar Photo-Fenton." Journal of Environmental Science and Health - Part A Toxic/Hazardous Substances and Environmental Engineering **41**(3): 457-473.

Congress, H. R.-.-t. (2009). "Produced Water Utilization Act of 2009." In GovTrack.us (database of federal legislation).

Diwald, O., T. L. Thompson, T. Zubkov, E. G. Goralski, S. D. Walck and J. T. Yates Jr (2004). "Photochemical activity of nitrogen-doped rutile TiO_2(110) in visible light." Journal of Physical Chemistry B **108**(19): 6004-6008.

Emilio, C. A., M. I. Litter, M. Kunst, M. Bouchard and C. Colbeau-Justin (2006). "Phenol photodegradation on platinized-TiO_2 photocatalysts related to charge-carrier dynamics." Langmuir **22**(8): 3606-3613.

EPA (1993). "Development Document for Effluent Limitations Guidelines and New Source Performance Standards for the Offshore Subcategory of the Oil and Gas Extraction Point Source Category." EPA-821-R-93-003. from http://yosemite.epa.gov/water/owrccatalog.nsf/1ffc8769fdecb48085256ad3006f39fa/969ed536d932393a85256d83004fd95c!OpenDocument.

Fridman, A. (2008). Plasma chemistry. Cambridge ;;New York, Cambridge University Press.

Fujishima, A., X. Zhang and D. A. Tryk (2008). "TiO_2 photocatalysis and related surface phenomena." Surface Science Reports **63**(12): 515-582.

Ghicov, A., J. M. Macak, H. Tsuchiya, J. Kunze, V. Haeublein, L. Frey and P. Schmuki (2006). "Ion Implantation and Annealing for an Efficient N-Doping of TiO_2 Nanotubes." Nano Letters **6**(5): 1080-1082.

He, C. H. and J. Gong (2003). "The preparation of PVA-Pt/TiO_2 composite nanofiber aggregate and the photocatalytic degradation of solid-phase polyvinyl alcohol." Polymer Degradation and Stability **81**(1): 117-124.

Im, J. S., M. I. Kim and Y. S. Lee (2008). "Preparation of PAN-based electrospun nanofiber webs containing TiO_2 for photocatalytic degradation." Materials Letters **62**(21-22): 3652-3655.

Jia, C. W., E. Q. Xie, J. G. Zhao and H. G. Duan (2007). "Co-doped anatase TiO_2 nanofibers fabricated by electrospinning." Journal of Applied Physics **101**(9): 093509-093504.

Kim, Y. B., D. Cho and W. H. Park (2010). "Fabrication and characterization of TiO_2/poly(dimethyl siloxane) composite fibers with thermal and mechanical stability." Journal of Applied Polymer Science **116**(1): 449-454.

Kwon, S., M. Fan, A. T. Cooper and H. Yang (2008). "Photocatalytic applications of micro- and nano-TiO_2 in environmental engineering." Critical Reviews in Environmental Science and Technology **38**(3): 197-226.

Li, D. and Y. Xia (2003). "Fabrication of titania nanofibers by electrospinning." Nano Letters **3**(4): 555-560.

Li, D. and Y. Xia (2004). "Direct fabrication of composite and ceramic hollow nanofibers by electrospinning." Nano Letters **4**(5): 933-938.

Li, W., Y. Wang, H. Lin, S. I. Shah, C. P. Huang, D. J. Doren, S. A. Rykov, J. G. Chen and M. A. Barteau (2003). "Band gap tailoring of Nd^{3+}-doped TiO_2 nanoparticles." Applied Physics Letters **83**(20): 4143-4145.

Lieberman, M. (2005). Principles of plasma discharges and materials processing. Hoboken N.J., Wiley-Interscience.

Lin, Z., A. Orlov, R. M. Lambert and M. C. Payne (2005). "New insights into the origin of visible light photocatalytic activity of nitrogen-doped and oxygen-deficient anatase TiO_2." Journal of Physical Chemistry B **109**(44): 20948-20952.

Linsebigler, A. L., G. Lu and J. T. Yates Jr (1995). "Photocatalysis on TiO_2 surfaces: Principles, mechanisms, and selected results." Chemical Reviews **95**(3): 735-758.

Macak, J. M., H. Tsuchiya, A. Ghicov, K. Yasuda, R. Hahn, S. Bauer and P. Schmuki (2007). "TiO_2 nanotubes: Self-organized electrochemical formation, properties and applications." Current Opinion in Solid State and Materials Science **11**(1-2): 3-18.

Martin, S. T., C. L. Morrison and M. R. Hoffmann (1994). "Photochemical mechanism of size-quantized vanadium-doped TiO_2 particles." Journal of Physical Chemistry **98**(51): 13695-13704.

Nakamura, R., T. Tanaka and Y. Nakato (2004). "Mechanism for visible light responses in anodic photocurrents at N-doped TiO_2 film electrodes." Journal of Physical Chemistry B **108**(30): 10617-10620.

Nakano, Y., T. Morikawa, T. Ohwaki and Y. Taga (2006). "Band-gap narrowing of TiO_2 films induced by N-doping." Physica B: Condensed Matter **376-377**(1): 823-826.

Ohno, T., M. Akiyoshi, T. Umebayashi, K. Asai, T. Mitsui and M. Matsumura (2004). "Preparation of S-doped TiO_2 photocatalysts and their photocatalytic activities under visible light." Applied Catalysis A: General **265**(1): 115-121.

Pelaez, M., N. T. Nolan, S. C. Pillai, M. K. Seery, P. Falaras, A. G. Kontos, P. S. M. Dunlop, J. W. J. Hamilton, J. Byrne, K. O'Shea, M. H. Entezari and D. D. Dionysiou (2012). "A review on the visible light active titanium dioxide photocatalysts for environmental applications." Applied Catalysis B: Environmental **125**: 331-349.

Qiu, Y. and J. Yu (2008). "Synthesis of titanium dioxide nanotubes from electrospun fiber templates." Solid State Communications **148**(11-12): 556-558.

Rengifo-Herrera, J. A., J. Kiwi and C. Pulgarin (2009). "N, S co-doped and N-doped Degussa P-25 powders with visible light response prepared by mechanical mixing of thiourea and urea. Reactivity towards E. coli inactivation and phenol oxidation." Journal of Photochemistry and Photobiology A: Chemistry **205**(2–3): 109-115.

Song, M. Y., D. K. Kim, K. J. Ihn, S. M. Jo and D. Y. Kim (2005). "New application of electrospun TiO_2 electrode to solid-state dye-sensitized solar cells." Synthetic Metals **153**(1-3): 77-80.

Szczepankiewicz, S. H., A. J. Colussi and M. R. Hoffmann (2000). "Infrared spectra of photoinduced species on hydroxylated titania surfaces." Journal of Physical Chemistry B **104**(42): 9842-9850.

Umebayashi, T., T. Yamaki, H. Itoh and K. Asai (2002). "Analysis of electronic structures of 3d transition metal-doped TiO_2 based on band calculations." Journal of Physics and Chemistry of Solids **63**(10): 1909-1920.

Umebayashi, T., T. Yamaki, H. Itoh and K. Asai (2002). "Band gap narrowing of titanium dioxide by sulfur doping." Applied Physics Letters **81**(3): 454.

Veil, J. A., M. G. Puder, D. Elcock and R. J. R. Jr. (2004). "A white paper describing produced water from production of crude oil, natural gas, and coal bed methane." Prepared for US Department of Energy - National Energy Technology Laboratory - W31-109-Eng-38.

Yu, H., J. Yu and B. Cheng (2007). "Photocatalytic activity of the calcined H-titanate nanowires for photocatalytic oxidation of acetone in air." Chemosphere **66**(11): 2050-2057.

Zaleska, A. (2008). "Doped-TiO2: A review." Recent Patents on Engineering **2**(3): 157-164.

CHAPTER 3

RESEARCH OBJECTIVES AND TASKS

3.1. OVERVIEW

This study is built on mature titanium dioxide/ultra violet(UV) processes that have been widely used for disinfection and advanced oxidation of organic contaminants. The result from this study could extend the photocatalytic treatment processes to visible light region, avoiding the need for an UV source. Degradation of petroleum hydrocarbons is selected as the first model system for application because oil spills occur frequently; and it is envisioned that if an effective photocatalyst could be prepared by utilizing visible light radiation, application of the catalyst to the contamination sites could be a new and economical approach of *in situ* contamination degradation. Another application is for the treatment of produced water associated with gas and oil production. This research could potentially provide a cost-effective approach for the produced water treatment and reuse.

To achieve the research goal as mentioned above, we aims at accomplishing the following three tasks.

3.2. PREPARATION OF VISIBLE LIGHT ACTIVATED 1-D TITANIUM DIOXIDE NANOMATERIALS BY ELECTROSPINNING AND PLASMA TREATMENT TECHNIQUES

3.2.1. Preparation of visible light activated titanium dioxide nanotube by non-thermal plasma treatment technique

In this task, we aim to synthesize TiO_2 photocatalyst as a thin solid foil containing packs of self-ordered nanotubes, then to perform plasma treatment for doping nitrogen atoms onto TiO_2 nanotubes at the surface of this thin foil. If it is successful then such approach can be expanded to a wide range of TiO_2 nanomaterials, leading to higher applicability of this photocatalyst.

The thin solid foil of self-ordered nanotubes of TiO_2 is prepared following the anodization method derived from Varghese et al. (Varghese, Gong et al. 2003). In this method, a thin foil of titanium (Ti) is used as the anode, at which the following processes occur when there is a DC current applied (Macak, Tsuchiya et al. 2007).

$$Ti - 4e^- \rightarrow Ti^{4+} \quad (15)$$

$$Ti + 2H_2O \rightarrow TiO_2 + 4H^+ + 4e^- \quad (16)$$

$$TiO_2 + 6F^- + 4H^+ \rightarrow [TiF_6]^{2-} + 2H_2O \quad (17)$$

$$Ti^{4+} + 6F^- \rightarrow [TiF_6]^{2-} \quad (18)$$

After this process, the self-ordered nanotubes of TiO_2 are formed at the surface of the Ti foil. At this stage, the formed nanotubes only contain amorphous TiO_2. Therefore, the thin foil is consequently subjected to the annealing process to convert amorphous TiO_2 into anatase TiO_2, before underwent nitrogen doping treatment.

As mentioned in Chapter 2, when the unique nanotubular structure needs to be preserved, available methods for nitrogen doping of self-ordered nanotubes of TiO_2 are very limited (Macak, Tsuchiya et al. 2007; Zaleska 2008). Successful nitrogen doping of self-ordered TiO_2 nanotubes without hampering the structure was carried out by either ion implantation or thermal treatment in NH_3 atmosphere. Because these methods require a high temperature, a non-thermal doping process would have advantages because of the lower energy requirement and avoidance of material damage when TiO_2-nanostructure coated subjects are processed.

We propose a novel method of doping the self-ordered nanotubes of TiO_2, which is to use the non-thermal radio frequency plasma discharge to dope nitrogen atoms into TiO_2 nanotubes with the aid of carbon monoxide (CO) as the initiating reagent. The fundamental hypothesis of this novel method is that carbon monoxide could be a catalyst/activator, based on the followings thermodynamic data (Fridman 2008).

In the plasma phase, the combination of nitrogen with oxygen is:

$$\tfrac{1}{2}\, N_2 + \tfrac{1}{2}\, O_2 \rightarrow NO \qquad \Delta H \approx 5.5 eV/mol \qquad (19)$$

However, such combination is limited by the dissociation of nitrogen molecule as follows:

$$N_2 \rightarrow N + N \quad \Delta H = 9.8eV/mol \qquad (20)$$

As the reaction (20) is too endothermic, it is generally known that reaction (26) occurs only in a powerful plasma discharge event (i.e., lightning strike during thunder storm). In non-thermal plasma, nitrogen molecules can be ionized, but at very small fraction of 10^{-6}-10^{-3} of total free molecules (Lieberman 2005).

When carbon monoxide is present, however, the combination of carbon monoxide with oxygen is thermodynamically favored because of the exothermic property of the related reaction.

$$CO + \tfrac{1}{2} O_2 \rightarrow CO_2 \quad \Delta H = -2.9eV/mol \qquad (21)$$

In the plasma, reaction (22) can be limited by the dissociation of carbon dioxide molecule. But this dissociation requires a large amount of heat input.

$$CO_2 \rightarrow CO + O \qquad \Delta H = 5.5eV/mol \qquad (22)$$

Therefore, it is hypothesized that carbon monoxide can more easily combine with oxygen atoms in the lattice of TiO_2, leaving oxygen vacancies for ionized nitrogen molecule to move in, resulting in the nitrogen doping of TiO_2. This hypothesis will be tested as the first research task.

With this study, we expect to investigate not only the doping capability, but also the limitation of the non-thermal plasma treatment technique.

3.2.2. Preparation of visible light activated titanium dioxide nanofibers by electrospinning technique

In this task we aim to synthesize TiO_2 photocatalyst as a nanofiber mat with a fiber supporting material containing nitrogen atom within its molecule; then to perform a mild heat treatment for doping nitrogen onto TiO_2 while still retaining the 1-D fibrous form of TiO_2 nanofibers.

The mat of TiO_2 nanofibers is prepared following the widely known electrospinning method. In a typical preparation, a suitable organic polymer is dissolved into an appropriate solvent to provide the electrospunable supporting substrate for the electrospinning process. Alkoxide titanium isopropoxide (TIIP) is chosen as the precursor for TiO_2 nanomaterial as similarly used in other studies (Li and Xia 2003; Li and Xia 2004; Chandrasekar, Zhang et al. 2009). In a standard preparation, liquid TIIP is dropwisely added to the supporting substrate under vigorous mixing conditions, then the

mixture is electrospun to produce a mat containing of polymer fibers coated/filled with TIIP. This mat is then hydrolyzed in a control manner for TIIP to convert into TiO_2 following the reaction as below.

$$Ti(OPr)_4 + 4\ H_2O \rightarrow\ TiO_2 + 4\ Pr\text{-}OH \qquad (23)$$

The prepared mat is then subject to a drying step to remove Pr-OH, as well as any excessive amount of moisture and solvent. Because only amorphous TiO_2 is produced in the hydrolysis step, universally the mat has to be annealed at temperature of 500^{o}C and above for amorphous TiO_2 to convert into crystalized forms of anatase and rutile, two forms exhibiting photocatalytic characteristics. Nevertheless such annealing step could lead to the other consequences, for example the supporting polymer is burnt off at high temperature, resulting in mechanically unstable TiO_2 nanofibers which are easily broken into smaller rods, therefore losing the advantages of 1-D nanomaterials as mentioned earlier.

In this study, we investigated a novel approach to prepare TiO_2 nanofibers with electrospinning process. The hypothesis herein is that by selecting a suitable polymer that is stable at high temperature and at the same time contains intra-molecule nitrogen atoms as the supporting substrate, together with controlling the annealing process for the crystallization and doping of TiO_2 nanofibers to occur, the as prepared TiO_2 nanofibers shall exhibit both the higher mechanical stability and the visible light activation while still retaining the 1-D fibrous structure.

This hypothesis, if proven, shall provide a highly effective method to prepare visible light activated TiO_2 nanofibers for industrial and domestic application. At the same time, we will explore the possibilities of developing the preparation technology to be simple and energy efficient and replacing the usage of harmful chemicals which are being phased out in the industry in order to achieve a less harmful and more environmentally sound technology.

3.3. CHARACTERIZATION OF VISIBLE LIGHT ACTIVATED 1-D TITANIUM DIOXIDE NANOMATERIALS

The crystal structure of TiO_2 will be characterized by the X-Ray Dispersion Spectroscopy (XRD) test. The XRD analysis is based on Scherrer equation (Cullity and Stock 2001; Chen and Mao 2007):

$$D = \frac{K\lambda}{\beta cos\theta}$$

where D is the intensity of the diffractive X-ray radiation, K is a dimensionless constant, 2θ is the diffraction angle, λ is the wavelength of the X-ray radiation, and β is the full width at maximum of the diffraction peak.

The recorded peak positions, intensities, widths and shapes of the recorded XRD spectrum will provide important information of the crystal structure, the crystallinity, and

the estimate of the crystal grain size. For instance, the broadening of a particular peak gives the information on the crystal size of an individual crystal domain. At the same time, the height of that peak gives the information on the periodicity of such crystal domain in the testing sample (Chen and Mao 2007). The XRD patterns of some TiO_2 nanomaterials are given in Fig 3.1.

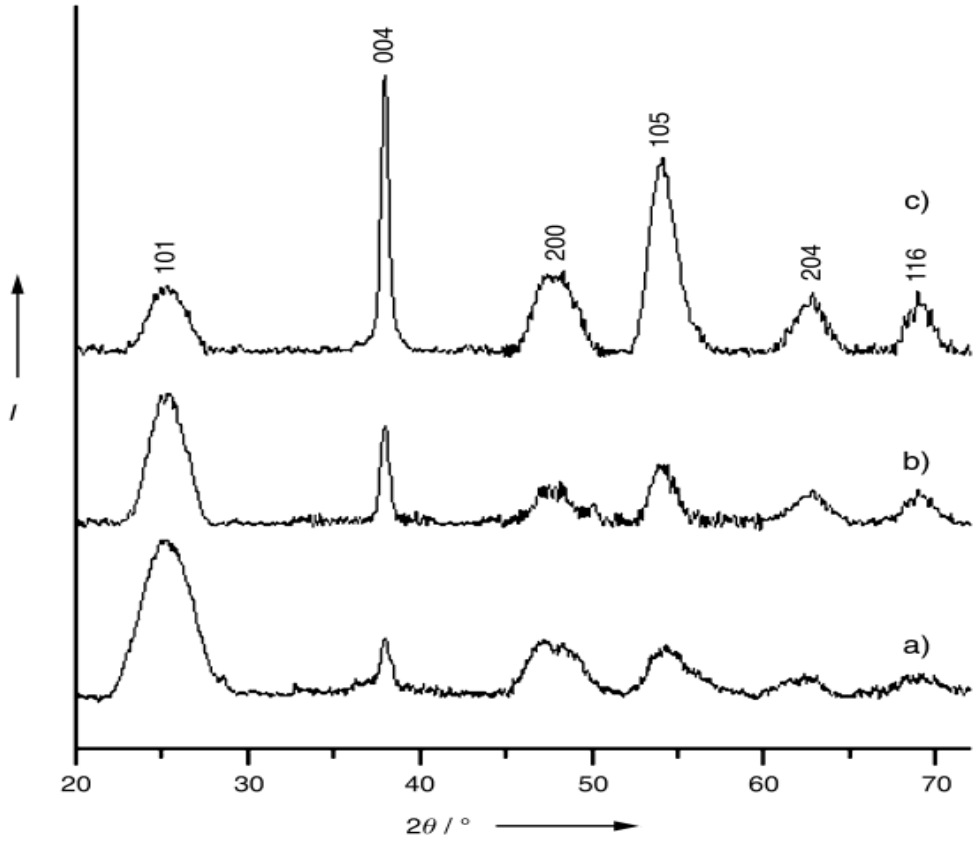

Figure 3.1. XRD patterns of titanium dioxide nanomaterials of different sizes (Zhang, Zhong et al. 2005).

When the nanoparticles size increases, the peak is narrowed (a) = spherical particles, (b) = 16-nm nanorod, and (c) = 30-nm nanorod.

Scanning Electron Microscopy (SEM) and Transmission Electron Microscopy (TEM) analyses will be used to examine nanostructures of TiO_2 at the surface of prepared photocatalysts. From literature review, the tube diameter of the expected nanotubes ranges from 15-300 nm (Macak, Tsuchiya et al. 2007), so SEM will have sufficient resolution to characterize such structures.

Optical property, or light absorption capacity in specific, of the as prepared TiO_2 photocatalyst will be measured via the light reflectance test. A blank sample of Ti foil subject will be used to set up the baseline for the optical test. Intensities of reflected radiations from the surface of the solid specimen are recorded over the continuous light spectrum from 190nm to 900nm. Actual light absorption of the as prepared photocatalyst will be deduced from the result of reflectance.

To determine the enhancement and activation of the as prepared TiO_2 photocatalyst, the degradation of Methylene Blue (MB) in water in the presence of as prepared TiO_2 samples will be conducted. Details of the reactor setup, experimental parameters, and respective analysis procedures are later given in research chapters 4, 5 and 6 in this dissertation

3.4. TESTING FOR SOLUBLE HYDROCARBONS REMOVAL USING AS PREPATED VISIBLE LIGHT ACTIVATED 1-D TITANIUM DIOXIDE NANOMATERIALS

In this task, we will evaluate the photocatalytic oxidation of the modified 1-D titanium dioxide nanomaterials under simulating solar radiation in batch reactors, with BTEX as model contaminants. Dark control tests and controls without any catalyst will be included to allow for proper data interpretation.

Concentration of dissolved petroleum hydrocarbons in batch reactors will be measured as a function of time. With the conditions of available instruments, a Total Organic Carbon (TOC) analyzer and Gas Chromatography coupled with Mass Spectrophotometer (GC-MS) will be employed to determine the total concentration of hydrocarbons in the aqueous phase. Kinetics data of BTEX removal by modified 1-D titanium dioxide nanomaterials shall be utilized for discussing the competence, limitation and implication of the application of visible light activated photocatalyst in treating water contaminated with hydrocarbon in actual field conditions.

REFERENCES

Chandrasekar, R., L. Zhang, J. Y. Howe, N. E. Hedin, Y. Zhang and H. Fong (2009). "Fabrication and characterization of electrospun titania nanofibers." Journal of Materials Science **44**(5): 1198-1205.

Chen, X. and S. S. Mao (2007). "Titanium dioxide nanomaterials: Synthesis, properties, modifications and applications." Chemical Reviews **107**(7): 2891-2959.

Cullity, B. D. and S. R. Stock (2001). Elements of X-Ray Diffraction. Upper Saddle River, NJ, Prentice Hall.

Fridman, A. (2008). Plasma chemistry. Cambridge ;;New York, Cambridge University Press.

Li, D. and Y. Xia (2003). "Fabrication of titania nanofibers by electrospinning." Nano Letters **3**(4): 555-560.

Li, D. and Y. Xia (2004). "Direct fabrication of composite and ceramic hollow nanofibers by electrospinning." Nano Letters **4**(5): 933-938.

Lieberman, M. (2005). Principles of plasma discharges and materials processing. Hoboken N.J., Wiley-Interscience.

Macak, J. M., H. Tsuchiya, A. Ghicov, K. Yasuda, R. Hahn, S. Bauer and P. Schmuki (2007). "TiO_2 nanotubes: Self-organized electrochemical formation, properties and applications." Current Opinion in Solid State and Materials Science **11**(1-2): 3-18.

Varghese, O. K., D. Gong, M. Paulose, C. A. Grimes and E. C. Dickey (2003). "Crystallization and high-temperature structural stability of titanium oxide nanotube arrays." Journal of Materials Research **18**(1): 156-165.

Zaleska, A. (2008). "Doped-TiO2: A review." Recent Patents on Engineering **2**(3): 157-164.

Zhang, Z., X. Zhong, S. Liu, D. Li and M. Han (2005). "Aminolysis route to monodisperse titania nanorods with tunable aspect ratio." Angewandte Chemie - International Edition **44**(22): 3466-3470.

CHAPTER 4

APPLICATION OF NON-THERMAL PLASMA TREATMENT FOR DOPING OF SELF ORDERED 1-DIMENSIONAL TITANIUM DIOXIDE NANOTUBES FOR PHOTOCATALYTIC ACTIVATION IN VISIBLE LIGHT

ABSTRACT

Self-ordered titanium dioxide nanotubes (TiNT) with their high specific surface area and 1-dimensional geometrical features can provide high photocatalytic efficiency. Efforts are being implemented to dope carbon and nitrogen on TiNT to achieve activation with visible light and enhanced photocatalytic efficiency. The widely known methods of doping by ion implantation and thermal treatment still have disadvantages. In this study, we developed a non-thermal plasma treatment process to dope nitrogen onto TiNT with an aim to preserve the tube structure and to reduce the energy input for the doping process. The as prepared film of TiNT after plasma treatment exhibited activation by visible light and improved efficiency in the degradation of methylene blue (MB) in water. This type of material might find wide environmental applications.

4.1. INTRODUCTION

Self-ordered nanotube of titanium dioxide was first prepared by anodization of titanium metal foil in 1999 (Zwilling, Darque-Ceretti et al. 1999; Macak, Tsuchiya et al.

2007). Together with the rapid development among studies focused on titanium dioxide nanomaterials and their photocatalytic phenomenon, titanium dioxide nanotube (TiNT) has gathered a strong interest among the variety of TiO_2 nanomaterials. It has been reported that the nanotube structure of TiO_2 provided more photocatalytic efficiency than the particle structure such as P25 made by Degussa. Laboratory-scale studies showed that although a thin film of TiNT has much less surface area compared to layers of P25 powder in the same mass (~ 8 times), the photocatalytic efficiency observed with TiNT was ~ 2 times higher than such P25 layers. Such improvement was accounted for by several factors, but the major one was that the structure of self-ordered nanotube provides a more optimized geometry for the diffusion of reactants to the surface and provided for a lower trapping and recombination kinetics of photo-induced electron-hole pairs (Macak, Tsuchiya et al. 2007). In addition to the better performance, the application of TiNT in a fixed form as a heterogeneous catalyst will eliminate the separation process which is necessary when powder forms of TiO_2 nanomaterial are used, resulting in simpler and potentially lower cost technologies in practical applications.

With such advantages, there is also a strong desire to dope TiNT with various dopants, particularly nitrogen, to enable the activation of photocatalytic effect with visible light. The key factor is that the tubular structure of TiNT must be retained after the treatment, however, few measures are available for nitrogen doping of TiNT. Up to now, in general there are two major methods for doping nitrogen onto TiNT. The first one is to use the ion implantation process in which a large dose of charged nitrogen atoms with high kinetic energy interacts with and penetrates into the TiNT. This technique was

found to heavily destroy or suppress crystallite structures of TiNT so that an annealing step was required to reconstruct TiO_2 crystals in order to regain photocatalytic effect (Macak, Tsuchiya et al. 2007). In the second method, TiNT is heated inside a nitrogen donor environment such as ammonia, urea, or nitrogen (Chen and Mao 2007) to acquired nitrogen doping. Although the crystallite structure of TINT is preserved after heat treatment, this technique required a large energy input as heat and a long processing time, which result in a very high energy demand to operate.

In this study, we explored the possibility of using non-thermal plasma treatment to dope nitrogen onto TiNT. The doping effect was investigated though characterizations and application of the as-prepared TiNT in photolytic degradation of organic dye in visible light. The fundamentals for this approach have been summarized in Chapter 2 of this thesis. If successful the non-thermal plasma treatment technique would provide a lower energy consumption and shorter processing time for doping nitrogen onto TiNT, while still retain the desirable 1-D nanotube structures, enable activation with visible light and improve the photocatalytic efficiency of TiNT, particularly for environmental engineering applications.

4.2. EXPERIMENTAL

4.2.1. Materials

Titanium metal foil 0.25mm thick, 99.7% metal basis (Ti, CAS 7440-32-6), hydrofluoric acid A.C.S reagent grade 48% (HF, CAS 364-39-3), and acetone (CAS 67-64-1) were purchased from Sigma Aldrich (St Louis, Missouri). Dimethyl sulfoxide (DMSO, CAS 67-68-5) and methylene blue (MB, CAS 61-73-4) were purchased from Fisher Scientific (Fairlawn, New Jersey). Titanium dioxide P25 (P25, CAS 13463-67-7) was purchased from Degussa Corporation (Ridgefield Park, New Jersey). Ultra high purity-grade nitrogen gas (N_2) was purchased from the University of Missouri (Columbia, Missouri). Carbon monoxide gas of 99.9% purity (CO, CAS 630-08-0) was purchased from Praxair (Columbia, Missouri).

4.2.2. Preparation of modified titanium dioxide nanotubes

4.2.2.1. Preparation of thin solid film of titanium dioxide nanotubes

The thin solid foil of TiO_2 was synthesized following the anodization method derived from Varghese et al (Varghese, Gong et al. 2003) as follows. In this process, a long and narrow Ti strip with dimension of 1 cm x 5 cm was cut from the original Ti foil. This strip was then cleaned 2 times with deionized (DI) water then 2 times with acetone in a sonication bath. After that, the cleaned Ti strip was dried in an oven at 115^{o}C in 4

hours then cooled down to room temperature. In the subsequent anodization step, the Ti strip was anodized in a two-electrode set up with the working solution containing 40 ml of DMSO and 5 ml of HF 48% solution with the direct current of 40 V for 24 hours. In this setup, the working electrode was a platinum (Pt) wire (0.025 cm diameter, 5 cm in length). Spacing between two electrodes was kept at 1 cm. The power supply, Hewlett-Packard 6202B (0-60V, 0.5A), was used to supply the DC current to the circuit. The solution was constantly mixed by a magnetic stirrer.

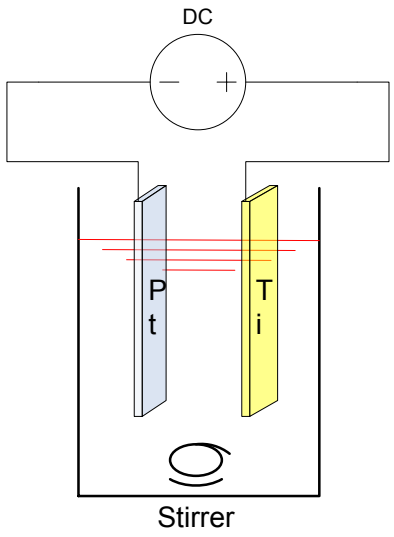

Figure.4.1. Anodization setup for formation of TiO_2 nanotubes

Subsequently, the Ti strip was collected rinsed with DI water and acetone several times again before annealed in the electric furnace for 5 hours and at 450^{o}C to convert amorphous nanotubes of TiO_2 at the surface of the strip into crystallite forms. After cooled down to room temperature, the strip was clean again with acetone and cut into square foils of TiNT with dimension of 1 cm x 1 cm to prepare for the plasma treatment.

4.2.2.2. Plasma treatment of titanium dioxide nanotubes

For the proposed research, a plasma reactor driven with RF power source, which was available in the Center of Surface Science and Plasma Technology of the University of Missouri, was used. The RF power generating system consisted of Advanced Energy RFX-600/ATX-600, which was capable of supplying energy rate of up to 100W. Chamber pressure was regulated by MKS Exhaust valve controller type 252. And the control of gas mass flows was carried out by MKS Mass-Flo controllers attached to a digital control panel. Flows of N_2 and CO gases were each controlled by separate mass flow controllers, which are adjustable to regulate the mass ratio of N_2/CO. Other controls of the plasma treatment process included pressure level, power input, and treatment time.

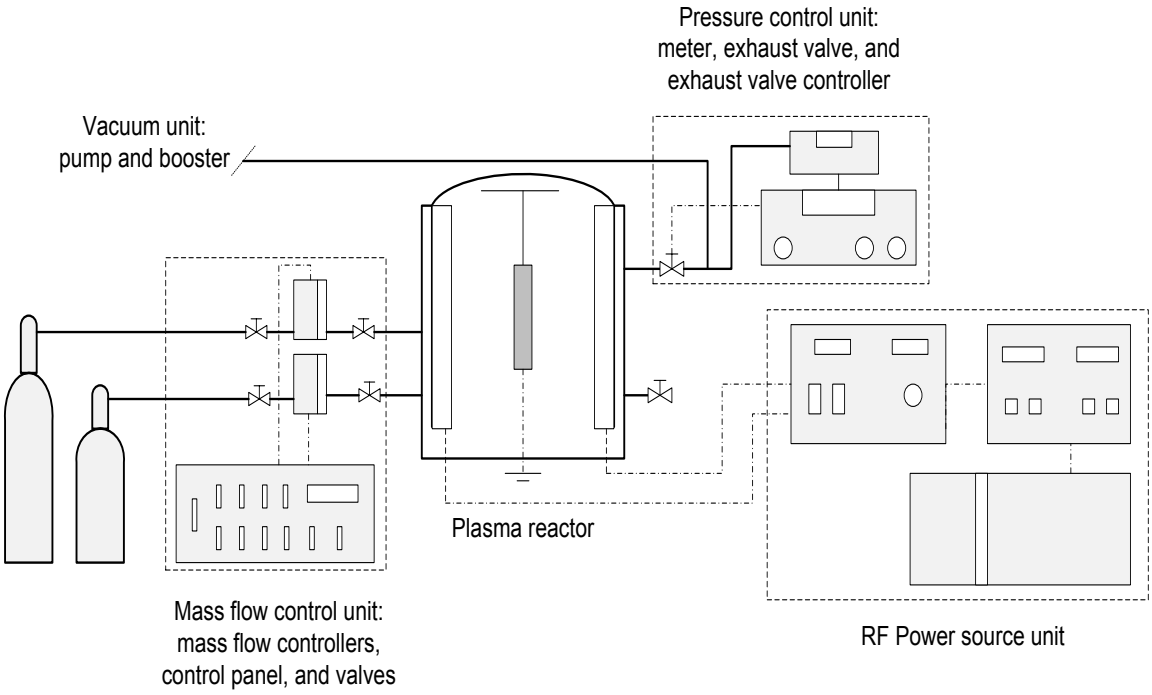

Figure 4.2. Plasma treatment setup for modifying TiO_2 nanotubes

TiNT foil was loaded into the plasma reactor as the floating object in the center between two plasma electrodes. Operating factors of the plasma treatment process were:

- Total gas flow rate: 6 sccm
- Plasma working pressure: 90 mTorr
- Input power: 5 W
- Treatment time: 10 min

Two (2) types of feed gas were used in the plasma treatment process, including N_2 only and a 1:1 mixture of N_2:CO, in order to test the hypotheses. After treatment, TiNT foils were rinsed several time with DI water and stabilized by drying at 115^{o}C in 12 hours.

4.2.3. Characterization of modified TiNT foil and evaluation of photocatalytic efficiency

The as prepared TiNT foils were examined for Scanning Electron Microscopy (SEM) and Electron Dispersive X-ray Spectroscopy (EDS) by FEI Quanta 600 FEG ESEM. Transmission Electron Microscopy (TEM) and Electron Diffraction (ED) characterizations of the nanotubes were performed on the JEOL 1400 Transmission Electron Microscope. Thin film X-ray diffraction (XRD) of as prepared TiNT foils was acquired by Scintag Pad V (CuKα radiation, detector solid Si, scan rate of 1^{o}/min). As prepared TiNT foils were also subjected to an UV-VIS reflection characterization using a

Shimadzu UV-VIS Recording Spectrophotometer UV2401PC. The control sample for the UV-VIS reflection characterization is a clean Ti metal foil.

In a typical experiment set up to measure the photocatalytic efficiency, each as-prepared TiNT foil was immersed into a beaker containing 20 ml of 0.5 parts per million (ppm) of methylene blue (MB). The beaker was first kept in a close container for 12 hours so any adsorption of MB on the glass wall, if there was any, would have been stabilized before start of the degradation tests. A Xenon lamp of 300 W was used as a light source. Optical filters were applied to the Xenon lamp to filter out radiations less than 400 nm and greater than 600 nm; all lights reaching to the reactor were in the visible range. At each time interval, 1 ml of the MB solution was withdrawn and its optical absorbance was measured at 670 nm by the spectrophotometer (Genesys 20, Thermo Scientific).

4.3. RESULTS AND DISCUSSION

4.3.1. Characterizations results

4.3.1.1 Characterizations of original titanium dioxide nanotubes before plasma treatment

SEM, TEM, ED and XRD images of the original TiNT foil before subjected to plasma treatment are presented in Figures 4.3-6 respectively. From the SEM image in Fig 4.3, it can be observed that original TiNT prepared from the anodization process

contain packs of vertical nanotubes. The diameter of an individual nanotube determined from TEM image in Fig 4.4 is about 150-200 nm.

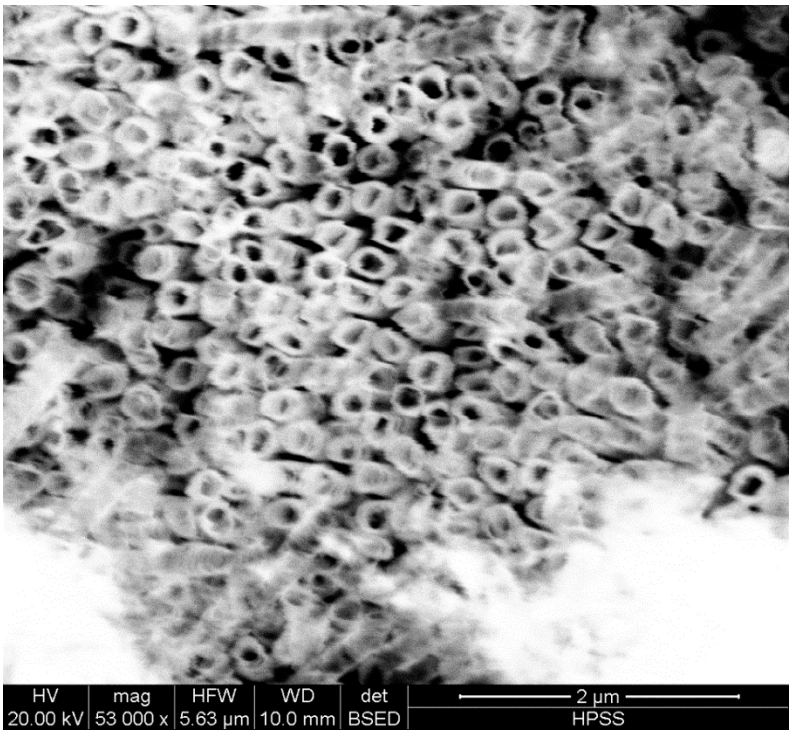

Figure 4.3. SEM image of titanium dioxide nanotubes before plasma treatment

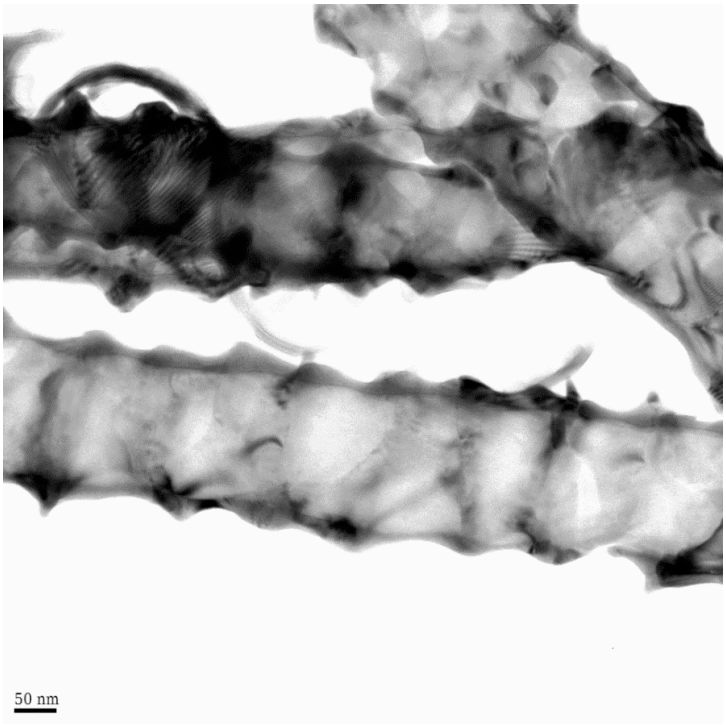

Figure 4.4. TEM image of titanium dioxide nanotubes before plasma treatment

Figure 4.5. ED image of a single titanium dioxide nanotube before plasma treatment

The electron diffraction (ED) pattern in Fig. 4.5 has showed that the individual nanotube is polycrystalline in nature, as the diffraction pattern clearly displayed two complete and distinctive diffraction rings around the nanotube.

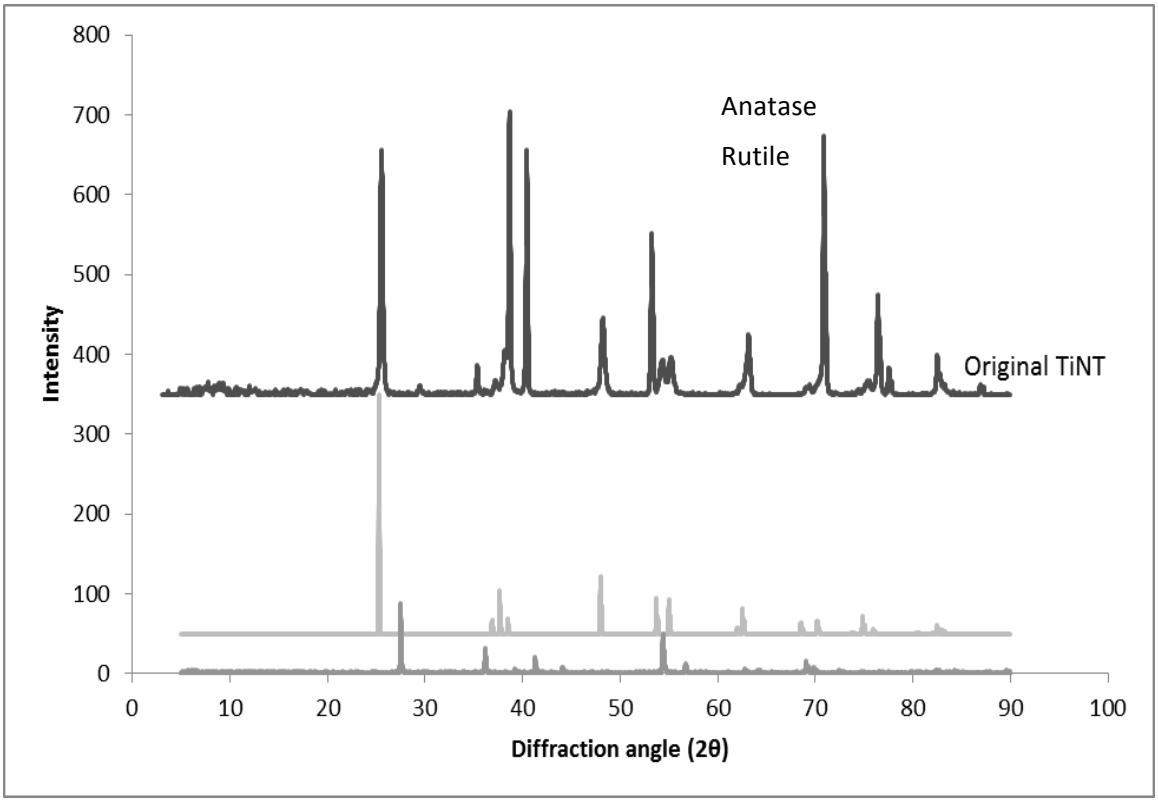

Figure 4.6. XRD pattern of titanium dioxide nanotube before plasma

When comparing XRD pattern of the original TiNT to XRD patterns of pure anatase and rutile as showed in Fig. 4.6, characteristic peaks of anatase at $2\theta = 25.5^{o}$, 38.6^{o}, 48.2^{o}, 54.3^{o}, 55.2^{o}, and 63.1^{o} corresponding to planes (001), (004), (200), (105), (211), and (204) were found in the original TiNT sample, while no chacateristic peaks of rutile could be found at the same time. This suggested that the dominant crystallite form of TiO_2 nanotubes in original TiNT sample is anatase.

In summary, the sample characterization results have proven that the prepared TiNT foil contain anatase TiO_2 nanotubes with diameter of 150-200 nm. This is consistent with the result reported in the literature (Varghese, Gong et al. 2003).

4.3.1.2. Characterizations of titanium dioxide nanotube after plasma treatment

SEM images of TiNT samples after treated in plasma are provided in Figures 4.7-10. In the TiNT sample treated with N_2 plasma (hereby namely N-TiNT), SEM images in Fig 4.7-8 revealed some nanotube openings were more or less fused together while most of nanotubes showed no visible damage. In comparison to the SEM image of the original TiNT sample showed in Fig 4.3, SEM images of N-TiNT indicated that tubular structure of TiNT was generally preserved after treated with N_2 plasma. Similar or even more significant damages on nanotube openings were found in the TiNT sample treated with N_2:CO plasma (hereby namely NC-TiNT). Many nanotube openings of NC-TiNT sample were collapsed as showed in Fig 4.9-10. It also could be observed that a portion of remaining nanotubes were blocked due to the fused opening and by the residue from surrounding damaged nanotubes.

As mentioned in the literature review, the nanotube structure of TiO_2 can be physically damaged due to the impact with a flux of energized nitrogen atoms during the ion implantation process. For example when Ghicov et al used ion implantation with nitrogen dose of 1×10^{16} ion/cm^2 with kinetic energy of 60 eV to dope nitrogen on TiNT,

significant damage to tubular structures and strong suppression of anatase crystalline forms were observed (Rengifo-Herrera, Kiwi et al. 2009). In non-thermal RF plasma, the concentration and the kinetic momentum of charged ions are 1 x 10^{10} ion/cm^2 and 10 eV respectively (Lieberman 2005), which are much lower than those in ion implantation. Therefore physical interactions between TiNT foil and charged N_2 ions during the plasma treatment were much weaker, resulted in the preservation of the tubular structure of N-TiNT.

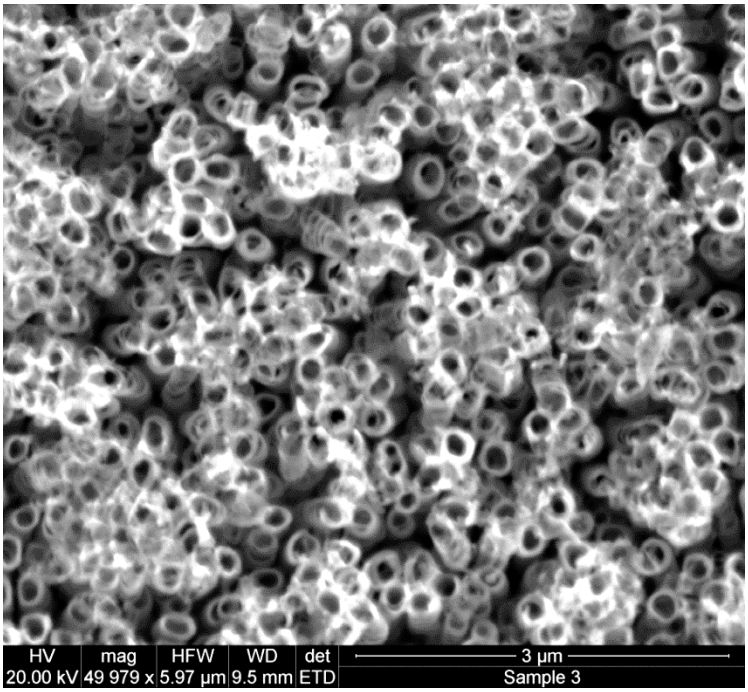

Figure 4.7. N-TiNT after having treated with N_2 plasma

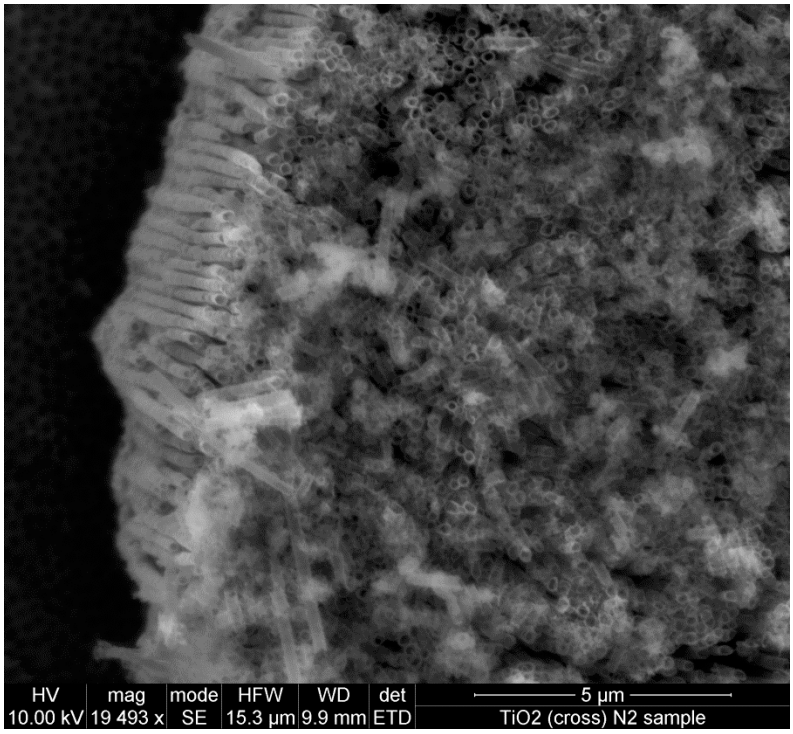

Figure 4.8. Cross-view of N-TiNT after treated with N_2 plasma

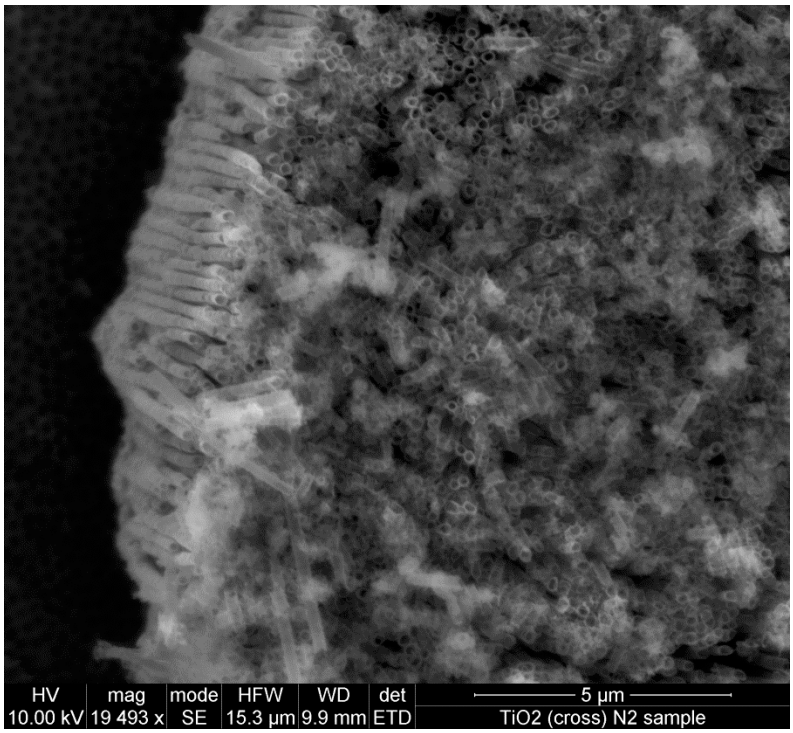

Figure 4.9. NC-TiNT after treated with N_2:CO plasma

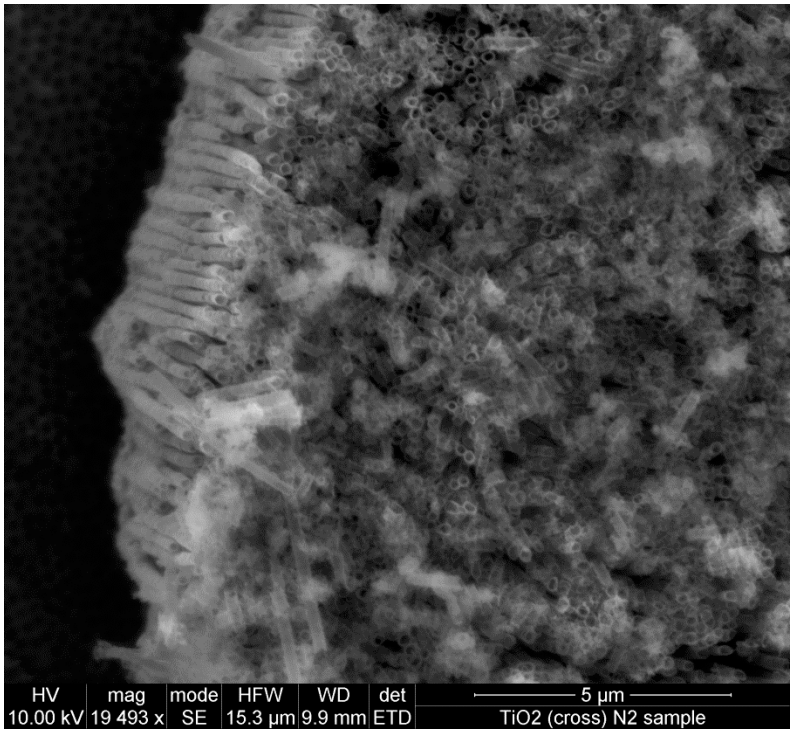

Figure 4.10. Crossview of NC-TiNT after treated with N_2:CO plasma

In line with the above argument, the clear increase in damage degree of NC-TiNT as observed has suggested that chemical processes played a significant role during the plasma treatment process. According to reaction (20) listed in Chapter 3, the plasma of N_2:CO gas mixture contained charged nitrogen ions from the dissociation of N_2 via reaction (27). However, charged oxygen atoms also could be formed via the following pathways:

$CO + O \rightarrow CO_2$ (this is reaction (21) as mentioned in Chapter 3)

$CO_2 \rightarrow C + O_2$ (23)

Oxygen atom for reaction (21) could come from latticed oxygen atoms in TiO_2 as hypothesized in Chapter 3. Reaction (23) is a well-known dissociation process of carbon dioxide gas in plasma (Fridman 2008). In term of standard oxidation potential, oxygen atom is clearly much higher than nitrogen atom due to the difference in electronegativity. Therefore, it is possible for oxygen atoms to interact with the surface of TiO_2 nanotube and oxidize defects of the polycrystalline structure and/or remaining titanium metal within the nanotube walls and openings, resulting in heavily fused and collapsed openings of these nanotubes.

Nevertheless, the damage to nanotube structures were considered insignificant as these SEM images showed the portion of TiO_2 nanotubes remaining in good structural. In addition, the effect of plasma treatment was only observed at the surface of the nanotubes, as side-view SEM images in Fig 4.8 and Fig 4.10 did not show major damage to the whole nanotube body. This again confirmed that non-thermal plasma treatment is only effective for the surface layer of material.

XRD patterns of N-TiNT, NC-TiNT are compared to that of original TiNT in Fig 4.11. The XRD pattern showed that the anatase crystallite form of nanotubes remained after the plasma treatment, with characteristic peaks of $2\theta = 25.5^o$, 38.6^o, 48.2^o, 54.3^o, 55.2^o, and 63.1^o corresponding to planes (001), (004), (200), (105), (211), and (204) being all found in the XRD patterns of N-TiNT and NC-TiNT foils. Therefore, it can be concluded that the applied plasma treatment technique did not suppress the crystallinity of TiO_2 within N-TiNT and NC-TiNT although physical damages were quite visible in these samples.

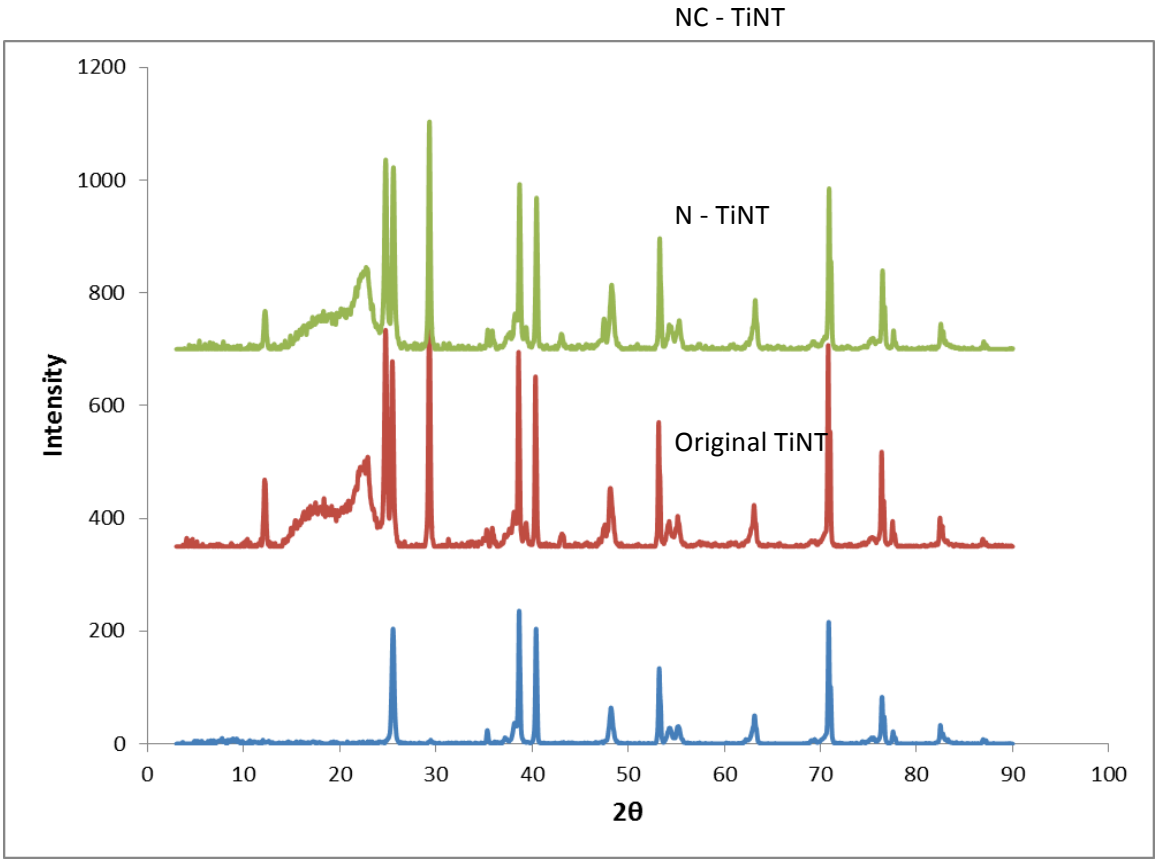

Figure 4.11. XRD pattern of plasma treated titanium dioxide nanotubes

It is noted that several new peaks appeared in the N-TiNT and NC-TiNT samples, particularly strong peaks at 2θ = 12.1, 22.2, 24.8, and 29.1. Further investigations suggested these peaks likely belong to carbonates phases which are mainly calcite ($CaCO_3$) and hydrotalcite (general formula $Mg_6Al_2(CO_3)(OH)_{16}{\cdot}4(H_2O)$). The source of these chemicals is unclear, they were likely caused by contamination occurred during the storing and handling of the material in the study. Nevertheless, these carbonates were not known to have any photocatalytic effect and therefore they did not pose any insignificant impact on the photocatalytic efficiency of the as prepared TiO_2 nanotubes investigated in this research.

4.3.2. UV-VIS characterization of TiNT samples

The UV-VIS absorption patterns of prepared TiNT, N-TiNT, and NC-TiNT foils, with the background level was the reflection pattern of unmodified Ti metal foil, are presented in Fig 4.12. Firstly, it can be observed that there was strong absorption in wavelength > 600 nm in all three samples. As nitrogen doping is known not to shift the absorption edge of TiO_2 to region > 600 nm (Chen and Mao 2007), the observed absorption in all three foils must be resulted from the diffraction of lights due to the nanotube structure at the surface.

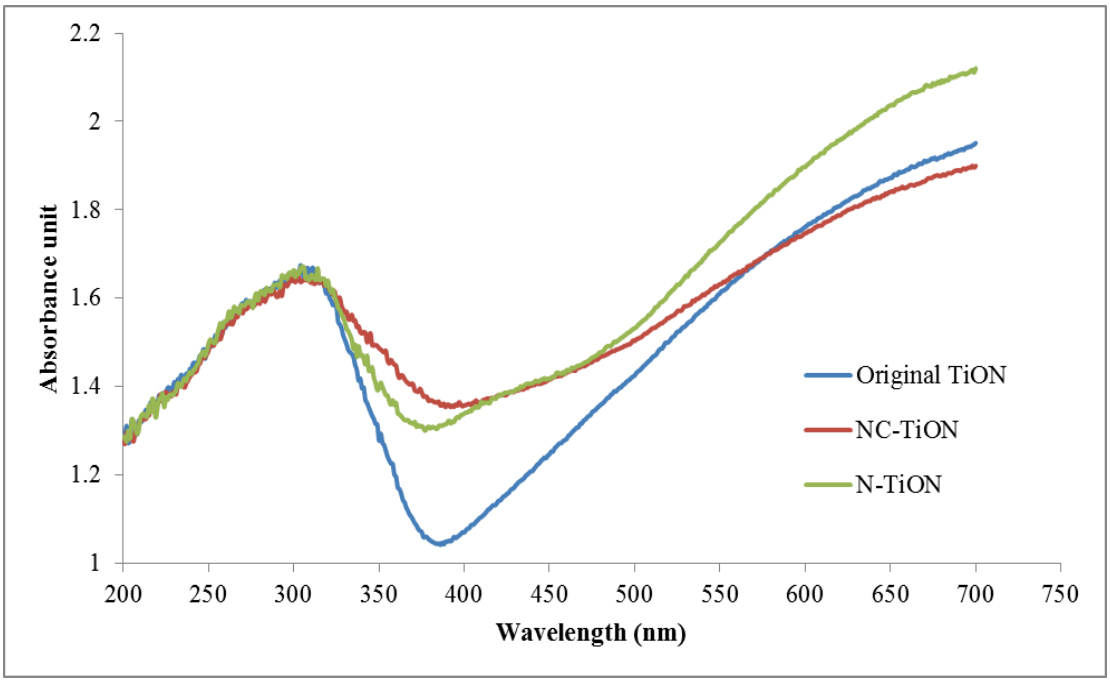

Figure 4.12. Optical absorbance of prepared TiNT foils in UV-VIS spectrum

The more important zone of wavelengths for consideration is the 200-550 nm zone containing UV and VIS radiations. In this zone, the original TiNT foil clearly showed that it only absorbed UV lights with wavelength < 380 nm, with the peak absorption at around 330 nm and rapidly decrease after 350 nm. This absorption pattern is a characteristic of pure anatase TiO_2 nanocrystals. As a result the TiNT was expected not to show any photocatalytic effect when radiated with visible light.

Compared to the original TiNT, the N-TiNT and NC-TiNT displayed similar absorption patterns in the UV zone of 200 – 340 nm with the peak absorption at around 330 nm. These similar patterns indicated that N-TiNT and NC-TiNT still contain a large portion of un-modified anatase TiO_2 within their structures, as having been confirmed previously via XRD patterns in Fig. 4.11, and maintain the ability to be activated in the UV region. However, the optical absorption patterns of N-TiNT and NC-TiNT from 340 nm and onwards were significantly different from the absorption pattern of original TiNT as illustrated in Fig 4.12. Firstly, the light absorption of N-TiNT and NC-TiNT did not decrease as sharply as original TiNT after 350 nm. Secondly, the light absorption slopes of N-TiNT and NC-TiNT extended into the visible light zone. And thirdly, there were significantly improved absorption by N-TiNT and NC-TiNT compared to TiNT in the visible light zone of 400 – 550 nm. These observations are consistent with the hypothesis that the plasma treatment process has doped nitrogen onto TiO_2 nanotubes and enabled them to absorb visible light.

Again as showed in Fig 4.12 in the wavelength range of 350 – 400nm there was a slight difference in light absorption between N-TiNT and NC-TiNT samples. The NC-TiNT had a higher light absorption, indicating that the N_2:CO plasma was able to facilitate a higher yield of nitrogen doping as proposed in the hypotheses. However, the observed increase was minor, so while our original hypothesis appears correct, the impact is not significant.

To further confirm the preparation is reproducible, another titanium metal strip was cleaned and undergone similar anodization and plasma treatment processes. These foils were named as “b” samples compared to the “a” samples which had been separately prepared in the previous preparation. The UV-VIS reflection patterns of these “b” samples compared to “a” samples are presented in Fig 4.13. Data on Figure 4.13 clearly showed that the UV-VIS reflection patterns were consistent between “a” and “b” samples, indicating that the preparation processes were reproducible in creating materials capable of visible light activation.

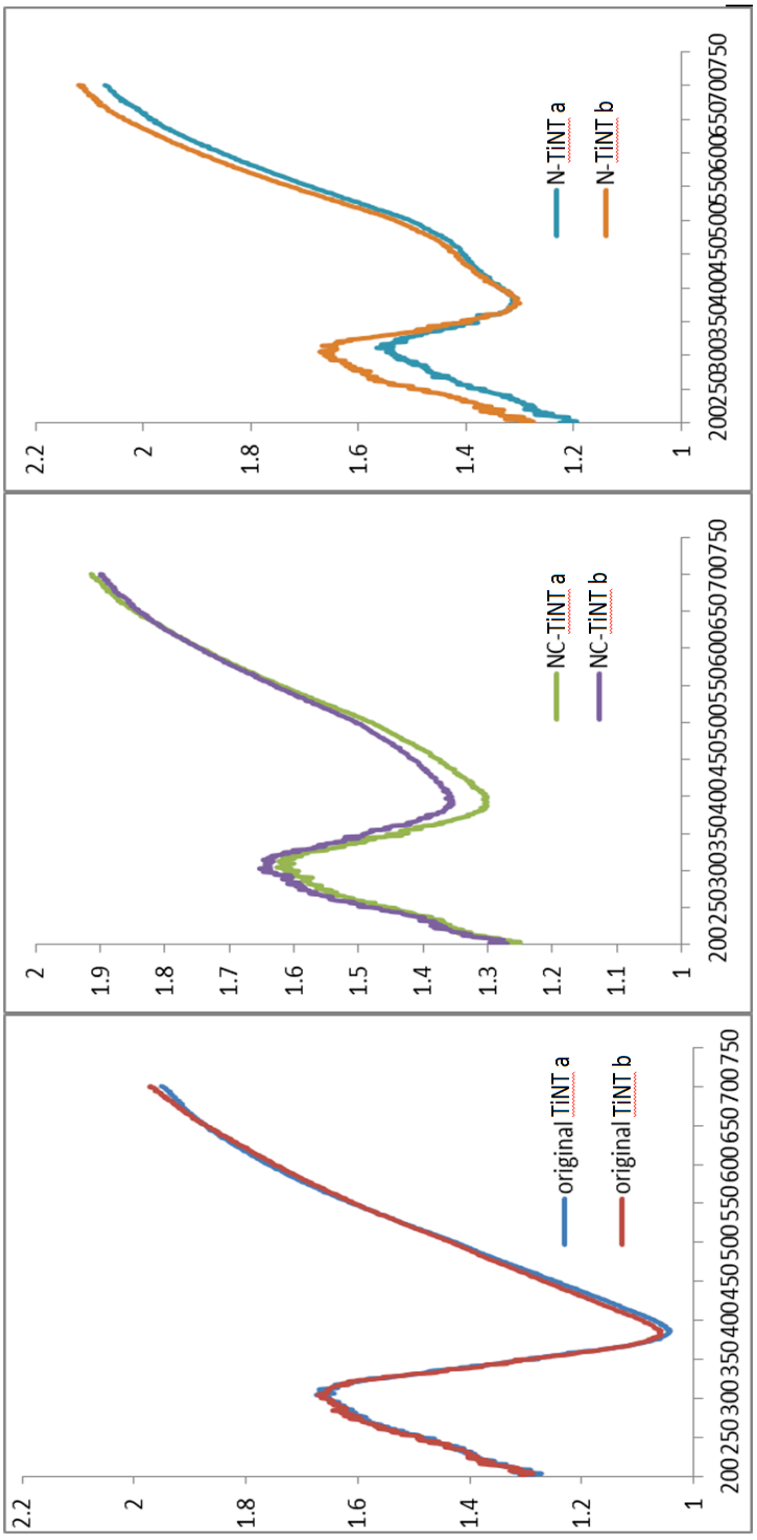

Figure 4.13. Comparison of UV-VIS absorption patterns among reproduced titanium dioxide nanotubes samples

4.3.3. Photocatalytic efficiency of as prepared titanium dioxide nanotube samples

Photocatalytic degradation kinetics of MB with the as prepared original TiNT, N-TiNT and NC-TiNT foils are presented in Fig 4.14 and Fig 4.15 as follows.

TiNT a

TiNT b

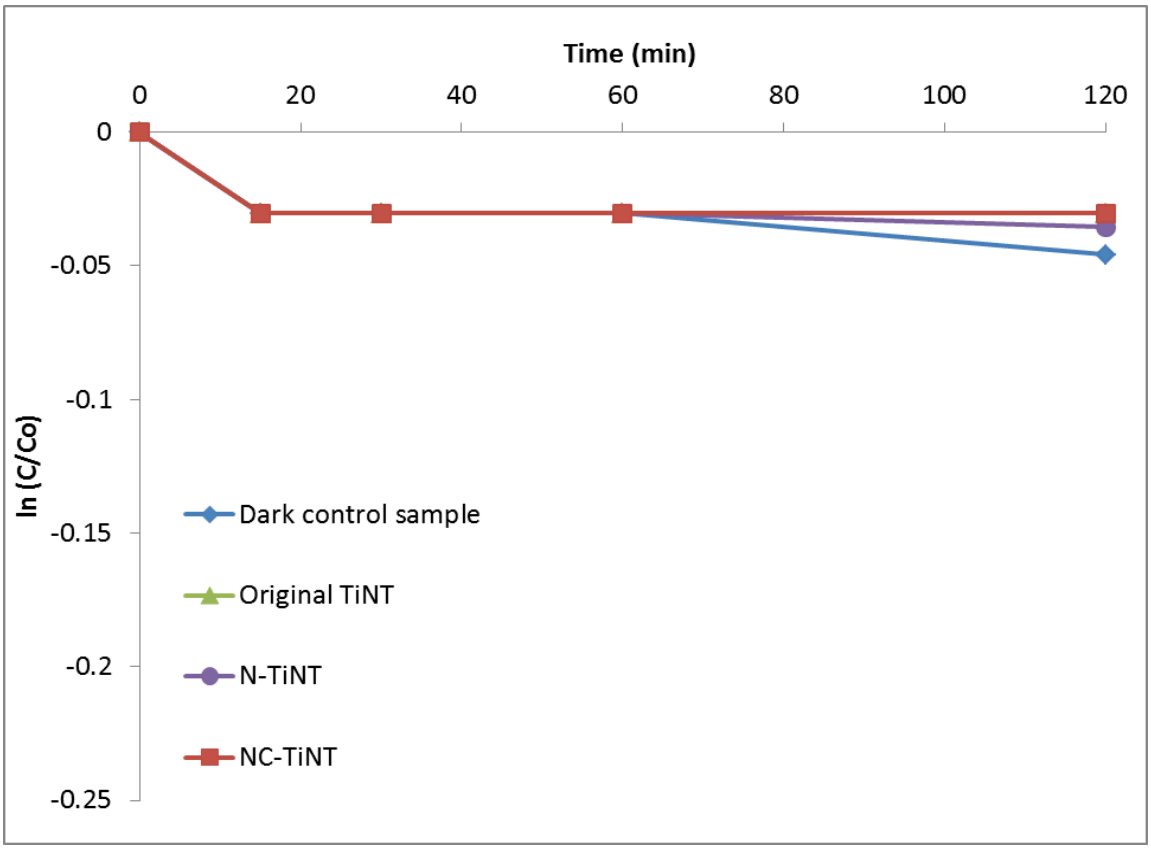

Figure 4.14. Methylene Blue removal with as prepared TiNT foils in dark conditions

(C = concentration of MB at time interval, C_o = initial MB concentration)

Data in Fig 4.14 demonstrated that in the dark tests MB removal rates by TiNT, N-TiNT, NC-TiNT and in the control test (without the photocatalyst) were similar to each other. And a negligible amount of MB was removed in these dark tests, which could be due to the adsorption of MB onto titanium nanotube surface and the reactor walls.

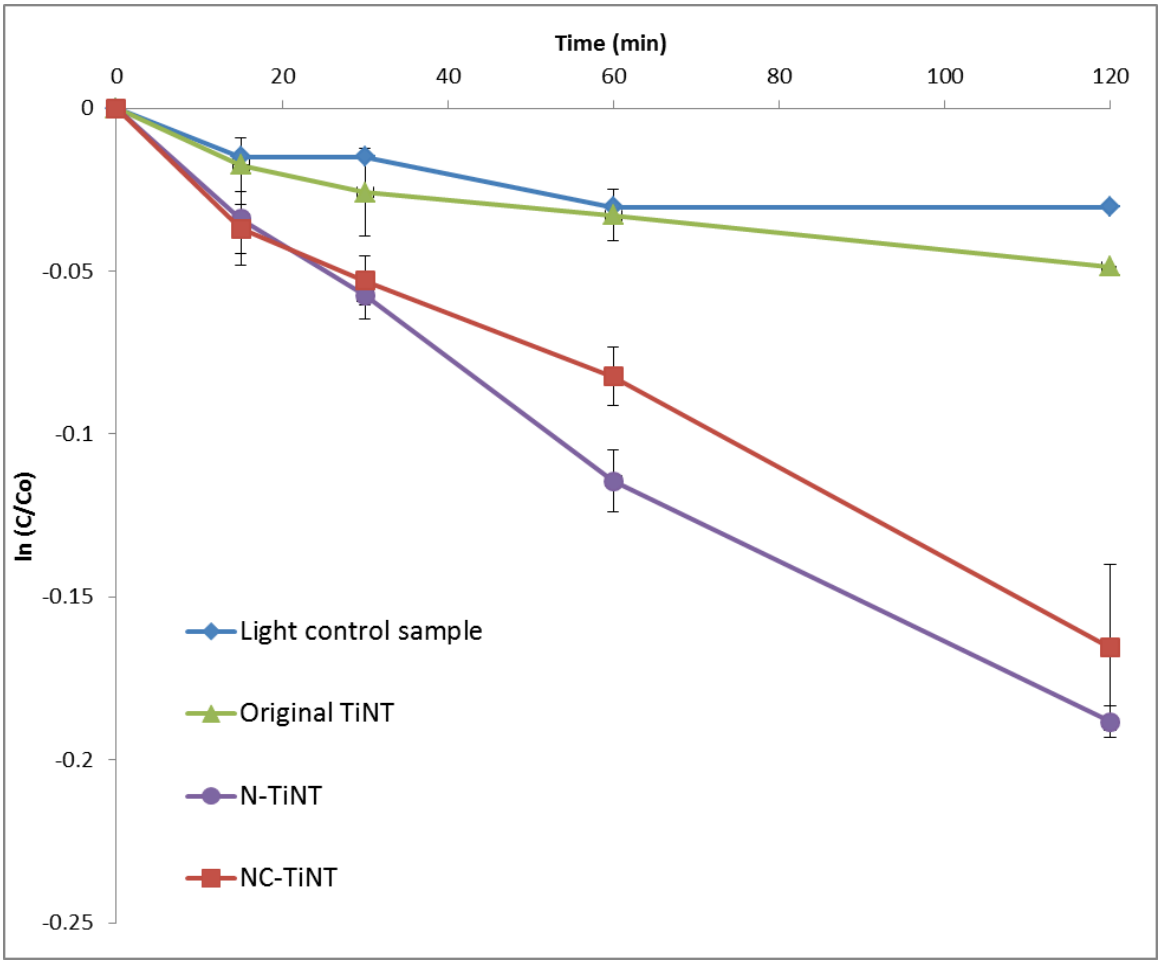

Figure 4.15. Methylene Blue removal with as prepared TiNT foils in light conditions

(C = concentration of MB at time interval, C_o = initial MB concentration)

In the light test, while the control and original TiNT tests still did not show any improved removal of MB comparing to the dark conditions, significant MB removal were observed with N-TiNT and NC-TiNT. More than 50% of MB was removed in 120 minute under the visible light radiation with N-TiNT and NC-TiNT. The removal rates of MB with N-TiNT and NC-TiNT in lighting condition were approximately linear with the

exposing time, indicating that the removal of MB with these catalysts follow a first order kinetics.

As only visible light with radiation > 400 nm was employed for MB degradation test, the results have proven that original TiNT was not activated with visible light as expected, but N-TiNT and NC-TiNT were activated with visible light. Such activation is due to nitrogen-doped TiO_2 nanocrystals resulted from the treatment process with non-thermal plasma as proposed in the hypotheses of the research.

Data in Fig 4.15 also showed that MB removal with N-TiNT was slightly higher than that of NC-TiNT. In the light reflection characterization, the NC-TiNT displayed a slightly better light absorbance than the N-TiNT as presented in Fig above. Thus, if only the light absorbance is considered then the NC-TiNT should display higher photocatalytic efficiency than the N-TiNT; but this was not observed in this research. Varghese et al (Varghese, Gong et al. 2003) reported that the photocatalytic efficiency of TiNT is governed mainly by the total effective surface area or the roughness of TiNT foil. Thus the explanation for the slight increase of MB removal observed with N-TiNT is likely due to the slightly higher total effective surface area of N-TiNT than that of NC-TiNT. As illustrated in SEM images in Fig 4.7 and Fig. 4.9, NC-TiNT surface was more damaged than N-TiNT surface during the plasma treatment due to the potential oxidation as discussed above. Moreover, many nanotubes on the surface layer of NC-TiNT were blocked from the oxidation or from the residue coming from other damaged nanotubes.

These two characters should result in a smaller total effective surface area of NC-TiNT, which then translated into the slightly higher removal of MB with N-TiNT.

4.4. CONCLUSION

TiNT prepared from a common anodization technique was successfully doped with nitrogen by the non-thermal plasma treatment. The doped TiNT showed activation with visible light and improved photocatalytic efficiency in the removal of MB. The material is very promising as a photocatalyst for treating spent water for reuse purposes, especially for areas where have high solar radiation rates but lack of access to safe water resources such as oil and gas fields at sea or in desert. Further experiments will start from this foundation to explore the capabilities as well as the limitations of this material in practical applications with various organic contaminants.

REFERENCES

Chen, X. and S. S. Mao (2007). "Titanium dioxide nanomaterials: Synthesis, properties, modifications and applications." Chemical Reviews **107**(7): 2891-2959.

Fridman, A. (2008). Plasma chemistry. Cambridge ;;New York, Cambridge University Press.

Lieberman, M. (2005). Principles of plasma discharges and materials processing. Hoboken N.J., Wiley-Interscience.

Macak, J. M., H. Tsuchiya, A. Ghicov, K. Yasuda, R. Hahn, S. Bauer and P. Schmuki (2007). "TiO_2 nanotubes: Self-organized electrochemical formation, properties and applications." Current Opinion in Solid State and Materials Science **11**(1-2): 3-18.

Rengifo-Herrera, J. A., J. Kiwi and C. Pulgarin (2009). "N, S co-doped and N-doped Degussa P-25 powders with visible light response prepared by mechanical mixing of thiourea and urea. Reactivity towards E. coli inactivation and phenol oxidation." Journal of Photochemistry and Photobiology A: Chemistry **205**(2–3): 109-115.

Varghese, O. K., D. Gong, M. Paulose, C. A. Grimes and E. C. Dickey (2003). "Crystallization and high-temperature structural stability of titanium oxide nanotube arrays." Journal of Materials Research **18**(1): 156-165.

Zwilling, V., E. Darque-Ceretti, A. Boutry-Forveille, D. David, M. Y. Perrin and M. Aucouturier (1999). "Structure and Physicochemistry of Anodic Oxide Films on Titanium and TA6V Alloy." Surface and Interface Analysis **27**(7): 629-637.

CHAPTER 5

ELECTROSPINNING AND IN SITU NITROGEN DOPING OF TITANIUM DIOXIDE/POLYACRYLONITRILE NANOFIBERS WITH PHOTOCATALYTIC ACTIVATION IN VISIBLE LIGHTS

(* This chapter has been published in Materials Letters ,Volume 82, 1 September 2012, Pages 102–104**)**

ABSTRACT

Titanium dioxide (TiO_2) nanofibers prepared by electrospinning method usually exhibit poor mechanical properties. In actual applications for water treatment, these fibers are easily broken into smaller pieces and a separation step is therefore required to recover the TiO_2 nanomaterials. In this research, visible light activated Titanium dioxide/Polyacrylonitrile (PAN) nanofibers have been prepared by the electrospinning process from Titanium isopropoxide (TIIP), PAN, and Dimethyl sulfoxide (DMSO) as solvent. The as prepared mat of nanofibers retained the original morphology and showed high photocatalytic efficiency under visible lights for the degradation of methylene blue (MB) in water, together with stable mechanical properties. This type of material might find wide environmental applications.

5.1. INTRODUCTION

Since the discovery of photocatalytic effect under UV radiation by Honda and Fujisima in the 70s (Fujishima and Honda 1972), many forms of titanium dioxide (TiO_2)

nanomaterial have been prepared and studied such as nanoparticle, nanotube, nanowire, nanorod, and nanosheet (Chen and Mao 2007). Among these forms, those nanotube and nanofiber with the 1-D characteristic, which is to have one dimension many times longer than the other ones, are of particular interest. These forms not only provide a high effective surface area but also a defined flow pattern resulted from geometrical characteristics, both of which greatly contribute to the improved efficiency of TiO_2 nanocrystals in practical applications (Macak, Tsuchiya et al. 2007; Chandrasekar, Zhang et al. 2009). Between nanotube and nanofibers, the latter has several advantages compared to the former. The preparation of TiO_2 nanotubes are mostly via the anodization of metallic titanium foil in solvents containing fluoride ion (Macak, Tsuchiya et al. 2007), which is inefficient for large scale applications. TiO_2 nanofibers can be prepared via the simpler, higher yield and lower cost electrospinning process (Chandrasekar, Zhang et al. 2009), and there is a great potential to use TiO_2 nanofiber in photooxidation processes, especially for the removal of organic pollutants in environmental systems.

Recently, many efforts have been carried out to prepare TiO_2 nanofibers by the electrospinning method, focused on two directions. The first direction is to electrospin an electrospinning dope containing a mixture of a spunable polymer and a TiO_2 precursor in an appropriate solvent (Li and Xia 2003; Chandrasekar, Zhang et al. 2009). In the second direction, the polymer is electrospun to create the template mat, then coated with TiO_2 precursors through immersion of the mat in a TiO_2 precursor solution in a separate step (Drew, Liu et al. 2003). Both preparation approaches, however, use an annealing step at

500-600^{o}C to create and activate TiO_2 nanocrystalllite within the prepared materials. During such annealing process, the organic polymer acting as a template is burnt off, leaving a porous mat containing hollow and pure TiO_2 nanofibers (Li and Xia 2003; Chandrasekar, Zhang et al. 2009). Inherently, such annealed TiO_2 nanofibers are highly unstable in term of mechanical properties, which in turn may limit their applications (Kim, Cho et al. 2010). In particular during their applications in aqueous photooxidation processes, these hollow nanofibers are easily broken into smaller pieces, so a separate separation step is required to recover the material. There is a critical need to improve the mechanical stability of TiO_2 nanofibers for such environmental engineering applications.

In addition, original TiO_2 nanomaterial can only activated with UV radiation due to the high energy band gap. As UV radiation is widely known to make up less than 10% of total solar radiation to the earth surface, the photocatalytic efficiency of pure TiO_2 nanomaterial was considered as limited. Therefore, there have been extensive studies to modify TiO_2 with a wide selection of dopants to narrow the original band gap and enable doped TiO_2 nanomaterials to be activated with visible lights. Among the experimented dopants, nitrogen and carbon are the most popular, and N-, C- and combined N and C-doped TiO_2 nanomaterials have been confirmed to be activated with visible light (Chen and Mao 2007).

To address the above mentioned mechanical stability issue and to achieve the visible light activated TiO_2 nanofiber, we aim to prepare the visible light activated TiO_2/PAN nanofibers with a simple electrospinning set up in this study. PAN has the

melting point of 317°C and crystalline anatase has been reported to form around 300°C from amorphous TiO_2 (Kim, Cho et al. 2010). Our hypothesis is that by preparing the TiO_2/PAN nanofibers via the electrospinning process, followed by anneal at around 300°C, the as-prepared nanofibers could retain the PAN template with anatase TiO_2 within the nanofiber structure. In addition, PAN could provide carbon and nitrogen for the potential doping of TiO_2 crystals during the annealing process. As a result, the as prepared TiO_2/PAN nanofibers might exhibit not only visible light activation but also better mechanical properties.

TiO_2/PAN nanofibers have been prepared in several studies. One group chose to prepare the PAN nanofibers first, then coated the fibers with TiO_2 nanocrystals (Im, Kim et al. 2008). The other groups prepared the TiO_2/PAN via the *in situ* electrospinning process, but did not investigate the photocatalytic efficiency of the prepared material (Hong, Li et al. 2006; Qiu and Yu 2008). All above studies used N,N dimethyl formanide (DMF) as the solvent for the polymer. In this study, we proposed to use DMSO in our preparation for two reasons. First, DMF is widely known to be a more toxic solvent and being gradually replaced in the industry, so it is desirable not using DMF. Second, the electrospinning of PAN in DMF require a high temperature to avoid solidification of the electrospun dope (Im, Kim et al. 2008). By using DMSO, we could carry out all preparation steps at room temperature. To our best knowledge, ours is the first effort to prepare TiO_2/PAN nanofibers via *in situ* electrospinning with DMSO as solvent at room temperature. This process if successful will offer a simple, low cost, high throughput and a green approach to prepare TiO_2 nanomaterials for practical applications.

5.2. EXPERIMENTAL

5.2.1. Materials

Titanium (IV) isopropoxide (TIIP, CAS 546-68-9) and acetone (CAS 67-64-1) were purchased from Sigma Aldrich (St Louis, Missouri). Polyacrylonitrile (PAN, CAS 250014-41-9, MW= 150,000) was purchased from Scientific Polymer Production Inc. (Ontario, New York). Dimethyl sulfoxide (DMSO, CAS 67-68-5) and methylene blue (MB, CAS 61-73-4) were purchased from Fisher Scientific (Fairlawn, New Jersey). Titanium dioxide P25 (P25, CAS 13463-67-7) was purchased from Degussa Corporation (Ridgefield Park, New Jersey). All chemicals were used without any further purification.

5.2.2. Electrospinning

An electrospinning dope was prepared as follows. At the beginning, 2 g of PAN powder was added into 10 ml of DMSO in a beaker then mixed by a magnetic stirrer in 24 hours to give a vicious and transparent polymer solution. Then 3 ml of this solution was vigorously mixed with 0.5 ml of acetone in a small glass vial in 1 hour. Still under vigorous mixing condition, 1 ml of TIIP was dropwisely added into the above mixture. The whole solution was mixed for 1 hour before loaded into a syringe for electrospinning.

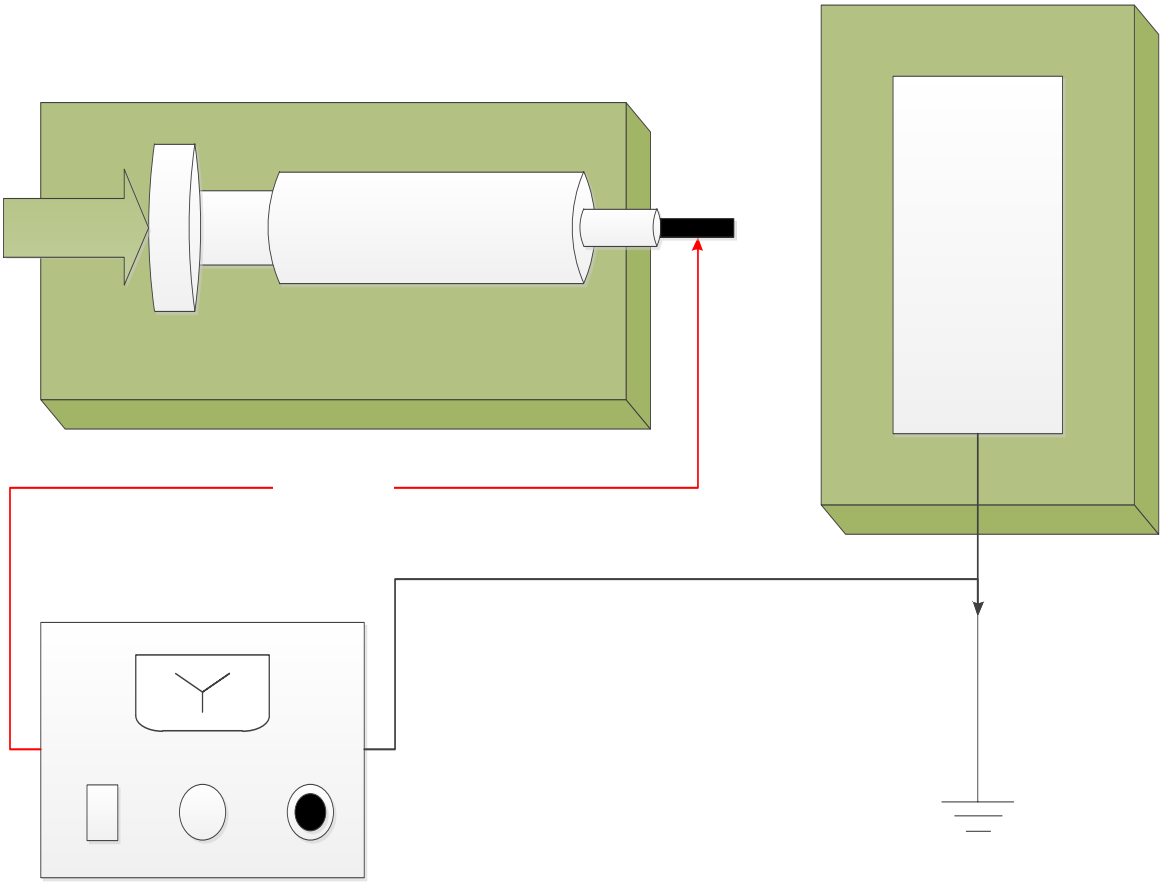

Figure 5.1. Instrumental set up for electrospinning of TiO_2/PAN nanofiber

The syringe needle diameter is of 22 G, and connected to a high voltage direct current power supply (ES30P-5W, Gamma High Voltage Research Inc., Ormond Beach, Florida). A grounded aluminum foil was used as a collector and placed 10 cm below the needle tip. Collectors were changed several times during the electrospinning. A voltage of 14 kV was applied between the needle and the collector. Pumping was provided by a syringe pump (Series 74900, Cole-Parmer Instrument Co.) at the rate of 0.025 ml/min. All of the above preparations were undertaken inside a fume hood at room temperature.

5.2.3. Post preparation and annealing

After the electrospinning process was completed, the electrospun mat was left intact inside the fume hood for 24 hours for the mat to be stabilized. The mat was then dried in a vacuum drier for 30 minutes, followed by rinsing several times with deionized (DI) water, then placed in DI water for 24 hours to allow a complete hydrolysis of TIIP. The mat was subsequently dried in an oven at 105^{o}C for 5 hours, annealed at 300^{o}C in a muffle furnace for 6 hours with the heating rate of 5^{o}C/min, and slowly cooled down to room temperature prior to storage and use.

5.2.4. Characterizations

The annealed TiO_2/PAN mats were examined for Scanning Electron Microscopy (SEM) and Electron Dispersive X-ray Spectroscopy (EDS) by FEI Quanta 600 FEG ESEM. Thin film X-ray diffraction of the annealed mat was acquired by Scintag Pad V (CuKα radiation, detector solid Si, scan rate of 1^{o}/min). The annealed mat was also subjected to an UV-VIS reflection characterization using a Shimadzu UV-VIS Recording Spectrophotometer UV2401PC.

5.2.5. Degradation of methylene blue under visible light

0.05 g of the as-prepared mat of TiO_2/PAN nanofibers was immersed into a beaker containing 20 ml solution of 0.5 parts per million (ppm) MB. The beaker was first kept in a close container for 12 hours so any adsorption of MB on the glass wall, if there

was any, would have been stabilized before start of the degradation tests. A Xenon lamp of 300 W was used as a light source. Optical filters were applied to the Xenon lamp to filter out radiations those are less than 400 nm and greater than 600 nm. At each time interval, 1 ml of the MB solution was withdrawn and its optical absorbance was measured at 670 nm by the spectrophotometer (Genesys 20, Thermo Scientific)

For comparison purpose, the similar experiment was carried with a thin film of P25 TiO_2. The preparation of thin film P25 is as follows. 0.015 g of P25 was dispersed in 3 ml of Isopropyl alcohol 70% via sonication in 20 minutes. The whole solution was transferred to a square glass slide of 1.5 cm x 1.5 cm, then finally heated at 105^oC in 2 hours to create a thin coating film of P25 on surface of the glass slide.

5.3. RESULTS AND DISCUSSION

After the electrospinning process, the collected fibers exhibited a white-yellow color, which changed into brown color after the annealing process. The annealed mat was also significantly reduced in size, only about one third of the original electrospun mat.

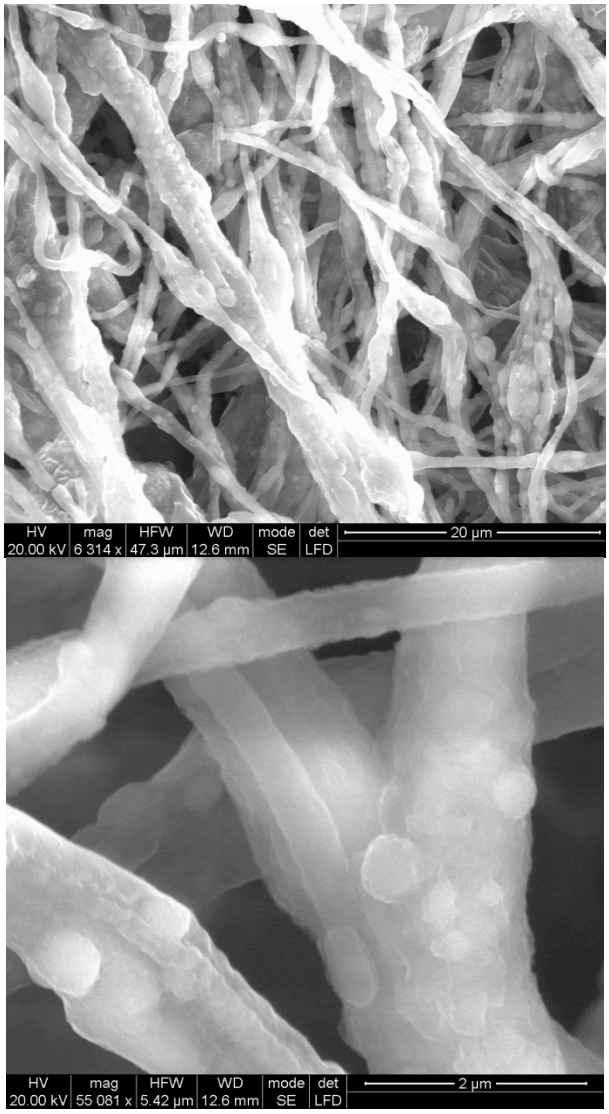

Figure 5.2. SEM images of the annealed TiO_2/PAN nanofibers

Fig 5.2 is the SEM images of annealed TiO_2/PAN nanofibers, showing that annealed TiO_2/PAN retained the fibrous shape, with fiber diameters ranged from approximate 200 nm to greater than 1 µm. The diameter of collected fibers is consistent with the diameter of the needle tip used in the electrospin. The larger needle tip was needed because the electrospun mixture showed the tendency of blocking the flow rapidly within 20-30 minutes under room temperature when needles with smaller

diameters were applied. DMSO has the boiling point of 189^{o}C and evaporates slowly at room temperature. We observed that as soon as TiO_2/PAN nanofibers deposited on the collecting foil, they quickly combined together to form larger fibers because the outer layer of the fibers were not solidified yet. While this issue could be overcome by using a constant rotating collector, we found that by adding acetone, the fluidity and the evaporation rate of the electrospun mixture could be improved, which helped the electrospinning of TiO_2/PAN fibers. However, the addition of acetone also decreased the viscosity of the electrospinning solution, which in turn resulted in many beads formed among fibers during the electrospinning process.

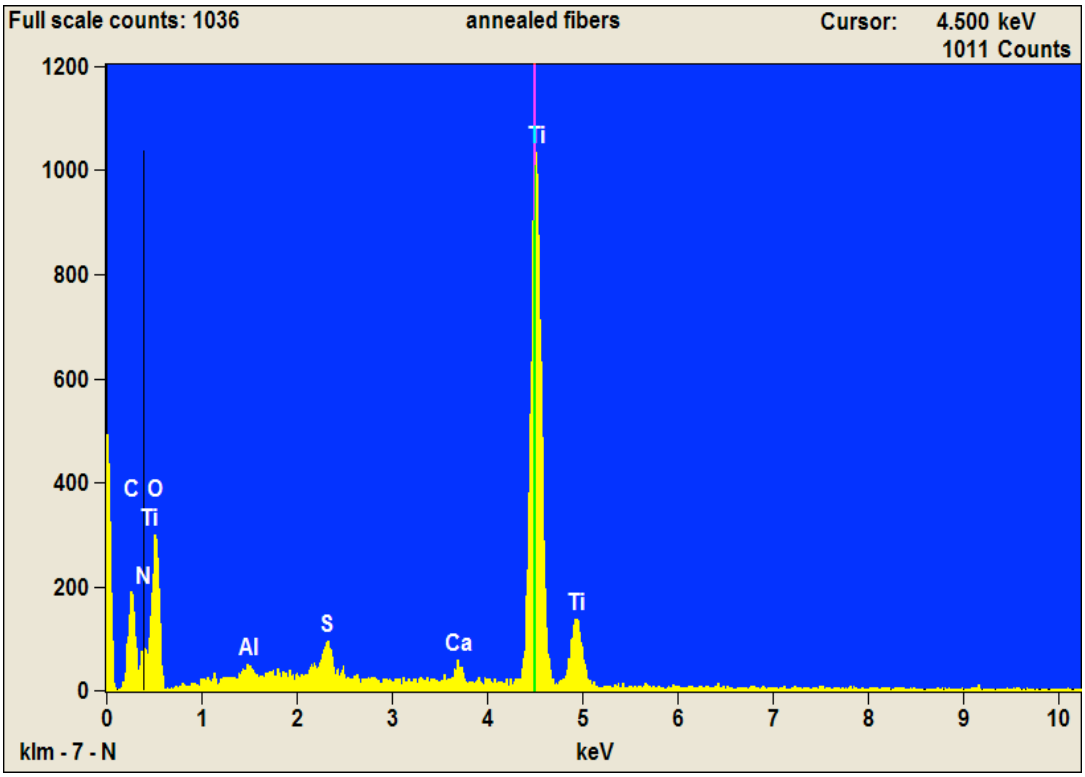

Figure 5.3. Qualitative EDS characterization of annealed TiO_2/PAN nanofibers

Fig 5.3 shows the EDS spectra that confirmed the presence of TiO_2 on the nanofibers. The overall annealed mat is highly porous and a large portion of TiO_2 deposits are under the "nodules" forms. Both of these features can result in a greater total effective surface area of material. The annealed mat of TiO_2/PAN can be rinsed with the water jet from laboratory DI water bottle and transferred among containers by tweezers without being broken as showed in Fig 5.4. These features imply that the annealed TiO_2/PAN nanofibers exhibits better mechanical properties and therefore would be highly suitable for environmental engineering applications.

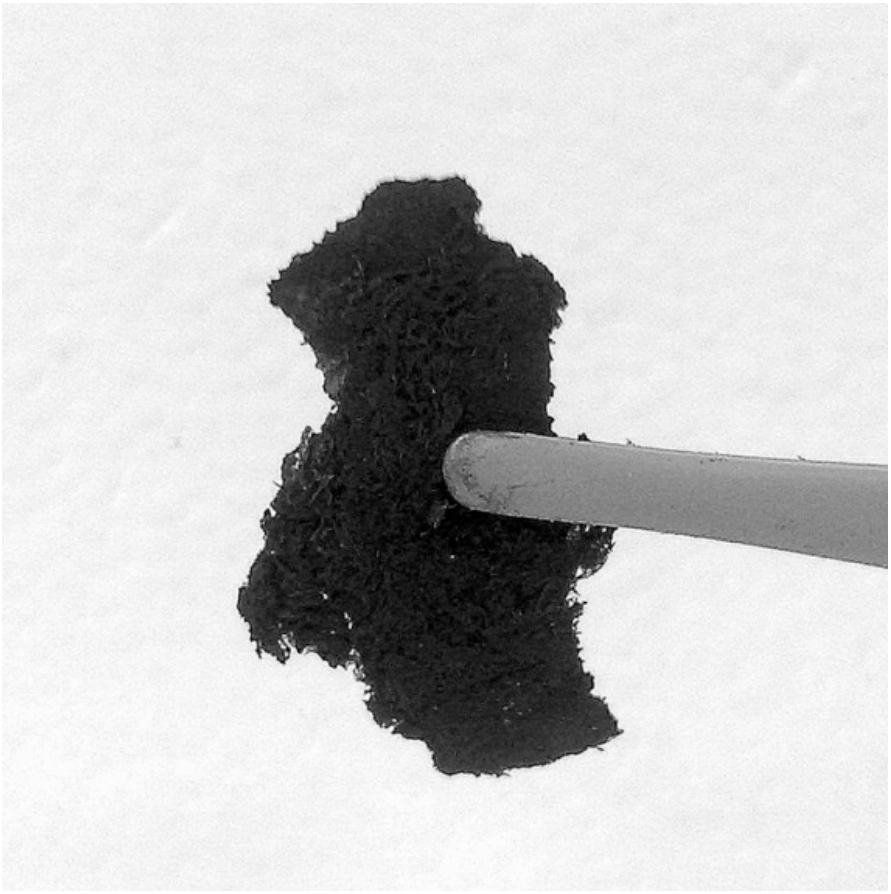

Figure 5.4. Annealed mat of TiO_2/PAN nanofibers picked up by tweezers

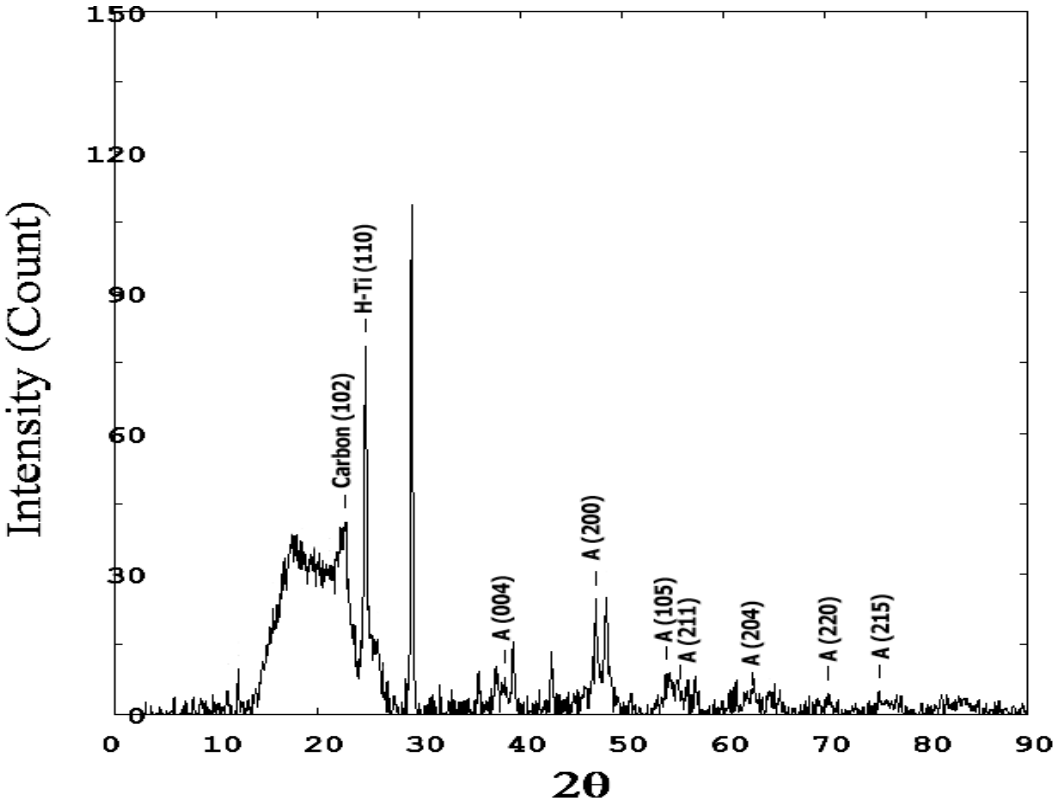

Figure 5.5. XRD pattern of TiO_2/PAN nanofibers

The XRD pattern of the annealed fibers (Fig 5.5) showed a broad peak around 2θ = 22.7^o that can be assigned for carbon (Im, Kim et al. 2008). The sharp peak at 2θ = 24.7^o suggests that the major crystal morphologies of TiO_2 in the nanofibers are hydrogen titanates (H-Titanates) (Mao and Wong 2006). H-Titanates are usually formed at around 300^{o}C during the anneal of hydrolyzed amorphous TiO_2, and could be transformed to anatase at higher temperature of 400-600^{o}C as reported in the literature (Yu, Yu et al. 2007). In our sample, however, while the major XRD peak of anatase at 2θ = 25.3^o (plane 101) could not be observed, which may be due to overlapping from the strong peak of H-Titanate, other weak peaks of anatase at 38.4^o, 48.4^o, 54.4^o, 55.7^o, 62.9^o, 70.3^o and 75.3^o corresponding to planes (004), (200), (105), (211), (204), (220) and (215) respectively are

visible. This indicates that a portion of H-Titanates has been converted into anatase in the annealed nanofibers in this study.

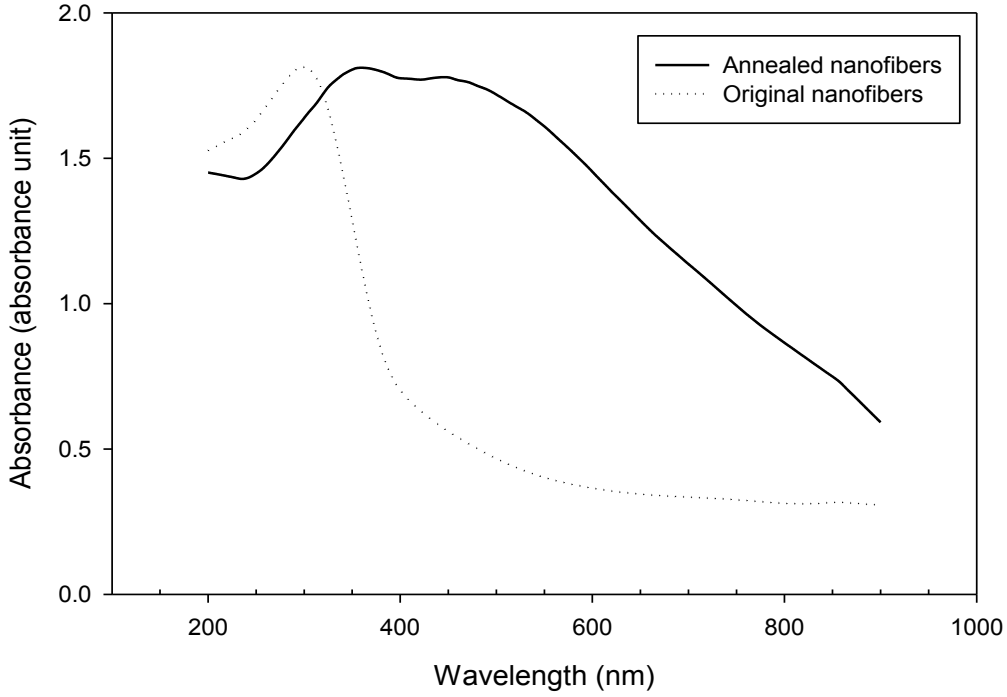

Figure 5.6. UV-VIS absorbance of as prepared nanofibers mats

The UV-VIS spectra of as prepared TiO_2/PAN nanofibers are showed in Fig 5.6 above. In the annealed mat, the absorption band was in the UV zone of wavelength < 330 nm. This is in agreement with the UV-VIS spectra of H-titania prepared by the other group previously (Mao and Wong 2006). After the annealing process, the peak absorption band shifted to 370-390 nm, proving that H-titania has been converted at least partially into anatase during the annealing process.

After the annealing process, the peak absorption band shifted to 350-390 nm, suggesting that H-titanate was converted into anatase during the annealing process.

Moreover, the near flat absorption edge extended far beyond the wavelength of 400 nm to the visible light zone, which likely results from the nitrogen-doped TiO_2, because it is well known that pure anatase TiO_2 has its light absorption sharply cut off in the UV zone before 400 nm. Additionally, a dark brown color of the annealed mat was observed following the carbonization of TiO_2/PAN nanofibers, which was consistent with the absorption increases in the visible light region.

Photocatalytic degradation kinetics of MB removal in the presence of the as-prepared TiO_2/PAN nanofibers are presented in Fig 5.7.

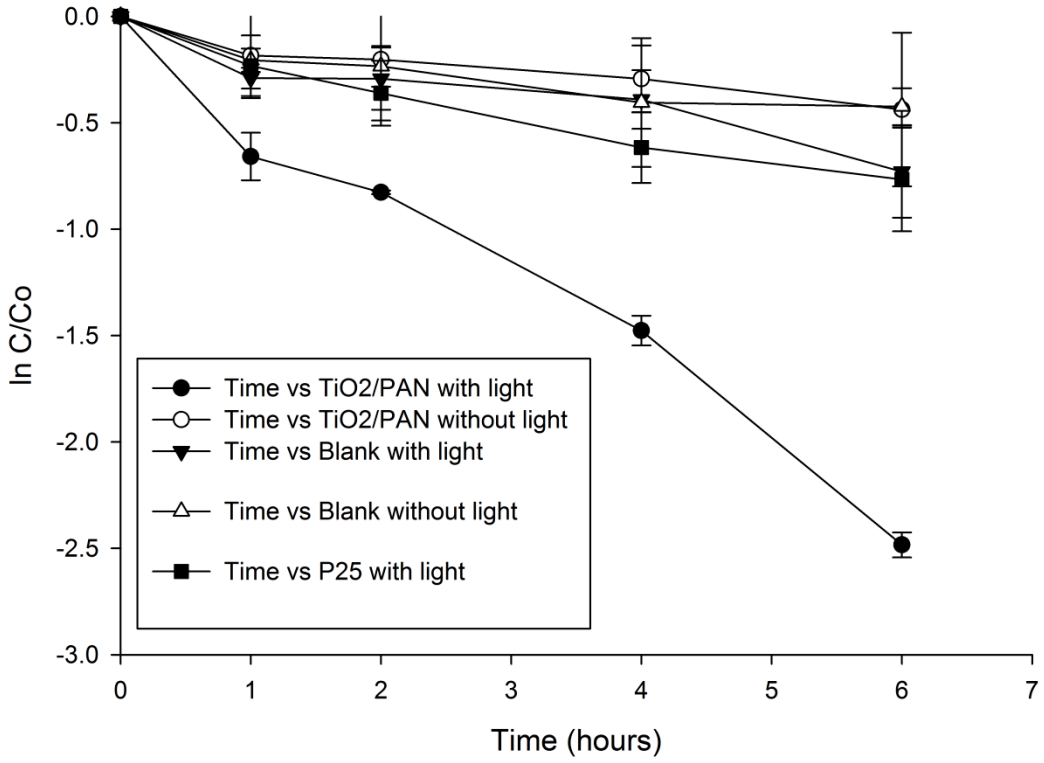

Figure 5.7 Catalytic degradation of methylene blue (MB) by the TiO_2/PAN nanofibers under visible light

(C = MB concentration at the time of sampling; Co = initial MB concentration)

Small amounts of MB removal were observed in blank samples (without any photocatalyst) in both light and dark conditions, which were attributed to the adsorption of MB to the reactor walls. MB removal rates observed with P25 exposed to visible light and with TiO_2/PAN nanofibers without light were similar to those in the blank samples. The results indicated that P25 was not activated with visible lights with a wavelength greater than 400nm. In the system with the TiO_2/PAN nanofibers that was exposed to visible lights, approximately 91.6% of MB was removed in 6 hours. Because H-titanate was reported to exhibit insignificant photocatalytic efficiency (Yu, Yu et al. 2007), the catalytic photooxidation of MB must be resulted from TiO_2 anatase crystals within TiO_2/PAN nanofibers. Moreover, the activation in the visible light suggests that TiO_2 anatase crystals have been doped to some degree with carbon or nitrogen as expected.

The results showed that the annealed TiO_2/PAN exhibits much higher photocatalytic efficiency in the visible light compared to P25, which is the current standard for TiO_2 applications as photocatalyst in the industry.

5.4. CONCLUSIONS

TiO_2/PAN nanofibers were successfully prepared by a simple electrospinning setup, at room temperature and with an environmentally-friendly solvent, DMSO. The annealed fibers still retain the fibrous forms and exhibit better mechanical properties during handling processes. Moreover, TiO_2 anatase crystals were grown within TiO_2/PAN nanofibers and doped with carbon and/or nitrogen during the annealing process at 300 ^{o}C,

resulting in the activation of the material in visible light. With the high photocatalytic efficiency, adequate mechanical properties, and easy preparation, TiO_2/PAN nanofibers are expected to have many environmental applications, including degradation of organic waste in industrial streams, treatment of produced water in oil and gas production industries, indoor air pollution treatment, and disinfections of water and living space. Further efforts are underway to improve the electrospinning process to produce smaller and more homogenous fibers, to understand the doping process for further enhancement of the photocatalytic efficiency, and explore industrial applications of the TiO_2/PAN.

REFERENCES

Chandrasekar, R., L. Zhang, J. Y. Howe, N. E. Hedin, Y. Zhang and H. Fong (2009). "Fabrication and characterization of electrospun titania nanofibers." Journal of Materials Science **44**(5): 1198-1205.

Chen, X. and S. S. Mao (2007). "Titanium dioxide nanomaterials: Synthesis, properties, modifications and applications." Chemical Reviews **107**(7): 2891-2959.

Drew, C., X. Liu, D. Ziegler, X. Wang, F. F. Bruno, J. Whitten, L. A. Samuelson and J. Kumar (2003). "Metal oxide-coated polymer nanofibers." Nano Letters **3**(2): 143-147.

Fujishima, A. and K. Honda (1972). "Electrochemical Photolysis of Water at a Semiconductor Electrode." Nature **238**(5358): 37-38.

Hong, Y., D. Li, J. Zheng and G. Zou (2006). "Sol-gel growth of titania from electrospun polyacrylonitrile nanofibres." Nanotechnology **17**(8): 1986-1993.

Im, J. S., M. I. Kim and Y. S. Lee (2008). "Preparation of PAN-based electrospun nanofiber webs containing TiO_2 for photocatalytic degradation." Materials Letters **62**(21-22): 3652-3655.

Kim, Y. B., D. Cho and W. H. Park (2010). "Fabrication and characterization of TiO_2/poly(dimethyl siloxane) composite fibers with thermal and mechanical stability." Journal of Applied Polymer Science **116**(1): 449-454.

Li, D. and Y. Xia (2003). "Fabrication of titania nanofibers by electrospinning." Nano Letters **3**(4): 555-560.

Macak, J. M., H. Tsuchiya, A. Ghicov, K. Yasuda, R. Hahn, S. Bauer and P. Schmuki (2007). "TiO_2 nanotubes: Self-organized electrochemical formation, properties and applications." Current Opinion in Solid State and Materials Science **11**(1-2): 3-18.

Mao, Y. and S. S. Wong (2006). "Size- and shape-dependent transformation of nanosized titanate into analogous anatase titania nanostructures." Journal of the American Chemical Society **128**(25): 8217-8226.

Qiu, Y. and J. Yu (2008). "Synthesis of titanium dioxide nanotubes from electrospun fiber templates." Solid State Communications **148**(11-12): 556-558.

Yu, H., J. Yu and B. Cheng (2007). "Photocatalytic activity of the calcined H-titanate nanowires for photocatalytic oxidation of acetone in air." Chemosphere **66**(11): 2050-2057.

CHAPTER 6

APPLICATION OF 1-DIMENSIONAL TITANIUM DIOXIDE NANOMATERIALS FOR THE PHOTOCATALYTIC DEGRADATION OF BENZENE, TOLUENE, ETHYLBENZENE AND XYLENE (BTEX) IN WATER UNDER VISIBLE LIGHT

ABSTRACT

1-dimensional titanium dioxide (TiO_2) nanomaterials including nanotubes and nanofibers were prepared to achieve activation under visible light with novel processing techniques. Nitrogen doped-TiO_2 nanotubes (N-TiNT) were prepared by anodization followed by plasma treatment, and N-doped TiO_2 nanofibers (N-TiO_2/PAN) were prepared by electrospinning with polyacrylonitrile as the template polymer. The photocatalytic efficiency under visible light of the two prepared 1-dimensional TiO_2 nanomaterials was investigated for the degradation of benzene, toluene, ethylbenzene, and m-xylene (BTEX), which are contaminants regularly found in produced water from oil and gas production activities. From the comparison of effectiveness among using the as prepared TiO_2 photocatalysts with other available techniques for treatment of produced water for reuse purpose, implications on the potential and limitation of the photooxidation process were provided.

6.1. INTRODUCTION

Aromatic hydrocarbons commonly found in produced water from oil and gas activities are hazardous to human and the environment. There is a need to develop more effective and efficient remediation techniques targeting these compounds, in the light of achieving safe reuse and discharge of produced water.

Advanced oxidation processes have been widely studied for treating hydrocarbon contaminated water. These processes explore high oxidizing power of hydroxyl radical $OH^{\cdot}$ in aqueous phase to oxidize organic carbons into the less harmful inorganic carbonates and carbon dioxide (Linsebigler, Lu et al. 1995). There is no involvement of oxidizing agents containing halogenous elements, so that the risk of forming harmful intermediates from the treatment process is much reduced. Among these advanced oxidation processes, the classic TiO_2/UV light system was one of the most widely applied methods (Chen and Mao 2007). Effective removal of petroleum-origin hydrocarbons in contaminated water, including aromatics such as BTEX, in contaminated water has been reported by the application of TiO_2/H_2O_2/UV light (Cho, Kim et al. 2006). Nevertheless, the known limitation of UV lights in solar radiation makes it impractical to build a solar system for treatment of these hazardous compounds in contaminated water on field, where direct uses of solar radiation are highly desirable because the approach could be more sustainable and economical.

The objective of this study was to investigate the application of modified 1-D titanium dioxide nanomaterials that have been proven to be activated with visible light, in the treatment of BTEX in produced water. Based on the collected results, implications on the future applicability of TiO_2 nanomaterials in practical water engineering application are discussed.

6.2. EXPERIMENTAL

6.2.1. Materials

6.2.1.1. Materials for the preparation of modified 1-D titanium dioxide nanomaterials

Titanium metal foil 0.25mm thick, 99.7% metal basis (Ti, CAS 7440-32-6) and hydrofluoric acid A.C.S reagent grade 48% (HF, CAS 364-39-3) were purchased from Sigma Aldrich (St Louis, Missouri). Ultra high purity-grade nitrogen gas (N_2) was purchased from Air-Gas (Columbia, Missouri). Titanium (IV) isopropoxide (TIIP, CAS 546-68-9) and acetone (CAS 67-64-1) were purchased from Sigma Aldrich (St Louis, Missouri). Polyacrylonitrile (PAN, CAS 250014-41-9, MW= 150,000) was purchased from Scientific Polymer Production Inc. (Ontario, New York). Dimethyl sulfoxide (DMSO, CAS 67-68-5) was purchased from Fisher Scientific (Fairlawn, New Jersey).

6.2.1.2. Preparation and characterization of modified 1-D titanium dioxide nanomaterials

From the stock materials as listed above, two types of modified 1-D titanium dioxide nanomaterials were prepared. The nitrogen-doped titanium dioxide nanotube (N-TiNT) was prepared through plasma treatment of anodized titanium metal foil, and the nitrogen-doped titanium dioxide/polyacrylonitrile nanofiber (N-TiO_2/PAN) was prepared via electrospinning of a spinning dope containing TIIP and PAN. Characterizations including SEM, TEM, XRD, EDS and UV-VIS were carried out for the as prepared N-TiNT and N-TiO_2/PAN catalysts.

Details of the preparation and characterization of N-TiNT and N-TiO_2/PAN catalysts have been described in previous Chapters 4 and 5 of this dissertation.

6.2.1.3. Materials for BTEX degradation experiments

Materials including benzene (CAS 71-43-2), toluene (CAS 108-88-3), ethyl benzene (CAS 100-41-4) and m-xylene (CAS 103-38-3) were used without any further purification.

6.2.2. Degradation of BTEX under visible light

A stock mixture of BTEX was prepared from 5.0 mL of benzene, 5.0 mL of toluene, 0.50 mL of ethyl benzene, and 2.50 mL of m-xylene. Composition of the above mixture was selected based on data reported in literature (Veil, Puder et al. 2004; Cho, Kim et al. 2006) in order to mimic the regular produced water in real world. Quantities of each BTEX components are listed in Table 6.1 as follows.

Table 6.1. Composition of BTEX stock solution

	Quantity (mL)	Mass (g)	TOC (g)	TOC (%)
Benzene	5.00	4.37	4.03	39.0
Toluene	5.00	4.34	3.95	38.3
Ethyl benzene	0.50	0.43	0.39	3.8
m-Xylene	2.50	2.16	1.95	18.9
Total	13.00	11.30	10.33	100

The stock mixture was stored in a closed vial and kept in the fridge when not using. For each degradation test, 10 µl of the stock BTEX mixture was added into the dark glass container with 120 mL of double distilled (DD) water, which then acted as the working solution in the experiment.

Illustration of experimental set up for the BTEX photocatalytic degradation test is provided in Fig 6.1 as below.

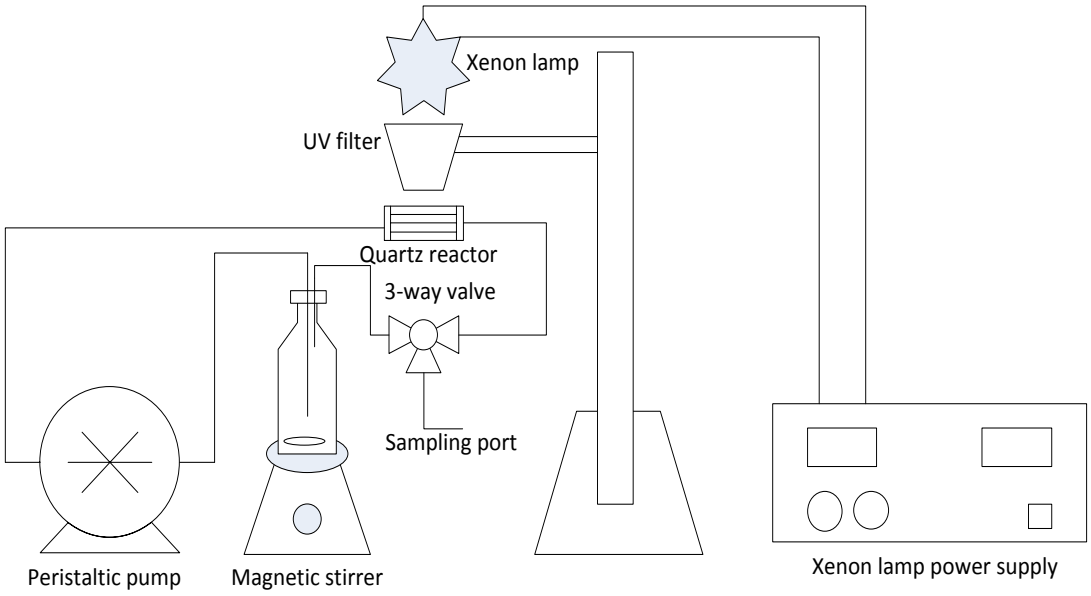

Figure 6.1. Experimental set up for the BTEX photocatalytic degradation test

As presented in Fig 6.1, the experimental set up included a dark glass bottle which acted as the container containing 120 mL of BTEX working solution, and a quartz tube of ~ 8 mL which acted as the main reactor of the whole system. BTEX working solution was circulated between the container and the reactor by a peristaltic pump, while constant mixing was provided via the magnetic stirrer for the container. The as prepared photocatalyst was placed in the middle section of the reactor. N-TiNT photocatalyst sample was provided in the form of a square film of 1 cm x 1 cm (with the template of titanium metal foil of 0.025 cm thick). Annealed TiO_2/PAN nanofibers were provided in the form of a mat of 0.02 g. A xenon lamp of 300W was provided with an UV filter directly above the quartz reactor so a stable working visible light was available for the photocatalytic degradation of BTEX.

Prior to turning on the lamp in each test, the BTEX working solution was circulated inside the system for 2 hours to minimize effects of adsorption and evaporation processes if there were any. Then at each time interval, 2.5 mL of BTEX solution was withdrawn from the 3-way valve into a glass vial, which was then sealed with plastic cover for determining total organic carbon (TOC). The analysis of TOC was carried out using Shimadzu TOC-V total organic carbon analyzer coupled with ASI-V autosampler. The conditions of the analysis are described as below:

- Number of determinations (per sample): 4
- Number of wash (with DI water): 2
- Acid (HCl 2N) add: 2%
- Sparge time: 6:00 min
- Injection volume: 50.0 μL

The detection limit of the TOC-V is 400 μg/L of TOC. Further supporting information of the TOC analysis and Shimadzu TOC-V instrument is given in section Supporting Information of this chapter.

During the experiments carried out with N-TiO_2/PAN nanofibers, samples of BTEX solutions withdrawn at various time intervals were also analyzed by gas chromatography-mass spectrophotography (GC-MS) in order to determine the concentration of individual BTEX components. The analysis of BTEX was carried out using Varian CP-3800 gas chromatograph coupled to a Saturn 2000 MS mass detector.

Samples were manually injected via the sample valve at the front injector without the use of an autosampler. The conditions of analysis are described as below:

- Number of determinations (per sample): 2
- Injection volume: 100.0 µL
- Gas chromatograph conditions:
    - GC column: Restek RTL-VRX, 60 m, 0.32 mmID, 1.8 µm film thickness
    - Carrier gas: Helium
    - Column oven: initial temperature of 35^{o}C with hold of 2.00 min; then ramped to 50^{o}C with rate of 10.0^{o}C per min and hold for 4.50 min; then ramped to 200^{o}C with rate of 20.0^{o}C per min and hold for 6.00 min. Total analyzing time is 18.00 min then the column oven is cooled down to 35^{o}C and then stabilized for 2.00 min before the next analysis.
    - Front injector: temperature of 125^{o}C
    - Front electronic pressure controller (EPC): initial pressure of 5.5 psi with hold of 2.00 min, then increased to 6.4 psi with rate of 0.60 psi per min and hold for 1.00 min, then increased to 14.4 psi with rate of 1.07 psi per min and hold for 6.00 min. Column flow is 1.2 mL per min with total flow of 14.0 mL per min. Split ratio: 10:1.
- Mass spectrophotometer conditions:
    - Ion trap temperature: 150^{o}C
    - Manifold: 40^{o}C

- Emission current: 50 µA
- Multiplier offset: 200 V
- Scan time: 0.43 sec
- Ejection amplitude: 15 V
- Max ion time: 2000 µsec
- Max reaction time: 40 msec
- Target TIC: 10000 counts
- Prescan ion time: 200 µsec

The GC spectrum of the stock working solution is provided in Fig 6.2 below for the determination of peak positions of benzene, toluene, ethylbenzene and m-xylene.

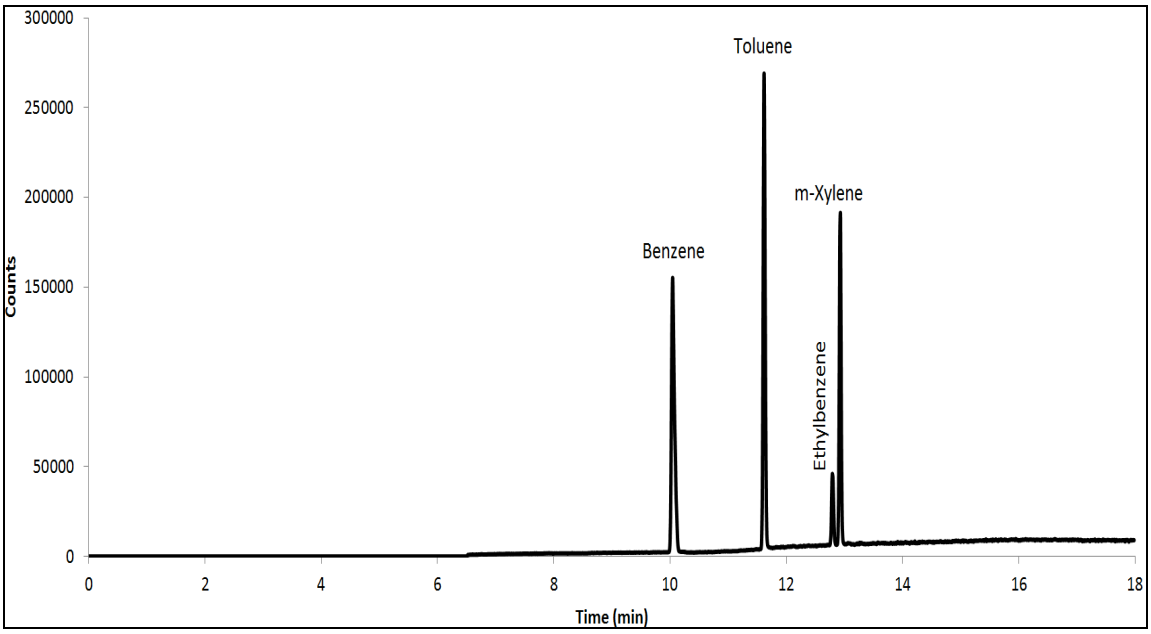

Figure 6.2. Standard gas chromatography spectrum of benzene, toluene, ethylbenzene and m-xylene recorded with GC-MS Varian CP-3800/Saturn 2000

The mass spectra of benzene, toluene, ethylbenzene and m-xylene acquired with Saturn 2000 MS detector in relation to the GC peaks are provided in the Supporting Information section for further information.

6.3. RESULTS AND DISCUSSION

6.3.1. Photocatalytic removal of BTEX in water with modified 1-D titanium dioxide nanomaterials under visible lights.

Three (3) sets of experiments were undertaken to determine the degradation patterns of BTEX with N-TiNT, including the control without photocatalyst but under radiating of visible lights (blank with light), the system with photocatalyst but in dark (N-TiNT with dark), and the system with the photocatalyst and under light conditions (N-TiNT with light). Observed degradation patterns of BTEX as indicated by the TOC values as a function of time are presented in Fig 6.3.

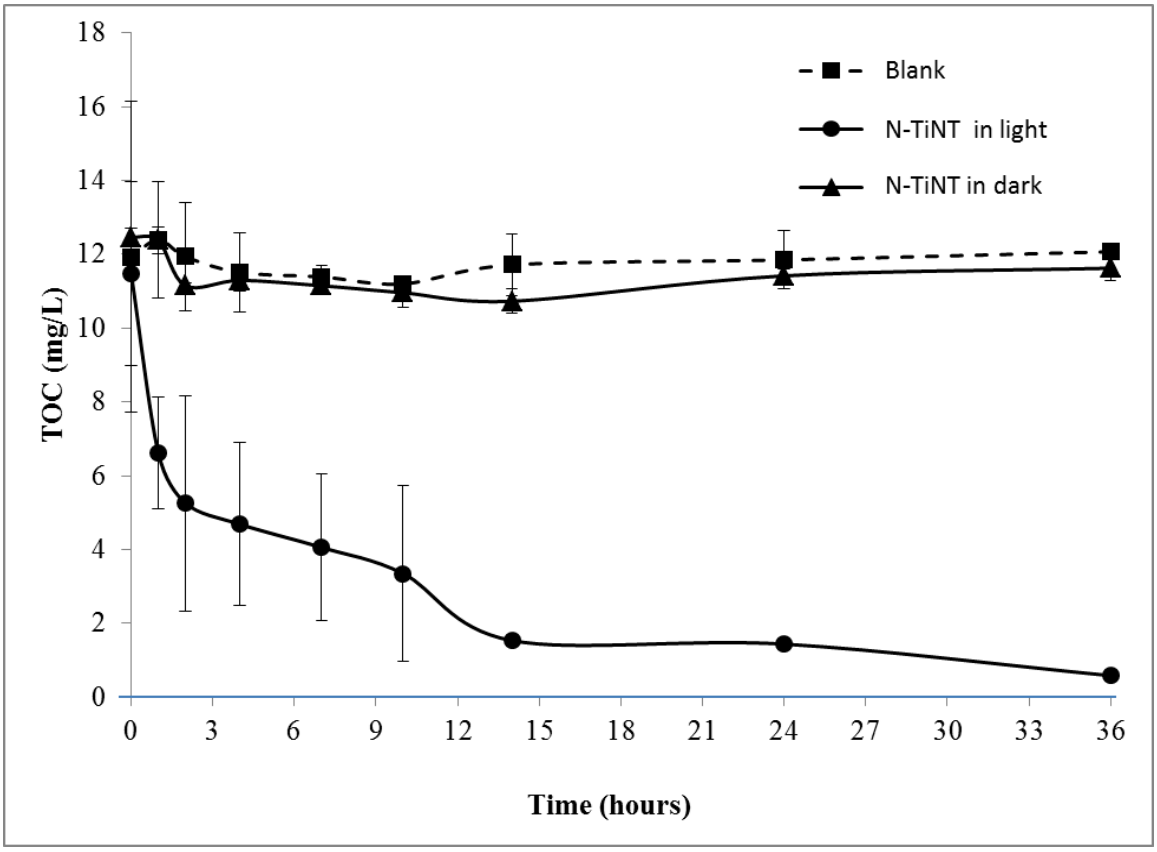

Figure 6.3. Treatment of BTEX in contaminated water with N-TiNT prepared by non-thermal plasma treatment

The results indicated that for the controls without the photocatalyst N-TiNT and with the photocatalyst N-TiNT but no light, the TOC values were essentially constant, indicating that the loss of BTEX through evaporation and adsorption was minimized. Any decrease of TOC must be resulted from the decomposition of aromatic hydrocarbons in the aqueous phase. Visible lights alone (without the photocatalyst) were not able to convert organic carbons into inorganic carbons in the solution. The presence of the photocatalyst N-TiNT but without light (N-TiNT dark experiments) also had no effect on the total TOC. When exposed to light, the removal of BTEX was observed when the photocatalyst N-TiNT was present. The overall removal of BTEX components was rapid

Blank

N-TiO_2/PAN in light

N-TiO_2/PAN in dark

at start, with 42.4 and 86.7 percentages of TOC were removed within 1 hour and 14 hours respectively. The removal of TOC continued afterwards but with a slower rate and reached 94.9% after 36 hours. These results confirmed that N-TiNT was activated with visible lights and the induced photocatalytic processes had oxidized BTEX components in the solution.

With a same experiment design, two (2) sets of experiments were carried out with the as prepared N-TiO_2/PAN nanofibers photocatalyst, the observed removal of BTEX is presented in Fig 6.4.

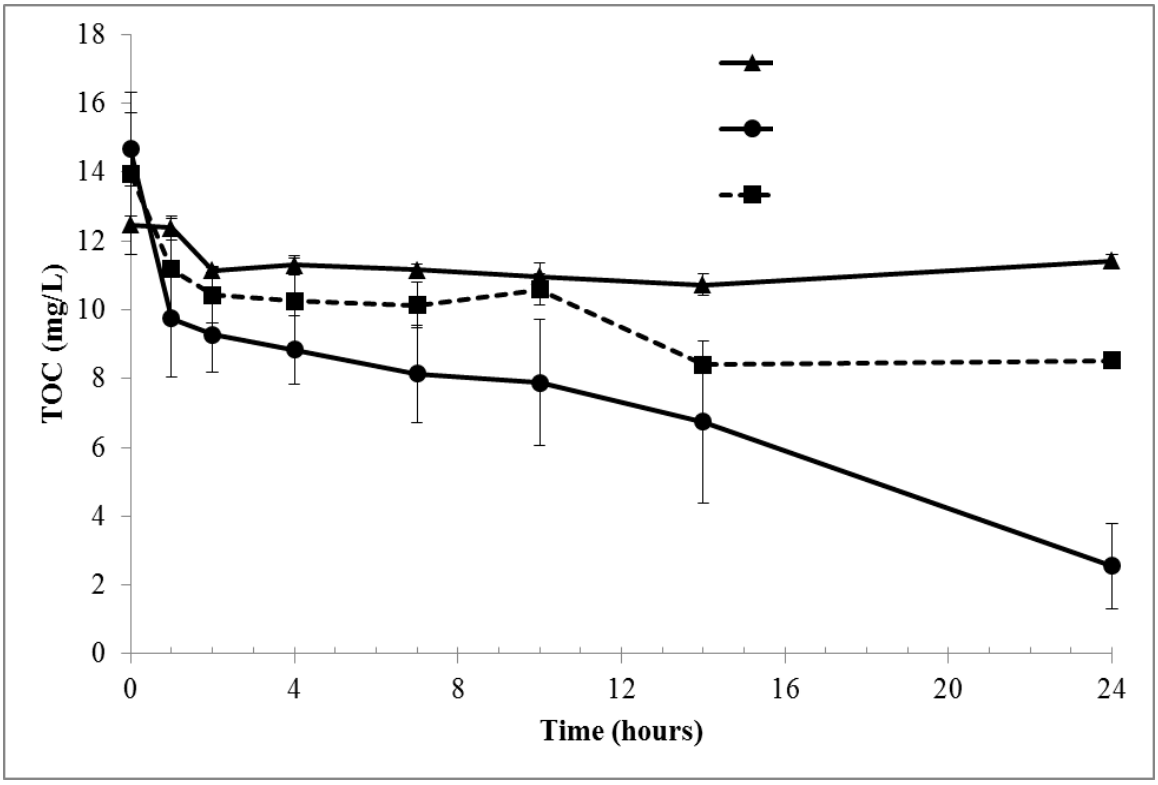

Figure 6.4. Treatment of BTEX in contaminated water with N-TiO_2/PAN nanofibers

It can be observed in Fig 6.4 that there was a small amount of BTEX removed in the dark test with annealed N-TiO_2/PAN nanofibers. After 1 hour of experiment without exposure to light, the TOC value decreased ~ 20% from 13.95 mg/L to 11.17 mg/L. Then there was no noticeable change in TOC value throughout the rest of the experiment. Hence, this observed removal is considered as being resulted from either the adsorption of BTEX onto the surface of annealed N-TiO_2/PAN nanofibers and/or some minimal evaporation during the stabilization period of the experiment. As PAN polymer alone is hydrophilic with no sorption of BTEX in produced water (Asatekin and Mayes 2009), the adsorption of BTEX components must be due to the presence of activated carbons at the surface of annealed N-TiO_2/PAN nanofibers.

When comparing to the data plotted in Fig 6.3 for N-TiNT, it is noted that the removal amount of BTEX components in the same dark conditions observed with annealed N-TiO_2/PAN nanofibers is slightly higher. During the annealing of prepared N-TiO_2/PAN nanofiber, the carbonization process of organic polymer material also occurred and created residual carbons, which at the same time were activated at the elevated temperature of the annealing process itself. These activated residual carbons served as effective adsorption centers for hydrocarbons in aqueous phase and therefore resulted in the high adsorption capacity of BTEX as observed with the annealed N-TiO_2/PAN nanofibers.

In tests with exposure to visible light, a clear removal of BTEX was observed with time. This confirmed the photocatalytic activation of TiO_2/PAN nanofibers with

visible light as reported in Chapter 5 of this dissertation. After 1 hour of experiment, ~ 33% of BTEX was removed with TOC value decreased from 14.67 mg/L to 9.74 mg/L. After 24 hour, ~83% of BTEX was removed with the final TOC value of 2.55 mg/L. Besides, GC-MS analytical results of samples withdrawn at specific intervals showed that benzene, toluene, ethylbenzene and m-xylene were removed simultaneously during the experiment process; as their respective peaks were all gradually decreasing from t = 0 to t = 24 hours as illustrated in Fig 6.5.

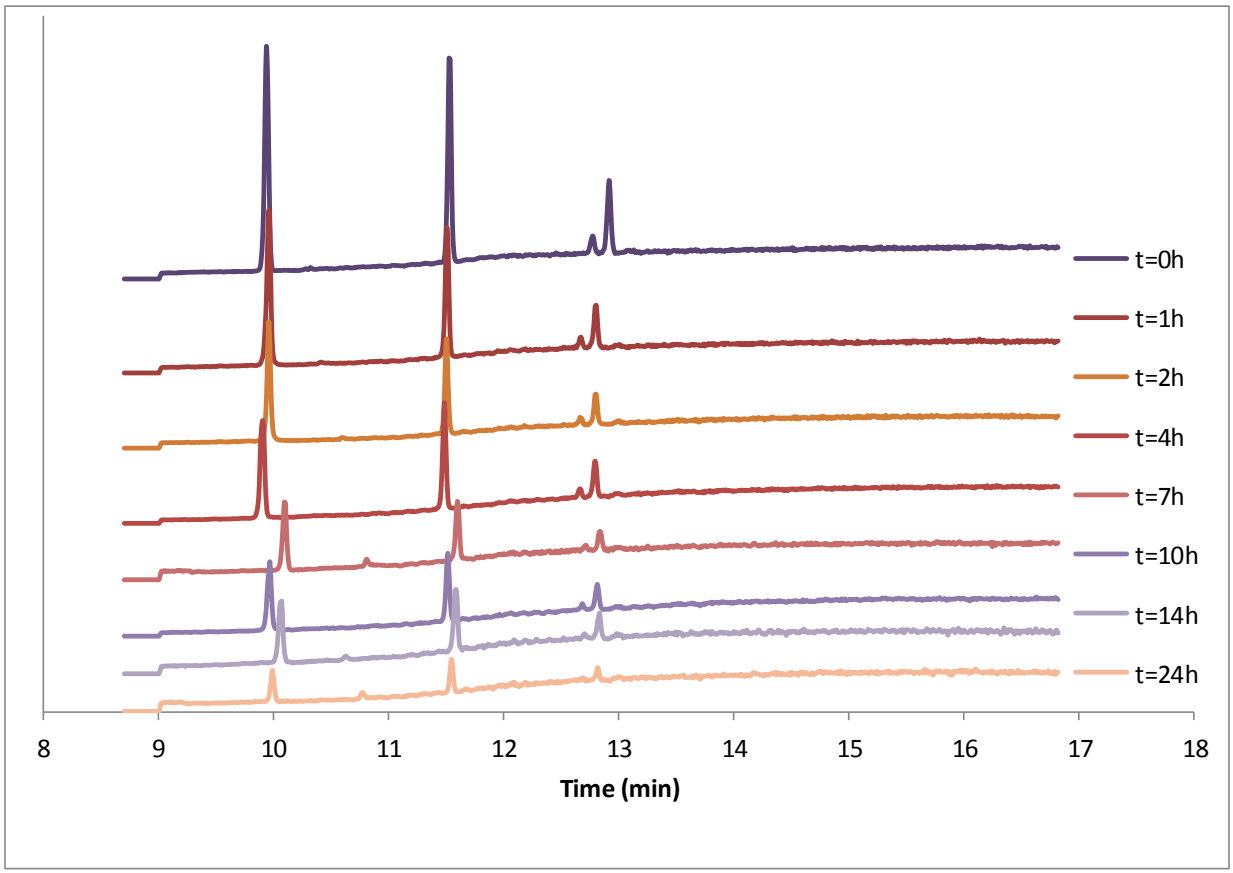

Figure 6.5. GC-MS spectra of BTEX working solution at specific time intervals in removal experiment with annealed N-TiO_2/PAN nanofibers and under exposure to visible light

(all spectra are in original scale)

The integrated area under each peak representing the concentration of each component was calculated and plotted in Fig 6.6.

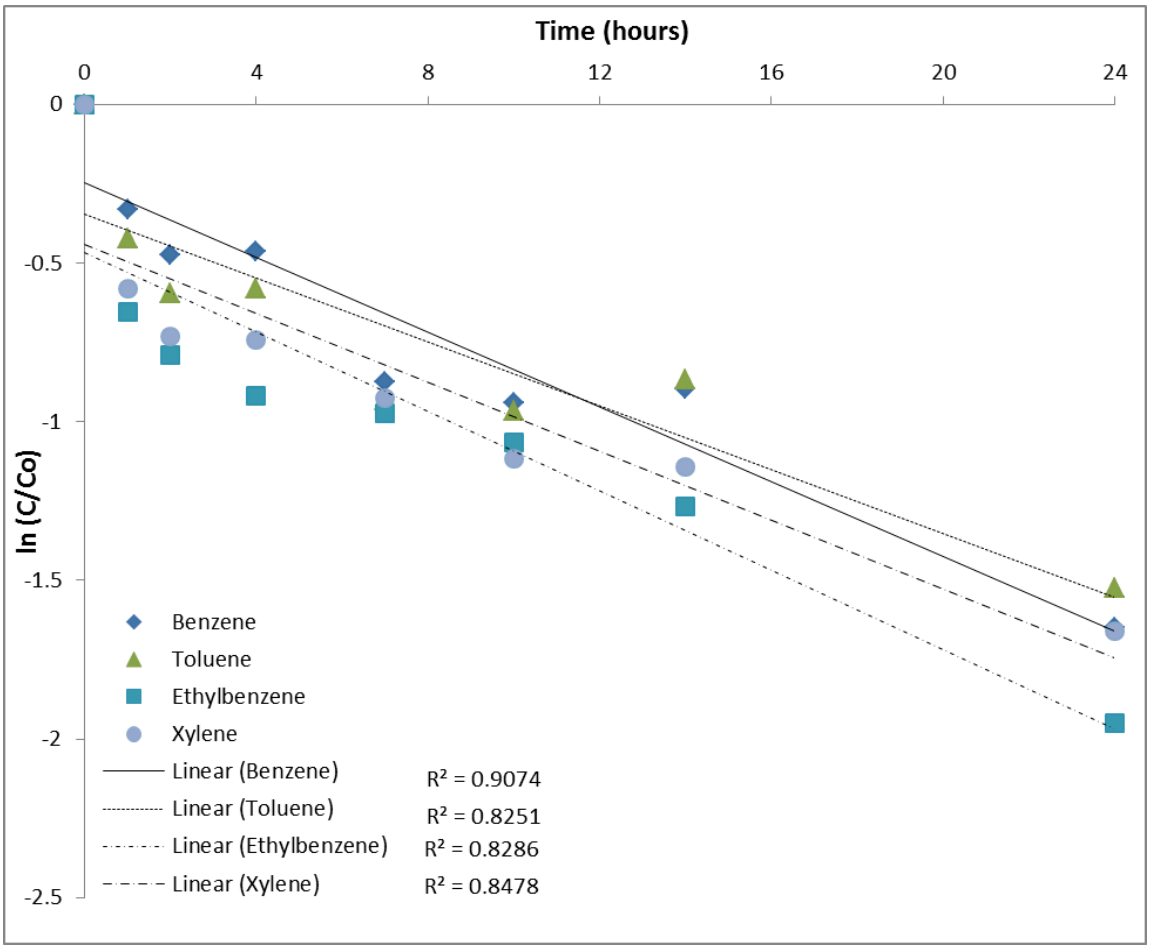

Figure 6.6. Removal rates of BTEX in removal experiment with annealed N-TiO_2/PAN nanofibers and under exposure to visible light

(C = concentration of relevant compound at specific time interval, C_o = initial concentration of relevant compound)

From Fig 6.6, the plotted data were found to have good linear fit with relevant correlation coefficient R^2 ranging from 0.83 to 0.91. This indicated that the removal of

each of BTEX components followed the first order kinetics: $ln[C] = ln[C_o] - kt$, which is in agreement with findings reported elsewhere (Chen and Mao 2007). Moreover, as the slopes of 4 linear trend lines in Fig 6.6 are nearly equal to each other, there is no noticeable difference among the removal rates of benzene, toluene, ethylbenzene, and m-xylene in experiments with annealed N-TiO_2/PAN nanofibers under exposure to visible light.

6.3.2. Implications on photocatalytic removal of BTEX in water with modified 1-D titanium dioxide nanomaterials under visible lights as a treatment technique.

Assuming the ratio among BTEX components in the working solution is unchanged during degradation experiments and using the data in Table 6.1, it is possible to compare the performance in removal of BTEX provided by N-TiNT/visible light and N-TiO_2/PAN/visible light systems with those of BAT and BPT which have been listed in Table 6.2.

Table 6.2. Comparison of BTEX removal efficiencies among N-doped titanium dioxide nanotubes/visible, BAT and BPT treatment techniques

Time	10 hours	14 hours	36 hours
Total BTEX in working solution in treatment by N-TiNT/visible light system (mg/L)	3.67	1.66	0.64
Total BTEX in working solution in treatment by N-TiO_2/PAN/visible light system (mg/L)	9.92	8.48	3.21 (24 hours)
Total BTEX in discharged effluent treated with BAT (mg/L) (EPA 1993)	5.881		
Total BTEX in discharged effluent treated with BPT (mg/L) (EPA 1993)	2.782		

From Table 6.2, N-TiNT/visible light system was capable of generating an effluent with lower total BTEX quantity compare to Best Available Techniques after 10 hours of treatment. The results show that it is possible for outdoor systems with visible light activated 1-D titanium dioxide nanomaterials to be utilized for treating hydrocarbon contaminants in water with free and sustainable solar energy. Besides, it should be noted that the BTEX removal was represented through the decrease of TOC values, which illustrates that the treatment process by photooxidation had completely mineralized BTEX, rather than into other organic intermediates which may still pose hazards to human health and the environment.

When the illuminating duration was extended, the photooxidation process induced by N-TiNT/visible light system was able to remove BTEX further. After 36 hours, the

TOC value in working solution was reduced to 0.64 mg/L which is closed to the detection limit (400 ppb) of the analysis instrument. After 14 hours which is closely equivalent to maximum daylight hours per day in the North America, the effluent treated by N-TiNT/visible light system contains less of total BTEX compared to Best Possible Techniques.

Although it was not possible to compare the efficiency between N-TiNT and N-TiO_2/PAN through undertaken experiments due to the different loads of photocatalyst in each set of experiment, it can be observed from Fig 6.3 and Fig 6.4 that the photocatalytic removal of BTEX between them shared a similar pattern. Therefore it is anticipated that the prolonged treatment with N-TiO_2/PAN/visible light will also result in a complete removal of BTEX in water.

6.4. CONCLUSIONS

Modified 1-D titanium dioxide nanomaterials with activation in visible light have been successfully employed in treatment of water contaminated with BTEX. Treatment techniques based on these photocatalyst were found comparable to existing BAT and BPT currently applied for produced water. Particularly, since the treatment time among experiments was chosen to resemble actual daylight hours on field, collected results from the study showed a promising potential for outdoor solar reactor to be established in actual conditions for treatment of contaminated water sources. In short, with only visible light being utilized for the degradation of hydrocarbon contaminants, treatment

techniques based on the applications of modified 1-D titanium dioxide nanomaterials can offer effective and sustainable detoxification options for environmental engineering purposes.

REFERENCES

Asatekin, A. and A. M. Mayes (2009). "Oil industry wastewater treatment with fouling resistant membranes containing amphiphilic comb copolymers." Environmental Science and Technology **43**(12): 4487-4492.

Chen, X. and S. S. Mao (2007). "Titanium dioxide nanomaterials: Synthesis, properties, modifications and applications." Chemical Reviews **107**(7): 2891-2959.

Cho, I. H., Y. G. Kim, J. K. Yang, N. H. Lee and S. M. Lee (2006). "Solar-chemical treatment of groundwater contaminated with petroleum at gas station sites: Ex situ remediation using solar/TiO_2 photocatalysis and solar Photo-Fenton." Journal of Environmental Science and Health - Part A Toxic/Hazardous Substances and Environmental Engineering **41**(3): 457-473.

EPA (1993). "Development Document for Effluent Limitations Guidelines and New Source Performance Standards for the Offshore Subcategory of the Oil and Gas Extraction Point Source Category." EPA-821-R-93-003. from

http://yosemite.epa.gov/water/owrccatalog.nsf/1ffc8769fdecb48085256ad3006f39fa/969ed536d932393a85256d83004fd95c!OpenDocument.

Linsebigler, A. L., G. Lu and J. T. Yates Jr (1995). "Photocatalysis on TiO_2 surfaces: Principles, mechanisms, and selected results." Chemical Reviews **95**(3): 735-758.

Veil, J. A., M. G. Puder, D. Elcock and R. J. R. Jr. (2004). "A white paper describing produced water from production of crude oil, natural gas, and coal bed methane." Prepared for US Department of Energy - National Energy Technology Laboratory - W31-109-Eng-38.

CHAPTER 7

CONCLUSION AND PERSPECTIVE

7.1. CONCLUSION

Visible light activated TiO_2 nanotubes were successfully prepared by the non-thermal plasma treatment with nitrogen as the working gas. The damage to tubular structures from the plasma treatment is not significant, or in other words the nanotube structures were mostly preserved, as desired. These findings are in good agreement with the objective of the experiment. However, observed results from the addition of carbon monoxide into the working gas are not adequate to fully support or to fully reject the original hypothesis that such an addition will aid the doping of nitrogen onto TiO_2 nanotubes. The noticeable effect observed when carbon monoxide was added into the plasma reactor was that the damage level to nanotube structures was more significant, which was resulted from the oxidation caused by carbon monoxide. It is believed that such damage can reach to an undesirable level when more extensive treatment is performed and therefore the more recommended plasma treatment technique in this dissertation should be the non-thermal plasma with nitrogen as the only working gas in order to retain specific advantages of TiO_2 nanotubes.

Besides, the employment of electrospinning technique with polyacrylonitrile as the template polymer has also brought success in the preparation of visible light activated TiO_2 nanofibers. The activation in visible light of the as prepared TiO_2 nanofibers is in

good agreement with the hypothesis set out when the preparation method was designed. In this dissertation it is considered that the overall preparation of nitrogen doped TiO_2 nanofibers by electrospinning method is more streamlined and effective yet requires less effort when compared with the preparation of nitrogen doped TiO_2 nanotubes via non-thermal plasma treatment. As TiO_2 nanofibers also share the advantages of 1-D geometrical characteristic with TiO_2 nanotubes, electrospinning as the preparation and modification method for 1-D TiO_2 nanomaterials is considered as a promising technique in the production of TiO_2 photocatalyst with enhanced efficiency for environmental engineering applications.

In the investigation with BTEX serving as model aromatic hydrocarbon contaminants in produced water, the as prepared TiO_2 nanotubes and TiO_2 nanofibers both had showed the ability to degrade these organic compounds under visible light. The decrease of total organic carbon value over the experimental time proved that BTEX were oxidized into inorganic carbon compounds which are CO_2 or CO_3^{2-} with none or very little toxicity. Data collected from GC/MS also showed the decreased concentration of BTEX components over time. In comparison with best possible and best available techniques for the removal of BTEX in water, the photo-oxidation based on modified 1-D TiO_2 nanomaterials is regarded as a promising treatment method with adequate effectiveness and high sustainability.

In summary, the findings reported in this dissertation have provided illustrations of successful novel techniques for preparation of visible light activated 1-D TiO_2

nanomaterials. As being newly developed, the reported techniques also carry with them opportunities of improvement and expansion. It is strongly believed that better techniques can be evolved based on the foundation constructed from the findings reported in this dissertation, as well as more effective and efficient 1-D TiO_2 nanomaterials that will be prepared to better meet technical and sustainable demands of environmental engineering applications.

7.2. RECOMMENDATIONS AND FUTURE RESEARCH

From this study, it has come to our knowledge that the preparation of visible light activated 1-D TiO_2 nanomaterial can be easily implemented by electrospinning technique. Compared to the complex preparation of nitrogen doped TiO_2 nanotubes which also requires a sophisticated plasma reactor with an expensive vacuum system, TiO_2 nanofibers can be prepared with simpler and more readily available instruments which are syringe pump and high voltage power generator. Moreover, the preparation time of visible light activated TiO_2 nanofibers was much shorter, and the final product yield was much larger. Furthermore the electrospinning technique itself provide a wide range of controls and modifications which have been reviewed earlier in this dissertation for customizing and bringing novel properties to the nanofibers. From this perspective, TiO_2 nanofibers have many advantages in term of preparation, especially when considering production at a larger scale. As a result, TiO_2 nanofibers herein are considered as the more effective 1-D structures of titanium dioxide nanomaterial for industry-wide application.

With this perspective, the author looks forward to implementing studies with TiO_2 nanofibers as prepared in following to the method reported in this dissertation in two directions as follows.

7.2.1. Improvement of physical properties and photocatalytic efficiency of modified TiO_2 nanofibers

In one approach, the author proposes to find an optimal multi polymers mixture to act as the support for TiO_2 nanofibers. This mixture shall provide TiO_2 nanofibers with similar in situ nitrogen doping while good mechanical strength is achieved across the mat of nanofibers. Good candidates for these studies are thermally stable polymers such as polybenzimidazole $(C_7H_4N_2)_n$ or silicon based inorganic polymers such as polydimethylsiloxane $CH_3[Si(CH_3)_2O]_nSi(CH_3)_3$. In another approach, nanomaterials made from metallic elements or metal oxides can also be introduced into the precursor dope to yield a product of TiO_2/metal/metal-oxide nanofibers which is able to provide higher photocatalytic efficiency. As mentioned in the literature review in Chapter 2, many metallic elements had been experimented as dopants for TiO_2 nanomaterials. Among them, various metals such as vanadium and lanthanum were able to enable not only activation with visible light but also higher photocatalytic efficiency. It is therefore expected that the addition of these materials will be beneficial to TiO_2 nanofibers. To develop an appropriate method together with to find the optimal mixture in order to yield TiO_2 nanofibers with better properties and performance will be a valuable and promising target for future research.

7.2.2. Applications of modified TiO_2 nanofibers for removal of newly established hazardous contaminants

Recently, more attention of scientific communities are being placed on new pollutants such as endocrine disrupting compounds (EDCs) and natural organic matters (NOMs). EDC is a group of chemicals that can interfere with hormone system of animal and human, and therefore is especially hazardous to biological lives. Known EDCs including pesticide DDT, Polychlorinated Biphenyls (PCB) and Bisphenol A (BPA) have been widely reported to cause cancer, birth defect and developmental disorder. NOMs are natural organic matters from plants and animals discharged to the environment. The presence of NOMs in water can lead to several complications in water treatment, ranging from biofouling of filtration system to harmful by-products during disinfection process. With the strong oxidation potential, it is expected that modified TiO_2 nanomaterials will be suitable for decomposing these unwanted substances. The actual effectiveness and efficiency in degradation of aqueous EDCs and NOMs by visible light activated TiO_2 nanofibers will be investigated in subsequent studies.

BACKGROUND INFORMATION

A. Operating principle of TOC with POC kit

On the Shimadzu TOC-V, the measured TOC is the total of NPOC which stands for Non-Purgeable Organic Carbon such as acetate, phenolate and etc., and POC which stands for Purgeable Organic Carbons such as volatile organic compounds such as BTEX, acetone and etc.

The operating diagram of TOC-V unit with POC kit is presented as follows:

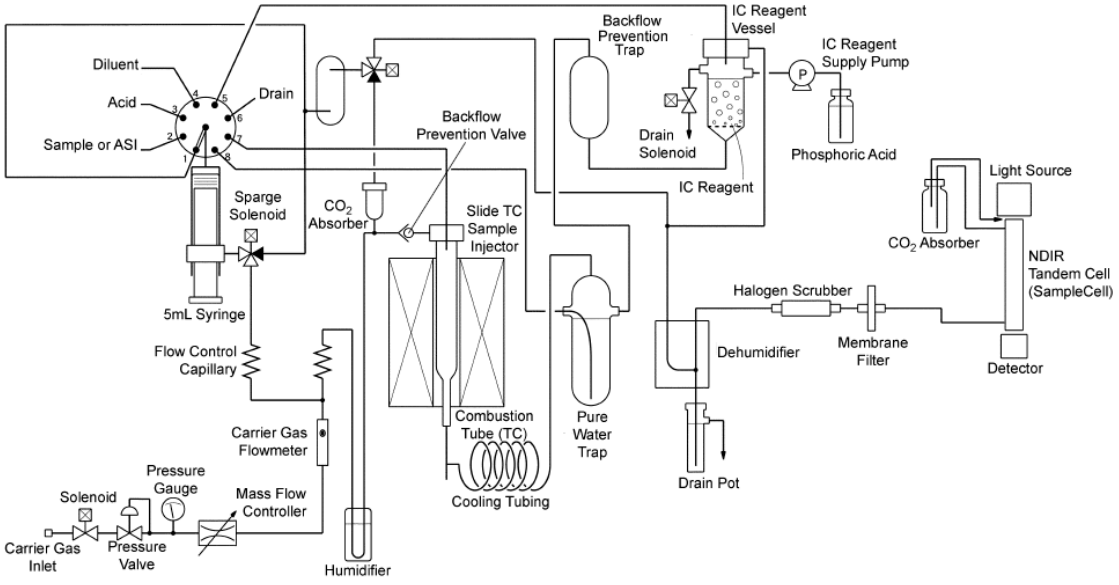

Firstly, the sample is acidified with HCl 2N solution to convert dissolved carbonates into CO_2:

$CO_3^{2-} + 2H^+ \rightarrow H_2O + CO_2$

Then the liquid sample is drawn through the LiOH column without sparging in order to remove CO_2 while POC and NPOC components are preserved for downstream analysis:

$$CO_2 + 2\ LiOH \rightarrow Li_2CO_3 + H_2O$$

POC and NPOC components are then completely burned in the combustion chamber to form CO_2 which is finally measured by an IR detector to give the analytical quantity of TOC.

Standard curve

The standard curve was established based on the 2-point-standard curve as recommended in the TOC operating instruction of the manufacturer. The following table shows data of the standard curve.

TOC of stock solutions (mg/L)	Peak Area
0	0.83
7.9	8.66
39.5	42.61

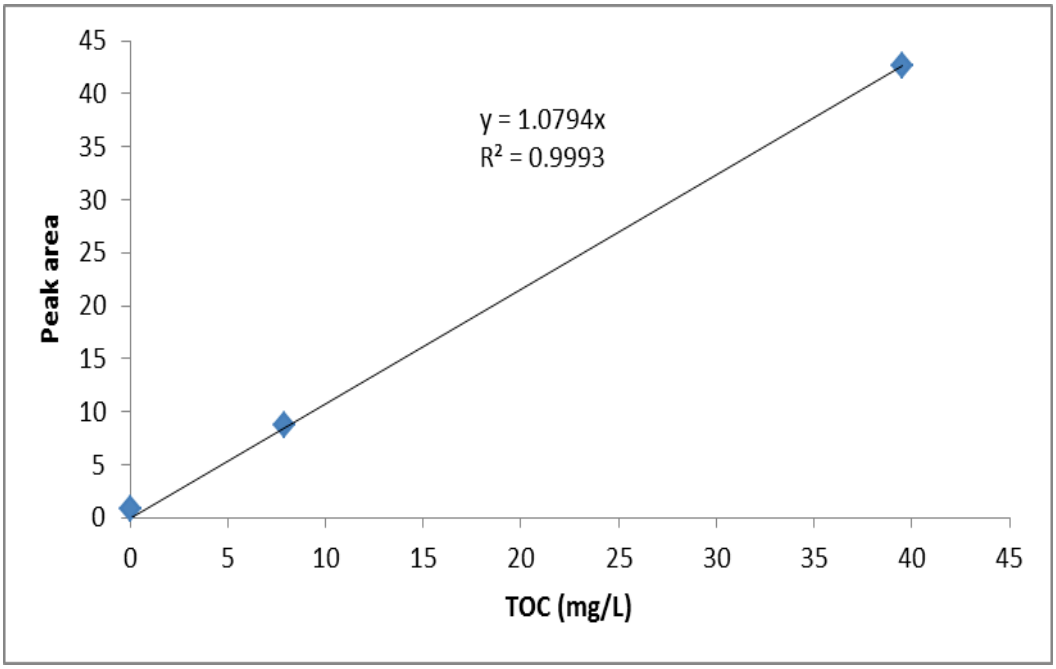

The R^2 factor of linear regression is approximate 1 in the above figure, which is in agreement with the operating instruction from the manufacturer.

Ethylbenzene

m-Xylene

Toluene

Benzene

B. Mass spectra of Benzene, Toluene, Ethylbenzene and m-Xylene acquired by Saturn 2000 MS.

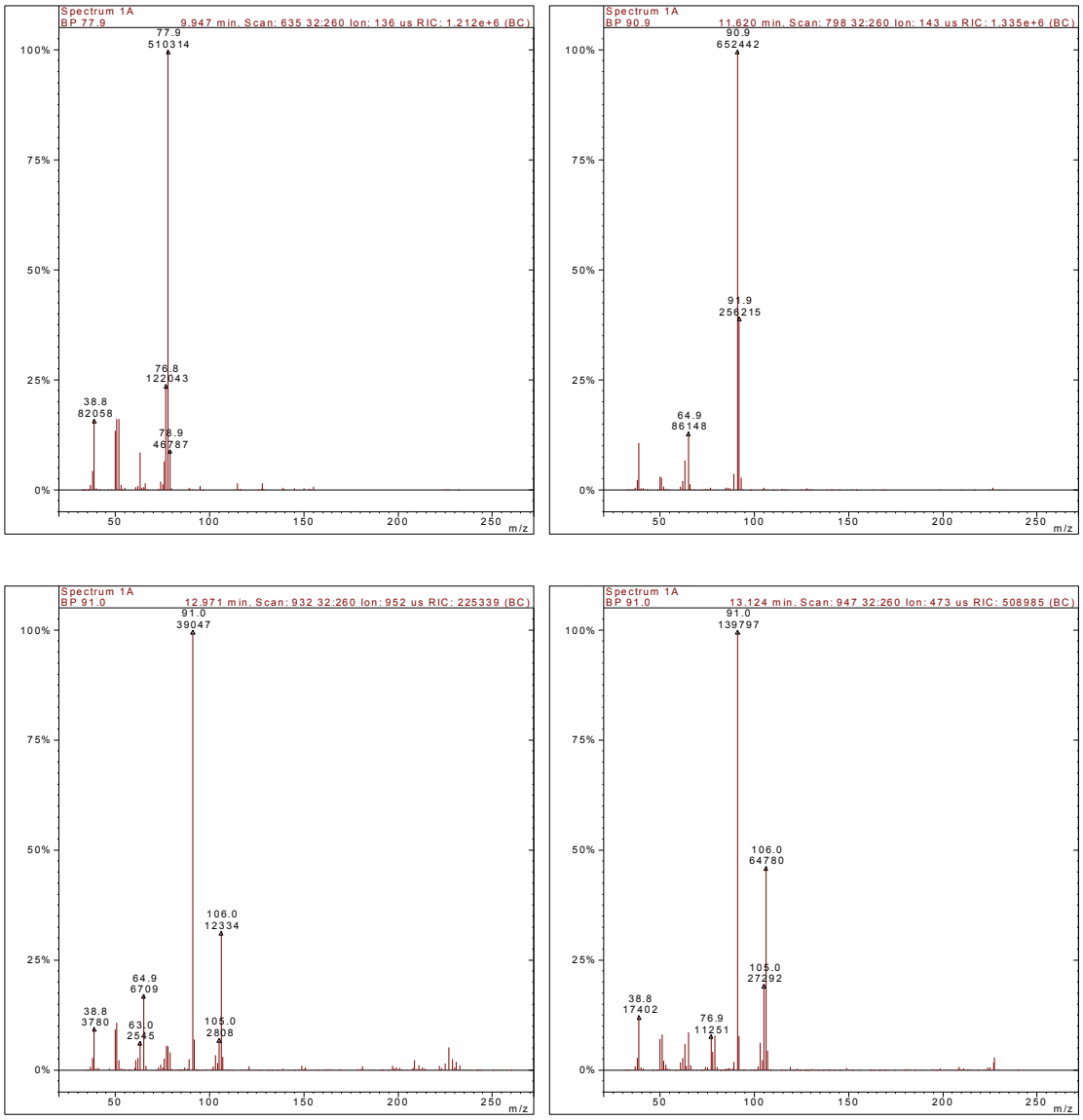

VITA

Huy Quang Nguyen graduated his Bachelor of Chemistry from one of the leading Vietnamese universities, Hanoi University of Sciences in 2001. Then in 2004, he achieved the degree of Master of Science in Environmental Engineering and Project Management at the University of Leeds, United Kingdoms. He joined Department of Civil and Environmental Engineering at the University of Missouri from 2007 to study toward Doctoral degree under the fellowship co-sponsored by Vietnam Education Foundation, the University of Missouri, and the Department of Civil and Environmental Engineering. Outside the time studying full-time for the Master and Doctor degrees, Huy has been working as an environmental engineer in the oil and gas sector in Vietnam, where he has participated in many key industrial projects such as Oil and Gas Production in Cuu Long Basin, National 1st Refinery, Phu My Power Plant, and Ca Mau Fertilizer Plant.